



Digitized by the Internet Archive
in 2019 with funding from
University of Alberta Libraries

<https://archive.org/details/Gould1964>

Thesis
1965
p. 25

THE UNIVERSITY OF ALBERTA

SOME PRELIMINARY EXPERIMENTS ON THE SPECIFIC HEAT OF
HELIUM FOUR ADSORBED IN 13X-ZEOLITE

by

Judith Ann Gould

A THESIS

SUBMITTED TO THE FACULTY OF GRADUATE STUDIES
IN PARTIAL FULFILLMENT OF THE REQUIREMENTS FOR THE DEGREE
OF MASTER OF SCIENCE

DEPARTMENT OF PHYSICS

EDMONTON, ALBERTA

December, 1964

UNIVERSITY OF ALBERTA

FACULTY OF GRADUATE STUDIES

The undersigned certify that they have read, and recommend to the Faculty of Graduate Studies for acceptance, a thesis entitled SOME PRELIMINARY EXPERIMENTS ON THE SPECIFIC HEAT OF HELIUM FOUR ADSORBED IN 13X-ZEOLITE, submitted by Judith Ann Gould in partial fulfillment of the requirements for the degree of Master of Science.

Date January 7, 1965

ABSTRACT

This thesis is a description of some experiments designed to test the feasibility of doing a detailed study of the specific heat of helium adsorbed in 13X-zeolite, an alumina-silicate with a regular cavity structure. The interest in this system arose from the controversy as to whether the first layer of adsorbed helium is solid or not. It was also hoped that this system would test the postulate (11) that helium is a quantum liquid if experiments were carried out with both helium three and helium four. The experiments reported here, however, were strictly of a preliminary nature and had only the following objectives: to develop some of the techniques, using helium four, necessary for doing a detailed examination of both the helium-four-and helium-three-zeolite systems, to measure an isotherm of helium four adsorbed in 13X-zeolite, and to obtain an estimate of the specific heat of helium four in the 13X lattice at liquid-helium temperatures above 1.8°K .

In view of these objectives three isotherms of helium four adsorbed in zeolite were done. These measurements showed that most of the gas was adsorbed at pressures lower than those measured on the manometers.

In addition, two heat-capacity runs were done in the temperature region 1.8 - 4.1°K with a bomb calorimeter: in the first run the calorimeter was filled with helium; in the second it was empty. The specific heat of helium four in zeolite was obtained by subtracting the results of the second run from that of the first. From this experiment the specific heat of helium adsorbed in 13X is significantly lower than that of the bulk liquid. No specific-heat maximum was observed but this is not surprising when the temperatures used and the manner in which the experiments were done are considered.

The preliminary study shows that the study of the helium - 13X system was worthwhile and should be continued in greater detail. Another group has already reported results for helium three in the zeolite (22).

ACKNOWLEDGEMENTS

A number of people assisted me greatly in this project and I would like to express my sincere appreciation of their aid.

Dr. F. D. Manchester, my research supervisor, gave many hours of his valuable time to discuss the project with me and to guide its execution.

During Dr. Manchester's absence, Dr. D. D. Betts, Dr. J. P. Franck and Dr. S. B. Woods assisted through a number of valuable discussions.

Without the assistance and advice of the technical staff this project would have been extremely difficult. I would like to thank Mr. P. Crouse and Mr. H. McClung for providing the liquid air and liquid helium necessary and for assembling some of the apparatus, Mr. N. Riebeek and Mr. J. Cuthiell for machining some of the metal apparatus and Mr. J. Legge and Mr. P. Alexander for making the glass apparatus.

Miss V. Miskew capably analyzed a few of the heat-capacity points. Miss H. Hufnagel was very co-operative and expert in her typing of the thesis. Miss J. Seale prepared some of the diagrams. The staff of the computing

centre obligingly processed the necessary programs and advised me on the most efficient methods available.

I would also like to thank the many other people who encouraged me in this work.

Very generous financial assistance was obtained from the National Research Council as it supported the experimental work and awarded me a National Research Council Bursary.

TABLE OF CONTENTS

	Page
ABSTRACT	i
ACKNOWLEDGEMENTS	iii
INTRODUCTION	1
Chapter 1. ADSORBED HELIUM	13
Adsorption Isotherms	16
Specific-Heat Measurements	22
The Onset of Superfluidity	24
Chapter 2. THE ADSORPTION APPARATUS	34
The Manometers	39
The Calibrated Volumes	40
The Dewar System	41
Powder Samples and Sample Containers	45
Chapter 3. OPERATION OF THE ADSORPTION APPARATUS	47
Calibration of the Apparatus	48
Adsorption Isotherms	51
Chapter 4. RESULTS OF THE ADSORPTION EXPERIMENTS	57
Dead Space Corrections	57
Errors in the Isotherm	60
Density of Zeolite Crystals	61
The Results	65
Chapter 5. THE SPECIFIC HEAT APPARATUS	73
The Calorimeter	73
General Features of the Specific Heat Cryostat	81
The Thermometer	85
Heater Circuit	86
Chapter 6. EXPERIMENTAL PROCEDURE ASSOCIATED WITH HEAT CAPACITY MEASUREMENTS	90
The Loading, Leak Detecting and Evacuation of the Calorimeter	90
Heat-Capacity Measurements	92

	Page
Chapter 7. THE HEAT-CAPACITY RESULTS	97
Method of Calculation	97
Errors in Procedure and Analysis	100
The Results	106
Chapter 8. DISCUSSION OF RESULTS	119
REFERENCES	135
Appendix I.	
Oil Density	A1
Appendix II.	
Calibration of Germanium Thermometer	A2
Appendix III.	
Results of Adsorption Experiments	A9
Appendix IV.	
Sample Calculation of Heat-Capacity Point	A12
Appendix V.	
Heat-Capacity Results	A16
Appendix VI.	
Schematic Diagrams of Manometer Usage in Adsorption Isotherms	A22

LIST OF TABLES

Table		Page
1.	Adsorption Volumes	42
2.	Definition of Symbols Used in Calculation of Measurements on Adsorption Apparatus	49
3.	Helium Atoms in 13X-Zeolite Cavities	121
4.	Helium Adsorbed in Zeolite Cavities	124
5.	A Comparison of Some Specific Heats of Helium	130
6.	Density of Apiezon B	A1
7.	Thermometer Calibration, Run 3	A6
8.	Thermometer Calibration, Run 4	A7
9.	Adsorption of Helium in Sample 1 at 4.1 and 2.1°K	A10
10.	Adsorption and Desorption of Helium in Sample 2 at 4.1°K	A11
11.	Heat-Capacity Results of Run A	A17
12.	Heat-Capacity Results of Run B	A20

LIST OF ILLUSTRATIONS

Figure		Page
1.	Model of the Large Cavity of 13X-Zeolite	6
2.	Model of the Unit Cell of 13X-Zeolite	8
3.	Transition Temperatures in Thin Helium Films	26
4.	Schematic Diagram of Adsorption Apparatus	35

Figure		Page
5.	Photograph of Adsorption Apparatus	37
6.	The Hydration of 13X-Zeolite	62
7.	Helium Adsorption in 0.202g. 13X-Zeolite	67
8.	Helium Adsorption in 0.516 g. 13X-Zeolite at Approximately 4.1°K	69
9.	Helium Adsorption Program of 13X-Zeolite	71
10.	Schematic Diagram of Calorimeter	76
11.	Photograph of Suspended Calorimeter	79
12.	Photograph of Specific-heat Cryostat	82
13.	Heater Circuit	88
14.	Heat Capacity of Dummy Calorimeter	103
15.	Heat Capacity of Runs A and B (analyzed by Method 2)	108
16.	Heat Capacity of Runs A and B (analyzed by Method 3)	110
17.	Heat Capacity of Adsorbed Helium as Obtained from Figure 15	113
18.	Heat Capacity of Adsorbed Helium as Obtained from Figure 16	115
19.	Specific Heat of Helium Adsorbed in 13X-Zeolite	117
20.	Error Curve for the Thermometer Calibration	A3
21.	Schematic Diagram of a Heat-Capacity Point	A13
22.	Schematic Diagrams of Manometer Usage in Adsorption Isotherms	A22

INTRODUCTION

Helium is an element with two stable isotopes: one of atomic mass four, having two protons and two neutrons in the nucleus; the other of atomic mass three, having two protons and one neutron. Both atoms are chemically inert. The liquids boil at low temperatures (helium four at 4.21°K (1) and helium three at 3.19°K); appear to have a liquid phase at 0°K ; and solidify only under pressure. In spite of the similarities, there are striking differences; liquid helium four exhibits a remarkable transition at 2.17°K , known as the lambda transition, to a superfluid phase when, among other changes, non-viscous ("superfluid") flow appears. The bulk liquid has a logarithmic singularity in its specific heat as measured on the saturated-vapour curve (2). As the density of liquid helium is increased the lambda transition occurs at lower temperatures and the lambda curve finally intersects the melting curve at 1.76°K and 29.6 atmospheres. Although a superfluid state in helium three, with a co-operative mechanism similar to the B.C.S.^{**} model for superconductors, has been postulated*, a possible phase transition to this state has been observed only recently at approximately $.0055^{\circ}\text{K}$ (4).

Since helium four has zero spin and is spherically symmetric, its interactions with other atoms are through

* a brief review is contained in (3)

** Bardeen-Cooper-Schrieffer

Van der Waals forces. Helium three, having spin $1/2$, can have a spin interaction as well as the Van der Waals. Both isotopes have a high zero-point energy. Any theory attempting to explain why the isotopes have markedly different behavior has had to rely on the fact that helium-four atoms are bosons obeying Bose-Einstein statistics and helium-three atoms are fermions obeying Fermi-Dirac statistics. Examples include the application of Bose-Einstein-condensation theory, reviewed by Atkins (1), Landau's theory of helium four (a review is contained in Superfluid Physics by Lane (5)), and a theory of helium three which is reviewed by Brueckner (6).

Any surface in contact with liquid helium four is covered with a thick film. Below the lambda-transition, the film exhibits such properties as behaving as a link for superfluid flow. Once the film has entered the superfluid phase, liquid can flow through the link to the lowest available level even if part of the flow path is uphill; this flow can be used to indicate the lambda transition. The properties of the saturated film are reviewed by Jackson and Grimes (7).

The unsaturated film, namely the film in contact with the solid wall at pressures lower than the saturated-vapour pressure, P_0 , usually exhibits a lambda transition

at a lower temperature than does the bulk liquid at P_0 ; however, what happens to the onset of superfluidity in the case of very thin films is not clear. It has been generally accepted that the first one or two statistical layers, being of solid density, exhibit properties similar to the solid; that is the atoms in these layers are immobile so that no superfluid transition can occur. Manchester (8,9) has observed superfluid transitions in the helium film at coverages low enough to cast doubt on this picture. This question is discussed fully in Chapter 1.

Since the idea that there is a solid-helium layer next to the wall is based on calculations involving the interatomic forces in the film, the conclusion that the first layer is solid applies to both helium four and helium three. Thus it would be interesting to attempt to observe, in very thin films either a spin degeneracy in helium three or a superfluid transition; the latter, especially, would indicate the presence of liquid helium. There is some possibility that adsorption on the surface would raise the superfluid transition to experimentally observable temperatures in the case of a boson system consisting of paired fermions. An increase in transition temperatures has been observed experimentally in some superconducting films, and the superconducting state in a metal is the basis for the superfluid model of helium three. For a given material these films exhibit a transition temperature increasing with decreasing film thickness (10).

Betts, Manchester, and Woods (11) have made two suggestions regarding the adsorption of helium. Firstly, by putting helium three in a regular, host lattice such as a zeolite crystal, the phonon interaction with the walls of the cavities might enhance the interaction between the helium atoms. This would raise the transition temperature of the postulated superfluid state in helium three. Specific-heat measurements would then show that helium three had a strong interaction with the zeolite lattice. Secondly, because the wavelength of helium is between eight and eleven angstroms* at liquid helium temperatures, the atom can not be localized. Thus liquid helium is a quantum fluid. Because of this, helium in the adsorbed state might remain fluid even if its density in that state was higher than that of the bulk, solid helium. Again the zeolite lattice, containing regular cavities a few angstroms in diameter, provides an interesting medium for examining this postulate. Since the cavities in the zeolite are intrinsic and the adsorption is almost completely internal, presumably the zeolite provides a more ideal adsorption surface with fewer surface imperfections than most other materials.

At the suggestion of Betts, Manchester, and Woods a program to study the specific heat of helium adsorbed in the Linde 13X-zeolite was initiated. The choice of medium had several advantages. Among them were the following:

* $\lambda = \left(\frac{h^2}{2mkT}\right)^{\frac{1}{2}} \quad (12)$

the cavity diameter, being approximately twelve angstroms (13), was only slightly larger than the wavelength of the free, helium atom; and zeolites were among the few available adsorbents in which enough helium was adsorbed at low coverages that a specific-heat maximum in a film of one or two "layers" could be detected if it were present.

Zeolites are hydrated crystals which occur naturally. Examples include chabazite, faujasite, analcite, heulandite and many others. The crystal structure of a number of these is discussed in the book by Wells (14). Similar crystals, among them the 13X-zeolite, have been produced synthetically and are available commercially. A review of some of their properties is contained in an article by Breck and Smith (15). The zeolites have an alumino-silicate structure which contains an intrinsic and regular pattern of pores in which water is absorbed. These pores are a few angstroms in diameter. The zeolites (16) have three types of pore structure: filamentary, plate-like and three dimensional. The last are the ones of interest here as they can be dehydrated to a large degree, often in excess of ninety per cent, without collapsing the pore structure. The pores can then be filled with other molecules as long as the replacements have a diameter smaller than the pore-neck.

Figures 1 and 2 show models of the 13X-zeolite, the one used in the following experiments. The structure has

Figure 1.

Model of the Large Cavity of 13X-zeolite

A cross-section of the large cavity of the 13X-zeolite is shown. The bounding sodalite units, each enclosing a small cavity, form one of the entrances between the large cavities. The sodium atoms, represented by large dark balls, partially block the entrances to the small cavities. The small dark ball (centre right) represents an aluminum ion. White balls represent oxygen atoms. No attempt has been made to show the complete cation structure. (The large dark ball (right edge, center) is an oxygen atom in shadow.)

Dr. H. W. Habgood of the Alberta Research Council very kindly allowed his models of the 13X-zeolite to be used in Figures 1 and 2.

All the photographs used in this thesis were taken by the Photographic Services of the University of Alberta.

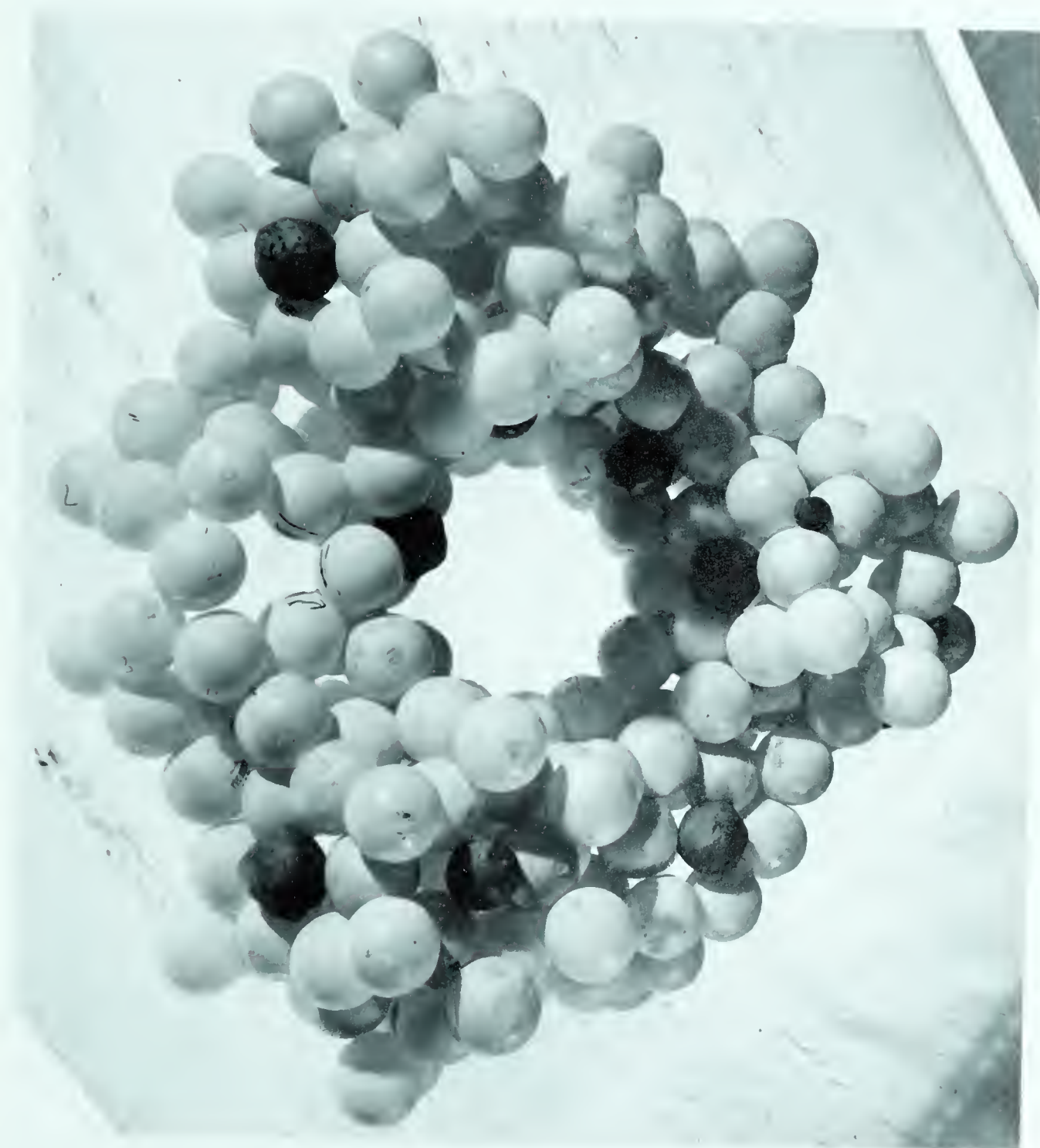
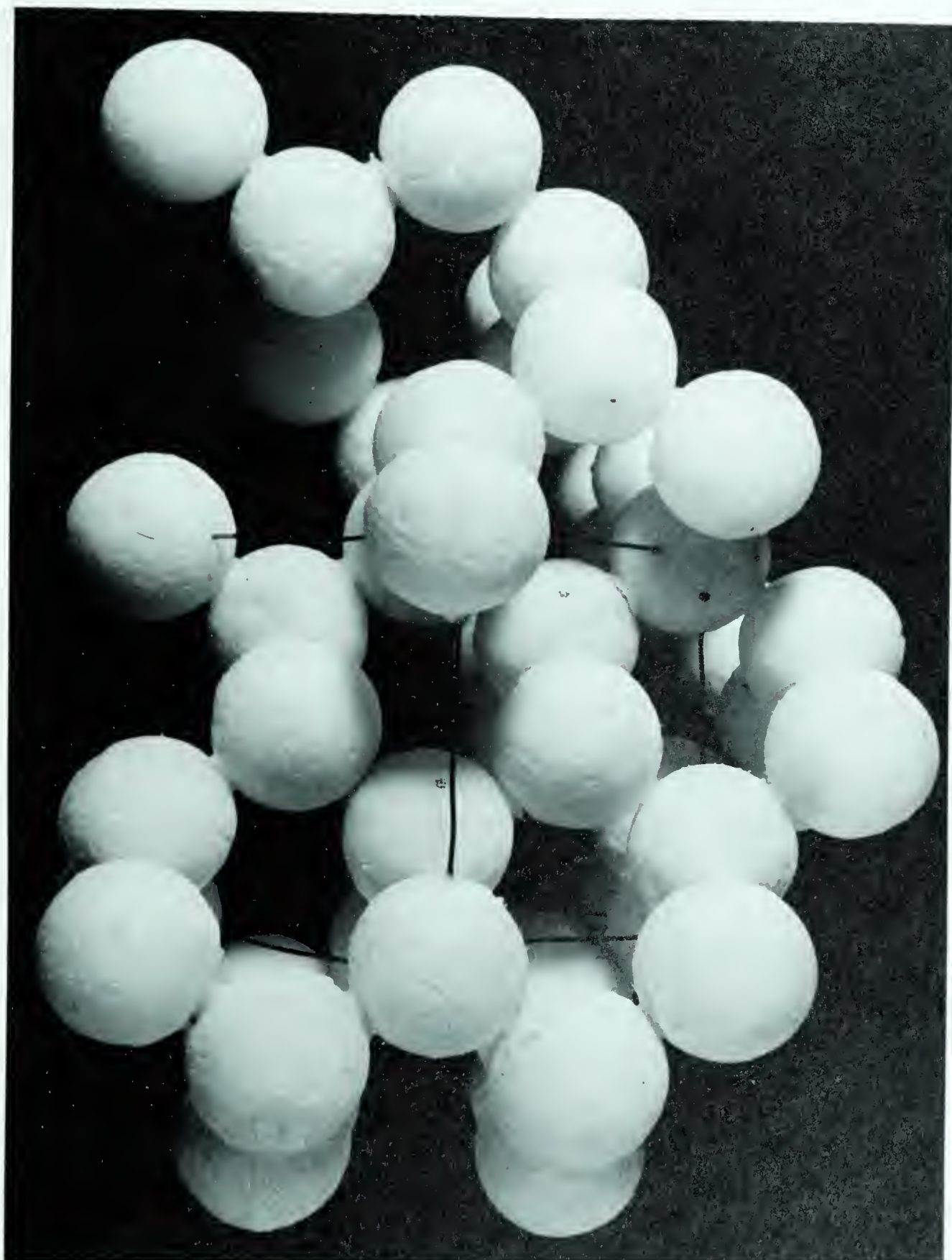


Figure 2

Model of the Unit Cell of 13X-zeolite

With each white ball representing a sodalite unit, the system of large cavities is shown. The wires in the picture outline a unit cell containing eight small and eight large cavities.



been determined by L. Broussard and D. P. Shoemaker (17). Basically it consists of $(\text{Si Al})\text{O}_4$ tetrahedra arranged in structural units known as sodalite units, the sodalite units being on a diamond lattice. The pore structure consists of eight large cavities and eight small cavities per unit cell. The entrance to the small cavities is through the interior of the large cavities. Normally only the large cavities will contain adsorbed molecules, excepting water. Dubinin (18) calculated that out of the 15,513 cubic angstroms per unit cell, the large cavities contain 6,490 cubic angstroms and the small 1,200 cubic angstroms. Thus a total of 7,690 cubic angstroms per unit cell is contained in the cavities.

Barrer and Bratt (19) measured the hydration isotherms of 13X and found that the anhydrous zeolite could adsorb approximately .33 gram of water per gram of anhydrous zeolite at 30°C . They also found that there was some irreversibility in the isotherms if the zeolite was heated above 270°C although it could be reversibly heated to 350° as long as the amount adsorbed was small. Thus these crystals can be dehydrated almost completely without excessive structural damage.

Experiments have already been done on the properties of helium in the 13X lattice. Santini (20,21) originally studied helium three in the 13X-zeolite to determine surface

effects in nuclear-magnetic experiments. From these experiments he and his co-workers concluded that helium three in this state was paramagnetic above two degrees Kelvin but that the results were not conclusive below this.

Lambert (22), using a sealed calorimeter, measured the specific heat of helium three in 13X. His first report indicated a maximum in the specific heat at approximately $.6^{\circ}\text{K}$ which was of the right magnitude to be caused by nuclear-spin ordering; however further measurements indicated that the observation of the maximum could not be repeated. Lambert also mentioned some measurements on the helium-four-zeolite system, but the results were not reported.

Several other experiments (23-26) have been carried out on adsorbed helium three and four recently. The adsorbents included copper and Vycor glass as well as zeolite. Unfortunately the papers have not yet been published.

This thesis describes some preliminary experiments on the measurement of the specific heat of helium four in 13X-zeolite. The experiments were designed to determine the advisability of continuing the study, using both helium four and helium three, at lower temperatures and a variety of coverages. In order that the heat capacity of a known amount of helium in the zeolite lattice be measured, some information about the adsorption isotherms was necessary;

for by using an adsorption isotherm the amount adsorbed could be obtained from a knowledge of the equilibrium pressure in contact with the zeolite. As there were no low-temperature, adsorption isotherms available, an experiment was set up for this purpose. After the discussion of earlier work concerning adsorbed helium in Chapter 1, this thesis will be divided into two parts: one dealing with the adsorption measurements and the other with the specific-heat measurements. The results of both sections will be discussed in Chapter 8.

Chapter 1. ADSORBED HELIUM

Analysis of data obtained from experiments on the adsorbed state can be quite complicated. For this reason a brief discussion of the analysis of heat-capacity curves to obtain the specific heat of an adsorbed gas is included. Only theoretical corrections will be included; additional corrections may be necessary under certain experimental conditions.

Hill (27) analyzed the thermodynamics of the adsorption of molecules on an inert adsorbent or in other words the thermodynamics of physical adsorption as distinct from chemical adsorption. The adsorbent was assumed to be unaltered in any of its physical properties by the adsorption. If the volume occupied by the adsorbate were negligible compared to the volume it would occupy in a gaseous state and if the perfect gas law could be applied, he found the isosteric heat of adsorption, q_{st} , to be defined by

$$\left. \frac{\partial \ln P}{\partial T} \right|_{\Gamma} = \frac{q_{st}}{PTv_g} = \frac{q_{st}}{kT^2}$$

v_g being the volume occupied by a molecule in the gas phase, P the equilibrium pressure above the adsorbate, Γ the number of molecules adsorbed per unit area. The isosteric heat could be calculated from plots of $\log P$ versus $1/T$ at constant coverage. It could also be measured calorimetrically.

The differential heat of adsorption, q_d , was related to the isosteric by

$$q_d = q_{st} - kT .$$

He considered a calorimeter containing an adsorbent with adsorbate and found that, if a quantity of heat, q , were added to the system, initially in thermal equilibrium,

$$C_\Gamma = \frac{q}{dT} - C_b - C_{vg} + q_d \frac{dN_s}{dT} ,$$

C_b being the heat capacity of the calorimeter, adsorbent, and addenda; C_{vg} the heat capacity of the unadsorbed gas in the calorimeter at constant volume; C_Γ the heat capacity of the adsorbed gas at constant coverage; dT the temperature change; and dN_s the number of molecules desorbed by the change in temperature. A relation between dN_s/dT and $\left. \frac{\partial N_s}{\partial P} \right|_{T,U}$, U being the adsorption area of the adsorbent, was calculated such that

$$\frac{dN_s}{dT} = - \frac{q_d P}{(kT)^2} \left. \frac{\partial N_s}{\partial P} \right|_{T,U} \left/ \left(1 + \frac{kT}{V} \left. \frac{\partial N_s}{\partial P} \right|_{T,U} \right) \right. ,$$

V being the dead space in the calorimeter. The differential $\left. \frac{\partial N_s}{\partial P} \right|_{T,U}$ can be obtained from isotherm data.

Another expression for $q_d \frac{dN_s}{dT}$ was used by Morrison et al.(28). From the perfect gas Law

$$kT(N - N_s) = PV ,$$

N being the total number of molecules. Thus

$$q_d \frac{dN_s}{dT} = q_{st} \frac{dN_s}{dT} + V \frac{dP}{dT} - \frac{PV}{T} .$$

If the pressure in the calorimeter were being monitored, dP/dT could be measured directly and dN_s/dT could be calculated from this. Thus all the quantities necessary for the specific-heat measurements were experimentally measurable.

A number of experiments have been carried out on helium in contact with a solid surface at less than its saturated pressure. These can be divided into three main categories for the purposes of this thesis; experiments on flow, isotherms and heats of adsorption, and experiments on specific heat. Since, as shown from Hill's analysis, the last two categories are of direct interest to specific-heat work, the results of these will be discussed in some detail. The flow experiments will be mentioned only in conjunction with the onset of superfluidity which is discussed briefly at the end of the chapter.

Adsorption Isotherms

Physical adsorption occurs when the molecules of an adsorbate are present on the surface of an adsorbent at pressures below the saturated-vapour pressure of the adsorbate. The adhesion between adsorbate and adsorbent is caused by attractive forces, which arise from the interaction of the electromagnetic field of each of the atoms involved, between the adsorbate and the adsorbent. Physical adsorption occurs when wave functions of the adsorbate are only slightly distorted by the presence of the adsorbent. If the distortion of the wave functions of the atoms (molecules) is so severe that electrons are either shared by the adsorbent and adsorbate or are transferred from one to the other so that a chemical bond is formed, then the adsorption is called chemisorption. A more complete discussion of the distinction is contained in reference 29 (p. 2). The distinction is not always clear; however helium atoms, being spherically symmetric, are definitely adsorbed physically.

When physical adsorption is present the adsorption forces are Van der Waals. These are electromagnetic in character and involve both the electrons and the nuclei of the interacting atoms. The interactions may be described as being between the dipoles and the multipoles of the adsorbate and adsorbent. These may be permanent multipoles belonging to the free atoms, multipoles induced by the presence of either the adsorbent or adsorbate, or multipoles induced instantaneously

by the interaction of the atoms. The last describes the interaction for the spherically-symmetric, helium-four atoms. When the atoms are so close that the electronic-wave functions overlap, a repulsive force arises. The complete interaction is commonly described by the Lennard-Jones(6-12) potential if no interaction higher than dipole-dipole is important (29, Chapter 2).

The early adsorption isotherms and heats of adsorption were measured at low relative saturations. Keesom and Schweers (30) measured isotherms of helium on glass and helium on gas layers adsorbed on glass from approximately 7.5×10^{-7} to 1.5×10^{-2} millimeters of mercury and from 1° to 9°K . From the step-like decrease in the heats of adsorption, which appeared to be temperature independent, they concluded that the first two layers were completed in this pressure range. Other isotherm work included helium on hydrated nickel sulphate (31), on charcoal (32), and on glass (33) from four to sixteen millimeters pressure.

Most of these early experiments were not analysed in terms of the generally accepted isotherm theories. These theories are reviewed in the book, Physical Adsorption of Gases by Young and Crowell. The most common isotherm relation applied to later experiments was the one developed by Brunauer, Emmett, and Teller (34), the "BET" isotherm.

The BET -isotherm equation contained two adjustable constants which could be fitted to each isotherm. One, v_m , represented the amount of gas in a monolayer. The other, c , was given by

$$c = \exp((E_1 - E_o)/RT) ,$$

E_1 being the energy of adsorption and E_o the heat of vaporization of the bulk liquid. The surface area of the adsorbent was estimated from v_m and the effective diameter of the adsorbate molecule when it was in the bulk liquid. Nitrogen isotherms taken at approximately 77°K have been used very successfully so that the area of the nitrogen molecule, 16.2 \AA^2 , has been used as a standard to obtain the effective areas of other adsorbates.

Frederikse and Gorter (35) using Fe_2O_3 ; Strauss (36); Long and Meyer (37); and Schaeffer, Smith, and Wendall (38) each reported that either the area of the powder was anomalously high when compared to the nitrogen isotherm or there was anomalous packing of helium on the surface. Frederikse obtained an effective diameter of between 2.05 \AA and 2.35 \AA for the adsorbed-helium atom whereas the liquid helium atom has a diameter of approximately four angstroms. Mastrangelo and Aston (39), when analyzing isotherms of helium on titanium dioxide, suggested that several layers were completed almost simultaneously and that Frederikse's first layer

actually corresponded to three layers of helium which were packed like atoms in solid helium. In 1956, Meyer (40) re-interpreted Bower's (41) experiments of helium adsorbed on aluminum foil at high pressures. He concluded that the first layer was completed when P/P_0 was approximately 10^{-10} and that the BET v_m was actually the amount of gas adsorbed before the heat of adsorption became equal to the heat of vaporization of the bulk liquid. His experiments on gold foil indicated that a monolayer had formed by P/P_0 equal to 10^{-7} . Hobson (42), using a magnetron gauge and a pyrex surface, found that the monolayer had formed below 10^{-9} mm. of mercury. Steele (43) modified the BET equation to allow the second layer to have an energy different from either E_1 or E_0 , and thus introduced a third parameter. About this time Singh and Band (44) calculated that the compression of helium into a dense monolayer actually made the Lennard-Jones potential repulsive so that the BET v_m could not be adsorbed in the monolayer unless a completely different type of interaction took place with an attractive potential of almost 1600 calories per mole.

In general, by 1956, researchers had decided that the first one or two layers of the adsorbed film were essentially solid. The reasons for this will be discussed more fully in another section. Analysing the results of some

isotherms of helium on titanium dioxide, Aston, Mastrangelo, and Tykodi (45) concluded that the change of slope in the modified BET plot of the isotherm between 2.6 and 3.4°K indicated a situation analogous to helium melting under high pressure. Most researchers had observed that the amount adsorbed at a given relative pressure, P/P_0 , increased with decreasing temperature. Exceptions included White, Chou, and Johnston (46) and Tjerkstra, Hooftman, and Van der Meydenberg (47) both of whom found the isotherms temperature independent. Brewer and Mendelssohn (48), using glass as their adsorbent, reported that v_m decreased with temperature and that the isosteres were discontinuous at the bulk-lambda temperature.

The heats of adsorption obtained from isotherms depended greatly on coverage but usually were somewhere between 100 and 30 calories per mole at low coverages. Near saturation the heat of adsorption approached the heat of vaporization, approximately 20 calories per mole. Several calorimetric determinations of the heat of adsorption have been performed at temperatures above 4°K. Theoretically the isosteric heat of adsorption is temperature independent. The results range from 700 to 200 calories per mole, again decreasing with increasing coverage. Heats calculated from isotherm data in the same set of experiments appeared to agree quite well with the calorimetric ones but there was not much overlap in the coverages used in each method.

A large advance in isotherm theory was made by Ross and Steele (51) who attempted to calculate an isotherm from the Lennard-Jones potential without any constants obtained from experimental isotherms. They felt that theory predicted the experimental isotherms of a monolayer of helium adsorbed on argon reasonably well.

A comparison of the adsorption isotherms of helium three and helium four on charcoal, made by Hoffman, Edeskuty, and Hammel (52) in the range up to P/P_0 approximately 0.95, showed that helium three had less tendency to adsorb at 2.45 degrees than helium four did at 3.95; however both were adsorbed by almost a factor of two more than nitrogen was at 75.6°K.

Although hysteresis had not been observed on the desorption branch of helium isotherms already mentioned, there was great interest in the problem of capillary condensation. This phenomenon was characterized by the capillary (53) or pore filling at one pressure but not desorbing until a lower pressure; hence a reproducible, hysteresis loop was formed. Kington and Smith (54) discussed this with regard to argon adsorbed on chromic-acid gel and Vycor glass--a glass with various-sized pores in it. They concluded that a theory in which the adsorption was controlled by the body of the cavity and the desorption by the neck was

most consistent with their results. Champeney and Brewer (55) measured the isotherms of helium and nitrogen on Vycor glass and observed a hysteresis loop in all but the 4.22°K one for helium. Dacy and Edwards (56), using a microbalance, were unable to obtain desorption points for the isotherms on saran charcoal because of long equilibrium times. Saran charcoal has a micropore structure with a minimum width between 10 and 15 \AA . Both groups concluded that one or two layers of adsorbed helium were present in the solid state.

The significance of the solid-layer theory will be discussed after the specific-heat measurements done on adsorbed helium have been reviewed.

Specific-Heat Measurements

Frederikse (57) measured the specific heat, near the lambda temperature, of helium adsorbed in various thicknesses on jeweller's rouge. Mastrangelo (58) did a similar experiment on helium adsorbed on titanium dioxide. Recently, in conjunction with some superflow experiments, Brewer et al. (59) measured the specific heat of helium adsorbed in the pores of Vycor glass. After their results had been corrected for the gas which desorbed during each heating period, each group of observers reported that the specific heat showed a maximum which was broader

and at a lower temperature than that in the bulk liquid. The extent of the smearing and the magnitude of the depression of the temperature of the maximum increased with decreasing coverage until the maximum disappeared at approximately three-layers coverage (BET) in Frederikse's experiment.

Of the three experiments the one performed by Frederikse was the only one having a low-temperature valve that could isolate the gas in the calorimeter. Mastrangelo measured the equilibrium pressure, the temperature and the volume of gas adsorbed as he obtained his heat-capacity measurements and later corrected his specific-heat measurements with the information. He also improved the thermal contact with the powder by having spring-loaded, randomly-drilled, copper sheets between layers of powder.

The appearance of an apparent phase transition in an adsorbed film near but below a phase transition in the bulk has been observed on several occasions. For example, argon (60) and nitrogen (61) adsorbed on titanium dioxide both showed specific-heat maxima at temperatures below the normal melting point.

Anomalous contributions to the heat capacities in annealed and irradiated silicon (62) and beryllium oxide (63) have been observed. The results have been explained by the diffusion of helium, produced during the

irradiation, into pockets produced by the annealing. The peaks are quite sharp and usually only slightly displaced from the temperature of the bulk-lambda transition. No estimate of the size of the pockets is given; however, Seidel and Keesom (62) thought the helium present had the density of the bulk liquid.

The Onset of Superfluidity

Specific-heat results were not the only experiments which reported the lowering of the lambda transition in films. Experiments on heat transfer in thin films and flow in narrow channels also showed depressions in the transition temperature which appeared to be a function of the relative pressure, P/P_0 . The transition temperatures obtained by Long and Meyer (64) from measurements of the rate of flow of the unsaturated film into a vacuum and those obtained by Brewer and Mendelssohn (65) from experiments measuring the heat transfer across films on glass and German silver were in close agreement; however, the experiments done on superflow in Vycor glass have, in general, a lower transition temperature than the above for a given relative pressure; the discrepancy being greater as the coverage decreased. Constrictions in the cavities of the Vycor were probably the cause of this additional lowering of the transition temperature as the narrowest part of the cavity would determine the superflow

properties. The specific-heat maxima were generally at higher temperatures than the superflow transitions. The onset of superflow and the heat-capacity maximum of helium (59) adsorbed in Vycor glass at approximately ninety-seven per cent saturation agreed quite well with each other and the results in reference (64). Figure 3 shows the transition temperatures obtained by Long and Meyer (64) and those obtained by Manchester (9).

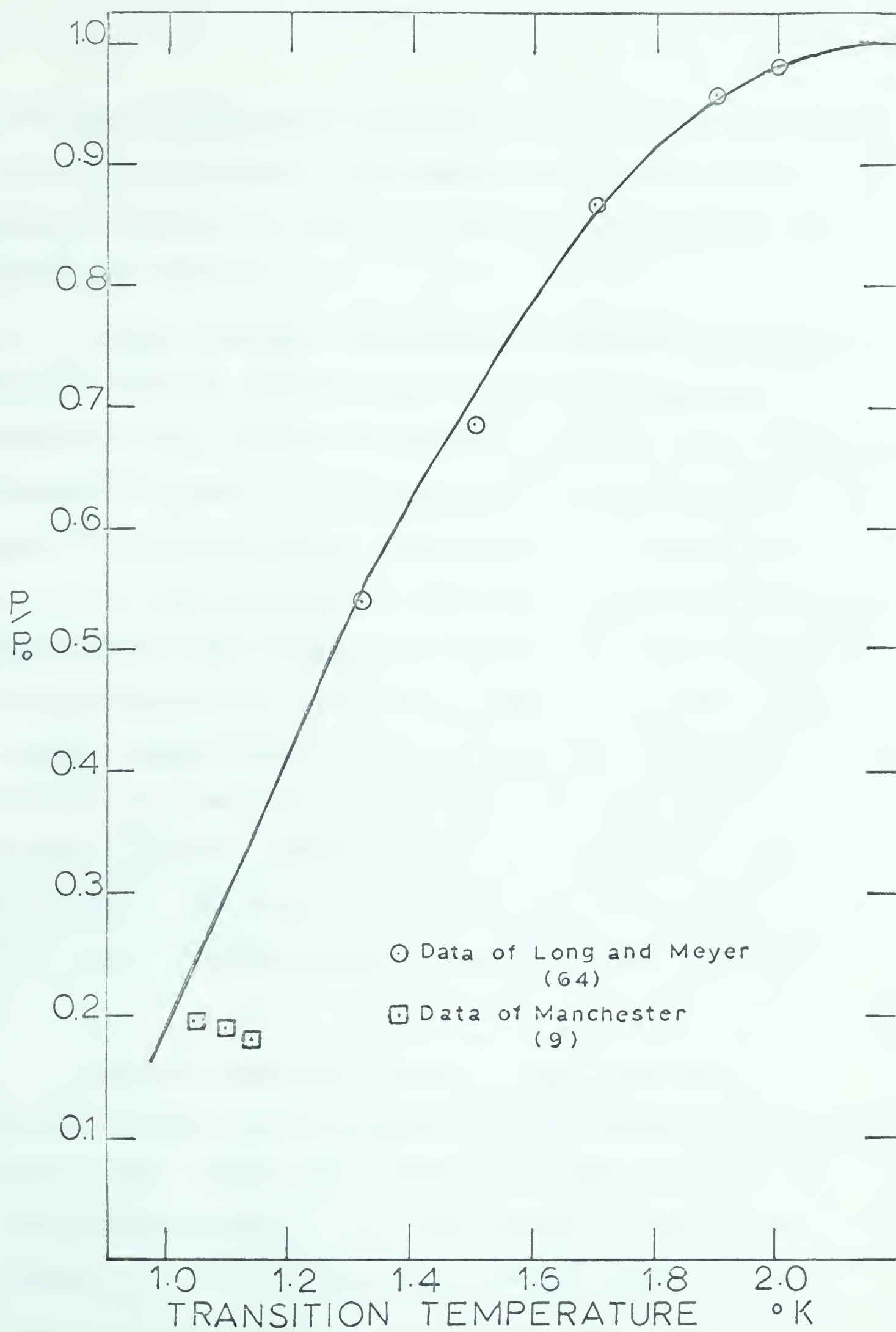
A number of semi-empirical theories have been developed to explain the peculiar features of the helium film. A brief review of them follows.

Application of the Bose-Einstein-condensation model of superfluid helium was unsuccessful in two dimensions, because the transition temperature went to zero as the area of the film increased. Ziman (67) postulated that liquid helium could be divided into small volumes, approximately 10^{-7} centimeters on a side, which were essentially independent. When this was applied to helium films, the agreement with the form of experimental results was not very good and, there was no physical justification for choosing the size of the volumes. An extension to the Bose-Einstein-condensation theory was developed by Singh and Pathria (12), who considered the effect of a bounded continuum with surface waves on the energy-gap-Bose-Einstein-condensation model, found that they could fit their

Figure 3

Transition Temperatures in Thin Helium Films

The relative pressure, P/P_0 , is plotted against transition temperature. The data used were those of Long and Meyer (64) and Manchester (9).



theoretical, transition-temperature curve to the experimental values of Long and Meyer (64) fairly well especially at low coverages; however two constants had to be calculated from experimental results.

Hecht (68,69), using Feynman's partition function, developed a theory in which the transition temperature was determined by the number of nearest neighbours. By increasing the number of layers in the experimental results by $3/4$, he managed to fit the specific-heat-transition temperatures quite well. Hecht attributed the lower transition temperatures obtained in the flow experiments to the fact that incomplete layers were present in the films. These incomplete layers, he thought, would affect the flow properties, which are essentially co-operative, by locally reducing below the calculated value the number of nearest neighbours in the outer layers. This discrepancy would not affect the specific-heat transition which is averaged over the entire film.

Another empirical theory of the transition temperature, based on the theories of film formation developed by Schiff (70), Atkins (71), Franchetti (72), and Matsuda and van den Meijdenberg (73), was proposed by Franchetti and Mazza (74). The interaction of helium films with the surface was first thought to be van der Waals (e.g. 70).

Later writers extended this theory to include zero-point energy (e.g. 71, 72, 73). From these theories Franchetti concluded that the helium film could be divided into three segments starting from the wall: a solid layer, a hampered layer unable to enter the superfluid state, and a liquid layer close to the bulk density. He calculated the fraction of the liquid in the hampered layer, θ , for thin films and pores. From experimental evidence he found

$$1 - \theta \sim (T/T_\lambda)^{5.6}$$

T being the transition temperature in the film, T_λ the bulk transition temperature. The agreement was moderately good at higher coverages but the theory was semi-empirical.

Ginzburg and Pitaevski (75) developed a theory, which they applied to the helium film, similar to the Landau-Ginzburg theory for superconductors. With the boundary conditions such that ^{the density of} the superfluid component would be zero at the wall of the solid and the surface of the film, they found that the transition would vanish at a critical thickness. Below this thickness a non-zero superfluid component could not satisfy the boundary conditions. In this model the transition temperature in the films was below that of the bulk liquid at P_0 . The nature of their approximations made it almost impossible to obtain any

comparison with experiment; however the Landau-Ginzburg theory^{*} with the extension derived by Douglass (77), predicted quite accurately the thickness at which the energy gap in a superconducting film became zero. It also implied that the transition temperature would increase with decreasing thickness in the film if the critical field of the film were larger than that of the bulk superconductors. This has been observed experimentally (10). Thus these theories cannot be completely ignored.

At the moment then there are no reliable theories available to predict the lambda-transition for a particular situation. The assumption has been made by many authors that the first layer is solid; however the impetuses for this assumption were the anomalously high v_m given by the BET isotherm, the lowering of the lambda transition with decreasing film thickness, and the fact that Frederikse (57) did not observe a transition in helium films approximately three BET layers thick. Since the transition occurs at a lower temperature, is broader, and contributes a smaller amount to the total heat capacity as the thickness of the film decreases, the fact that a transition was not observed is not surprising.

* for a review see (76).

Mastrangelo (58) compared the lowering of the transition in films with the lowering of the λ transition in the liquid under pressure; however the phase transitions observed in adsorbed nitrogen (61) and argon (60) would have been above the bulk melting temperature if these films had corresponded to the bulk substance under pressure. This invalidated Mastrangelo's analogy. Apparently using the results of the BET model for confirmation, several authors (eg. 71) have calculated a density for the first layer equivalent to the solid density. To do this they introduced an effective pressure caused by the Van der Waals interaction of helium with the solid surface. However the BET theory assumed that only the first adsorbed layer interacted with adsorbent; thus the two theories were contradictory and should not be compared.

The BET isotherm (29, p. 159) cannot be taken seriously in the case of helium. To calculate the isotherm several approximations were made: the atoms were assumed to be adsorbed on fixed sites with no lateral interaction and no interaction of the adsorbate with the adsorbent above the first layer. In addition, classical statistics were used. In the case of helium at four degrees, it is very doubtful that any of these approximations hold. Since the wavelength of the free atom is approximately eight angstroms, the atom

cannot be localized and quantum statistics are probably necessary. From the anomalous results for helium given by this isotherm neither of the other assumptions hold.

Experimental calculations of the density of the film are difficult to evaluate. Unless there is a known confining volume in which the film is held, the accuracy of the method of assigning atoms to layers in the helium film can be questioned. Calculations of film thickness, especially for thin films are dominated by the model of adsorption used. Even if the layer assignment is correct there is no reason for assuming that the density-phase relation which exists in bulk helium is the same in adsorbed helium.

Although the assumption that there is a solid layer is implicit in most theories of the transition temperature, Franchetti (74) and Hecht (69) are the only ones whose theories of the transition temperature depend explicitly on this assumption. Ginzburg and Pitaevski (75) postulated a liquid-helium-I layer at the surface of the solid. Experimental evidence in favour of this picture has been observed by Manchester (8, 9) and Buckley (8) who found oscillations in their films which indicated superfluid transitions in films a little more than a layer thick.

The zeolite cavity, as will be shown later, can contain only about four "layers" of helium across the diameter of its large cavity if adsorption in such a small volume can be considered a layer process. Thus if the first layer be a solid, no transition should be seen in the system. The lack of a transition does not necessarily mean that the first layer is a solid; the smallness of the cavities could inhibit the formation of the superfluid phase in liquid helium. Unfortunately the experiments reported here were not detailed enough to draw any conclusions about the existence of a transition in helium adsorbed in the zeolite cavities.

Chapter 2. THE ADSORPTION APPARATUS

The adsorption apparatus, shown in Figures 4 and 5, was very similar to many others used for the same purpose. Basically it consisted of a calibrated volume with manometers, a sample chamber, a gas-storage flask connected to a charcoal trap used to clean the gas; a mercury-diffusion pump capable of attaining pressures of about 10^{-7} millimeters of mercury, and a high-speed, mechanical backing-pump. To protect the manometers from contamination by gases liberated by rubber pumping tubes, a flexible, metal hose was used instead of a rubber tube. To eliminate vibration this was strapped to two cement-filled, metal bars mounted as saw-horses.

The oil manometer was positioned so that it could be used to measure pressure differentials. That is the pressure of a charge of gas admitted to the calibrated volumes was measured on the mercury manometer if the pressure was above six centimeters of mercury. By closing stopcock E before the sample chamber was opened, it was possible to measure the change in pressure caused by gas adsorption on the oil manometer. The change in pressure was known almost as accurately as the initial pressure. This meant that the major limitation on the accuracy of the system

Figure 4

Schematic Diagram of Adsorption Apparatus
(not in proportion)

A	mercury manometer
B	cold trap
C	line to fore-pump
D	oil manometer
E	stopcock to isolate oil-manometer arms
F	line to diffusion pump
G	three calibrated volumes for gas-adsorption measurements
K	mercury-calibrated volume
H	to sample chamber
J	2000 ml. gas-storage flask
L	charcoal trap for cleaning gas used in adsorption
M	sample chamber
N	manometer tube
O	Styrafoam ring
P	dewar cap
Q	Helium-transfer-and-recovery assembly
R	syphon guide
S	support rods

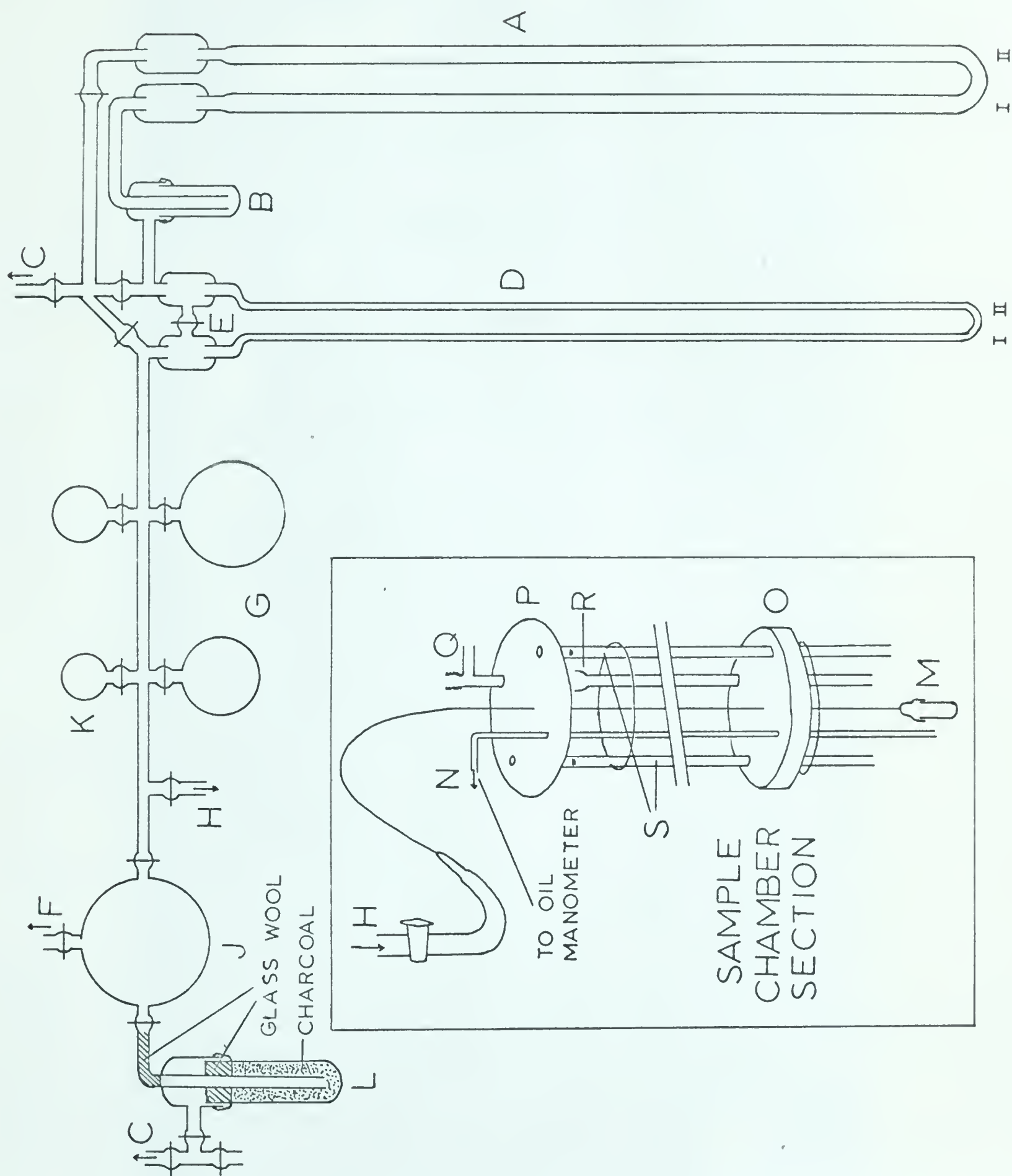
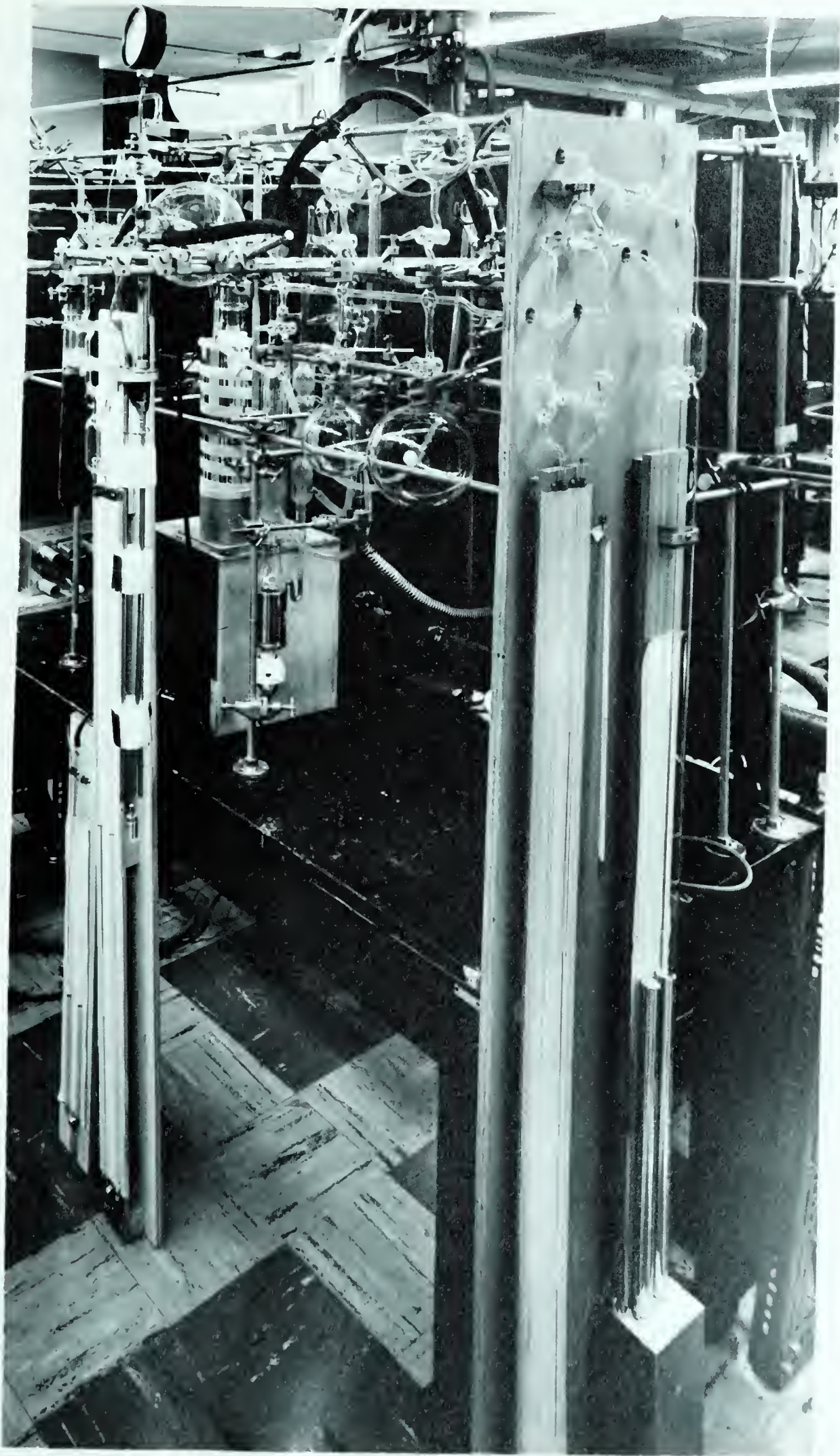


Figure 5

Photograph of Adsorption Apparatus





was temperature fluctuations as the calibrated volumes were not mounted in a constant temperature bath. For this reason most corrections less than one per cent were neglected.

The adsorption apparatus was used in four ways: firstly, to calibrate the apparatus with helium gas; secondly, to do a trial run in which an isotherm of nitrogen on titanium dioxide (anatase) at liquid-nitrogen temperatures was measured; thirdly, to measure helium isotherms on 13X-zeolite; and fourthly, to load the bomb-type calorimeter (see Chapter 5). Each type of experiment required slight modifications to the apparatus. Except for the modifications for the trial run, these will be described after the basic part of the apparatus has been discussed.

The Manometers

The oil manometer was made from two four-foot lengths of two-millimeter, precision-bore tubing. The radius of the arm nearest the calibrated volumes was checked by measuring with a travelling microscope the length of a short column of mercury in the tube and then weighing the mercury. To three figures the average radius of the tube was 1.00 millimeters. The manometer fluid was Apiezon B, the density of a sample from the same bottle having been measured roughly. The results are quoted in Appendix I.

The mercury manometer first used was made from five-millimeter-bore tubing. Before the adsorption runs on zeolites, this was replaced by a two-centimeter-precision-bore manometer, the internal diameter of which was specified by the manufacturer as .8659 inch (2.100 cm.^{*}). The manufacturer's values of the bores on both these manometers were accepted as the corrections caused by them were second order. The mechanical pump was used to provide the reference pressure.

The Calibrated Volumes

The volume of the 100 ml. flask, K, was found by doing a mercury volume determination at a known temperature. After the flask had been cleaned and weighed, it was almost filled with mercury. To remove the air bubbles in the mercury, the flask was pumped out by a fore-pump until no bubbles were visible. The mercury level was then adjusted until the stopcock bore was completely full. The stopcock was then closed, the excess mercury removed, and the mercury flask weighed on a triple-beam balance calibrated to 0.1 gram. This was done twice. The density of the mercury was obtained from reference (78). The results, being 94.785 c.c. and 94.780 c.c., were much better than expected. The buoyancy correction of about 0.006 c.c. was neglected

* i.d. tolerance \pm 0.0002 inches (Wilmad Glass Co.)

THE UNIVERSITY OF CHICAGO PRESS

THE UNIVERSITY OF CHICAGO PRESS
530 N. Dearborn Avenue
Chicago, Illinois 60610-5708
U.S.A.
Telephone: (773) 837-3000
Fax: (773) 837-0861
Internet: <http://www.uchicago.edu>
E-mail: orderdept@uchicago.edu
The University of Chicago Press is a not-for-profit organization.
All profits are used to support the Press's publishing program.
The Press is an equal opportunity institution.
All rights reserved. No part of this publication may be reproduced, stored in a retrieval system, or transmitted, in any form or by any means, electronic, mechanical, photocopying, recording, or by any information storage and retrieval system, without permission in writing from the University of Chicago Press.

THE UNIVERSITY OF CHICAGO PRESS
530 N. Dearborn Avenue
Chicago, Illinois 60610-5708
U.S.A.
Telephone: (773) 837-3000
Fax: (773) 837-0861
Internet: <http://www.uchicago.edu>
E-mail: orderdept@uchicago.edu
The University of Chicago Press is a not-for-profit organization.
All profits are used to support the Press's publishing program.
The Press is an equal opportunity institution.
All rights reserved. No part of this publication may be reproduced, stored in a retrieval system, or transmitted, in any form or by any means, electronic, mechanical, photocopying, recording, or by any information storage and retrieval system, without permission in writing from the University of Chicago Press.

THE UNIVERSITY OF CHICAGO PRESS

as the scale seemed only sensitive to 0.2 gram at the weights being used. The lack of sensitivity meant a 0.4 gram error in weight or a 0.03 c.c. error in volume would not be unlikely. Thus 94.78 ± 0.01 c.c was the accepted volume.

The volumes of the other three flasks, nominally 250, 500, and 1000 c.c., in the calibrated volume; the glass tubing from the flask J to the stopcock E; and the tubing between arm II of the oil manometer and arm I of the mercury manometer were measured by gas-expansion methods using the known volume, K . These methods will be described in the next chapter when the procedure for using the apparatus is developed.

Again the results were much more consistent than could be expected. The measurement for each section was repeated not less than three times and the results with standard deviations are given in Table 1 with the results for the known volume.

The Dewar System

Since the isotherms of helium adsorbed on zeolite were to be done at liquid-helium temperatures, a suitable dewar system had to be devised. The helium dewar had a 2 1/2 inch inner diameter. It was a glass dewar with slits in the silvering to permit observation of the helium level.

TABLE 1

ADSORPTION VOLUMES

Volume Name	Volume (c.c.)
gas line (tubing E to J)	68.73 \pm 0.16
250 ml.*	354.40 \pm 0.12
500 ml.*	564.05 \pm 1.82
1000 ml.*	1132.90 \pm 0.54
manometer volume* (5 mm. bore)	289.26 \pm 0.49
manometer volume (5 mm. bore)	220.56 \pm 0.52
manometer volume* (2 cm. bore)	519.86 \pm 0.44
manometer volume (2 cm. bore)	451.13 \pm 0.46
known volume	94.78 \pm 0.01

* including gas-line volume

THE
JOURNAL OF THE
ROYAL ANTHROPOLOGICAL INSTITUTE

CONTENTS	PAGES
THE ANTHROPOLOGY OF THE FUTURE	1
THE ANTHROPOLOGY OF THE PAST	10
THE ANTHROPOLOGY OF THE PRESENT	20
THE ANTHROPOLOGY OF THE FUTURE	30
THE ANTHROPOLOGY OF THE PAST	40
THE ANTHROPOLOGY OF THE PRESENT	50
THE ANTHROPOLOGY OF THE FUTURE	60
THE ANTHROPOLOGY OF THE PAST	70
THE ANTHROPOLOGY OF THE PRESENT	80
THE ANTHROPOLOGY OF THE FUTURE	90
THE ANTHROPOLOGY OF THE PAST	100
THE ANTHROPOLOGY OF THE PRESENT	110
THE ANTHROPOLOGY OF THE FUTURE	120
THE ANTHROPOLOGY OF THE PAST	130
THE ANTHROPOLOGY OF THE PRESENT	140
THE ANTHROPOLOGY OF THE FUTURE	150
THE ANTHROPOLOGY OF THE PAST	160
THE ANTHROPOLOGY OF THE PRESENT	170
THE ANTHROPOLOGY OF THE FUTURE	180
THE ANTHROPOLOGY OF THE PAST	190
THE ANTHROPOLOGY OF THE PRESENT	200
THE ANTHROPOLOGY OF THE FUTURE	210
THE ANTHROPOLOGY OF THE PAST	220
THE ANTHROPOLOGY OF THE PRESENT	230
THE ANTHROPOLOGY OF THE FUTURE	240
THE ANTHROPOLOGY OF THE PAST	250
THE ANTHROPOLOGY OF THE PRESENT	260
THE ANTHROPOLOGY OF THE FUTURE	270
THE ANTHROPOLOGY OF THE PAST	280
THE ANTHROPOLOGY OF THE PRESENT	290
THE ANTHROPOLOGY OF THE FUTURE	300

So that the temperature of the helium bath could be lowered by reducing the vapour pressure, the dewar was fitted with a copper-glass seal, that had a brass collar which in turn could be connected to a brass dewar cap by a Wood's metal seal. The entire length of the dewar and seal was about 26 inches.

The pumping tube for the sample chamber and the manometer tube to measure the bath temperature were anchored to the dewar cap. In addition two quarter-inch, inconel tubes acted as supports for three styrafoam rings, spaced along the rods to reduce radiation effects. Slits were cut near the top of the tubes to prevent oscillations from forming in a standing column of gas. The cap was also fitted with a standard helium-transfer-and-recovery assembly. This also provided the pumping tube for lowering the bath temperature. The recovery line was modified so that a high-speed, mechanical pump, fitted with a needle valve, could be connected for this purpose.

The manometer tube, an eighth-inch, inconel tube with its open end level with the sample chamber, was attached to an oil manometer. Since the isotherms were measured at approximately four degrees and two degrees, the oil manometer read the difference between atmospheric and bath pressure for the former and the bath pressure

1. The first part of the paper discusses the importance of the study and the objectives of the research. It also provides a brief overview of the literature review and the methodology used in the study.

2. The second part of the paper presents the results of the study. It includes a detailed analysis of the data collected and the findings of the research. The results are presented in a clear and concise manner, with appropriate use of tables and figures to illustrate the data.

3. The third part of the paper discusses the conclusions of the study and the implications of the findings. It also provides a summary of the key points of the research and a final conclusion. The paper is written in a professional and academic style, with a focus on clarity and accuracy.

directly for the latter. In the first case atmospheric pressure was measured on a Fortin barometer. In the other a mechanical pump provided the reference pressure.

The pumping tube for the sample chamber was one meter of one-millimeter, inconel tubing. It was connected to the adsorption apparatus by an eighth-inch, kovar seal and a brass ferrule. The sample chamber hung from the bottom of this tube. (Figure 4)

When the calorimeter was being loaded, the brass, dewar cap and its attachments were replaced by a wooden cap that was taped to the dewar. The cap had a slit in it for the pumping tube instead of a hole. Thus the tube could be slid out of the cap sideways instead of being drawn out of it. This made it possible to seal the calorimeter while it was still at helium temperatures. The procedure will be discussed in Chapter 6.

If the apparatus was set up for an adsorption run, a large glass dewar with viewing slits surrounded the helium dewar so that the latter could be completely immersed in liquid air. If the liquid-air level was maintained, the helium dewar could usually go about eighteen hours without being re-filled. With the bath at two degrees, the dewar would need refilling after about five or six hours.

Powder Samples and Sample Containers

The powder used for the experiments was 13X-zeolite powder produced commercially by Linde Gases Division of Union Carbide. Samples used in the adsorption and heat-capacity experiments were heated to a maximum of between 250 and 260°C* until the pressure was 2×10^{-7} mm. of mercury as read on a Martin gauge. This took between one and two weeks as the temperature was increased so that the pressure did not exceed 10^{-4} mm. of mercury during the heating. The heater was a small wire-wound, asbestos-insulated tube which fitted around the sample holder. The temperature was measured by a copper-constantan thermocouple placed between the heater and the sample holder. The calibration given in reference (78) was used.

The sample chamber for the first isotherm consisted of a small glass container with a kovar-glass seal. The volume of the container, found by a mercury determination, was 6.77 ± 0.01 c.c. After the sample had been weighed, the chamber, containing the sample, was soldered to the one-millimeter inconel tubing. The powder was dehydrated in situ and the adsorption isotherm was carried out without removing the powder from the vacuum system. The isotherm done at two degrees and the first four-degree isotherm were done on this sample. A later isotherm was done

* No irreversibility in the water isotherms was observed in this temperature region (Barrer and Bratt (19)).

THE HISTORY OF THE

The history of the world is a vast and complex subject, encompassing the lives of countless individuals and the events that have shaped our planet. From the dawn of time to the present day, the human story is one of constant change and evolution. The early years of our species are marked by a struggle for survival, as our ancestors sought to adapt to their environments and overcome the challenges of a harsh world. Over time, however, the human mind began to develop, and with it, the capacity for reason and imagination. This led to the creation of art, the development of language, and the establishment of societies and civilizations. The history of the world is a testament to the resilience and ingenuity of the human race, as we have overcome countless obstacles and achieved remarkable feats of achievement. The story of the world is a story of hope and possibility, a story that continues to unfold before our eyes.

The history of the world is a vast and complex subject, encompassing the lives of countless individuals and the events that have shaped our planet. From the dawn of time to the present day, the human story is one of constant change and evolution. The early years of our species are marked by a struggle for survival, as our ancestors sought to adapt to their environments and overcome the challenges of a harsh world. Over time, however, the human mind began to develop, and with it, the capacity for reason and imagination. This led to the creation of art, the development of language, and the establishment of societies and civilizations. The history of the world is a testament to the resilience and ingenuity of the human race, as we have overcome countless obstacles and achieved remarkable feats of achievement. The story of the world is a story of hope and possibility, a story that continues to unfold before our eyes.

using a brass sample chamber with a volume of 1.70 ± 0.03 c.c. Because the solder joint connecting the lid of the chamber with the bottom was a soft-solder one, the powder was dehydrated and then transferred to the sample chamber. How much the crystal re-hydrated during this time is not known. A similar procedure was followed when the sample was prepared for the calorimetric measurements. A kovar-glass seal and a ground-glass joint, each with an isolating stopcock, were "teed" into the high-vacuum side of the diffusion pump outside the calibrated area so that this section of the apparatus would be undisturbed when samples were being dehydrated.

The manometers were read with a Gaertner cathetometer* capable of being read to .005 cm. Except for the helium gas used in the last adsorption run, the helium was obtained from the Air Reduction Corporation. The nitrogen and other helium gas was purchased from Canadian Liquid Air. Before being admitted to the storage flask, J, (Fig. 4) the gas was cleaned in a charcoal trap immersed in liquid air.

*

The Department of Metallurgy kindly lent the Physics Department the cathetometer for these experiments.

Chapter 3. OPERATION OF THE ADSORPTION APPARATUS

The procedure and the method of calculating the results are so closely related that they are most easily discussed together. After a brief discussion of some corrections, the rest of the chapter will be devoted to this.

Rough calculations showed that gas expanding adiabatically into the Pyrex glass adsorption system could take approximately half an hour to attain thermal equilibrium if the expansion cooled the glass substantially. This was very conservative but pressure readings were never taken until at least half an hour had elapsed after the admission of a gas charge. Similar calculations showed, using the data of Rogers et. al. (79), that less than 0.3 c. c. of helium under standard temperature and pressure conditions would diffuse through the glass in a day. Since most of the points were taken in about eight hours, this correction was ignored. No correction could be applied for the gas being adsorbed by the oil in the manometer because no conclusive evidence could be obtained as to the amount being significant. In addition no corrections were made for capillary depression or, in the case of the two-centimeter-diameter, mercury manometer and the oil

THE HISTORY OF THE UNITED STATES

The history of the United States is a story of growth and change. It begins with the first people who lived on this land, and continues through the years of exploration, settlement, and the struggle for independence. The story is one of a people who have built a nation of freedom and opportunity, and who have played a leading role in the world.

The early years of the United States were marked by the struggle for independence from Great Britain. The American Revolution was a fight for the right of self-government, and it was a fight that was won. The United States was born, and it has since then grown into a great nation.

The story of the United States is a story of progress and achievement. It is a story of a people who have built a nation of freedom and opportunity, and who have played a leading role in the world. The story is one of a people who have overcome many challenges and who have achieved many great things.

The history of the United States is a story of growth and change. It is a story of a people who have built a nation of freedom and opportunity, and who have played a leading role in the world. The story is one of a people who have overcome many challenges and who have achieved many great things.

manometer, any consistent inequality in the zero level of the manometers. A correction of -0.025 cm. was applied to the five-millimeter-bore mercury manometer. As already mentioned the calibrated volumes and manometers were not in a constant-temperature bath; this was probably the biggest single source of error in the experiment. For this reason an uncalibrated, mercury thermometer, graduated to 0.1°C , was thought sufficient to measure the temperature of the manometers.

Calibration of the Apparatus

To obtain the pressure change in the manometer volume caused by the shift in the oil level, the manometer volume had to be measured. This was the volume between the null level of the oil in arm II of the oil manometer and the mercury level in arm I of the mercury manometer. For measurement purposes the null level of the mercury manometer was taken as the mercury level; the additional volume caused by the change in mercury level during pressure measurements, was added to the basic value. The manometer volume was found by measuring the manometer volume and the gas-line volume, the volume of the tubing from E to J (Fig. 4), together and then the gas-line volume alone. From this the manometer volume could be calculated.

TABLE 2

DEFINITION OF SYMBOLS USED IN CALCULATION
OF MEASUREMENTS ON ADSORPTION APPARATUS

Symbol	Definition
V_k	known volume--mercury calibrated volume
V_g	gas-line volume--the tubing from J to E (fig. 4)
V_m	manometer volume
V_s	volume of any other section to be calibrated
V_c	calibrated volume
V_a, V_d	volume in the sample chamber (S.T.P.)
ΔV_m	change in volume caused by shift in mercury-level in manometer
ΔV	change in volume caused by shift in oil-level in manometer
P_1	initial pressure
P_o	pressure read on the oil manometer
ΔP	$\Delta V P_1 / (V_m + \Delta V_m)$ pressure change in manometer volume caused by shift in oil level--applicable only when oil manometer and mercury manometer are being used together.
P_d	$P_o + \Delta P$ --when both manometers are in use $P_1 - P_2$ --when one manometer is in use
P_2	final pressure in calibrated section of the system, $P_1 - P_d$ when both manometers are being used. ($P_1 + P_d$ during the desorption run.)

- Note: 1) All quantities are defined so that they are positive.
2) Pressure is quoted in g./cm.² The mercury density was obtained from the Chemical Rubber Handbook (78); the oil densities from the measurement reported in Appendix I.

THE
JOURNAL OF THE
ROYAL ANTHROPOLOGICAL INSTITUTE

Page	Page
1	1
2	2
3	3
4	4
5	5
6	6
7	7
8	8
9	9
10	10
11	11
12	12
13	13
14	14
15	15
16	16
17	17
18	18
19	19
20	20
21	21
22	22
23	23
24	24
25	25
26	26
27	27
28	28
29	29
30	30
31	31
32	32
33	33
34	34
35	35
36	36
37	37
38	38
39	39
40	40
41	41
42	42
43	43
44	44
45	45
46	46
47	47
48	48
49	49
50	50
51	51
52	52
53	53
54	54
55	55
56	56
57	57
58	58
59	59
60	60
61	61
62	62
63	63
64	64
65	65
66	66
67	67
68	68
69	69
70	70
71	71
72	72
73	73
74	74
75	75
76	76
77	77
78	78
79	79
80	80
81	81
82	82
83	83
84	84
85	85
86	86
87	87
88	88
89	89
90	90
91	91
92	92
93	93
94	94
95	95
96	96
97	97
98	98
99	99
100	100

The manometer and gas-line volumes were measured together using the mercury manometer alone. One volume correction had to be applied: the change in volume ΔV_m caused by the change in pressure from essentially zero to P_2 . Helium gas at pressure P_1 in volume, V_k , was expanded into $V_m + V_g$ which had been evacuated. Thus

$$V_m + V_g = \frac{(P_1 - P_2)}{P_2} V_k - \Delta V_m \quad (1)$$

The gas-line and other volumes were calibrated by evacuating V_k , admitting helium gas to the section to be calibrated, measuring the gas pressure on the mercury manometer, isolating the oil-manometer arms, and expanding the gas into the known volume. Including the changes in volume caused by shifts in the manometer levels, the formula to calculate $V_s + V_g$ was

$$V_s + V_g = \frac{P_2}{P_d} (V_k - \Delta V) \quad (2)$$

With V_s zero in equation (2), equations (1) and (2) could be used to calculate V_m and V_g in about two successive approximations. The first time this was done the five-millimeter-bore manometer was in the system. When the two-centimeter-bore manometer replaced it, the gas-line

volume was already known. Once V_m was known all the other volumes could be calculated in a straight-forward manner.

Adsorption Isotherms

The helium isotherm required a slightly different procedure. A few general remarks will be made before the equations used to interpret the data are calculated.

Because mercury vapour is trapped in cold spots, when the sample was in the system, care was taken never to expose it to the mercury manometer. When the sample was being pumped, a liquid-air trap separated the sample from the mercury manometer. During an experiment the stopcock at E always isolated the sample from the manometer when the stopcock to the sample chamber was open.

After the sample had been dehydrated, if it had not been prepared in situ, it was sealed into the sample chamber and connected to the adsorption apparatus as described in Chapter 2. In this case the sample was then evacuated for one day at room temperature. This was also done between adsorption runs*. The inner dewar was then soldered into position; and, after the system had been pre-cooled by pouring a little liquid air into the helium dewar, the inner dewar was immersed in liquid air and helium was transferred.

* This was insufficient to remove all the helium (Fig. 9)

The criterion for equilibrium in an adsorption point was a little difficult to state. Each point took about eight hours to obtain so that only two or three points were taken per day. Unless the points were taken in the morning after a gas charge had been left to adsorb overnight, the measurement was taken twice, one hour apart. If the reading was substantially unchanged or if there were signs of desorption on an adsorption point, the second reading terminated the point. The overnight points were often terminated with only one reading. The time that the oil manometer took to reach equilibrium was not insignificant as the oil tended to wet the walls when it was displaced.

Slight differences in procedure occurred for the different isotherms. During the first four-degree one, the helium level was adjusted to a set level by boiling the excess off, a hundred-watt bulb shining through the slit being the heat source. In the second and last four-degree isotherm, the helium level was not adjusted in any way before a point was taken and liquid air was not added within a half hour of taking a measurement. These precautions were necessary because of the apparent desorption at the high-pressure end of the first isotherm (Appendix III, Fig. 7). During the last run, observations showed that the height of the helium on the millimeter tubing to the sample chamber,

caused significant differences in the amount of gas contained in the sample chamber at high pressures.

Since the time that the dewar could be maintained at two degrees was limited; an initial equilibrium was obtained at four degrees, at the low pressure end of the isotherm, and then the bath pressure was lowered. This reduced the time required at the reduced pressure considerably. At higher pressures, the gas had to be adsorbed at two degrees to prevent part of the last gas charge from desorbing at four degrees. The reduced temperature was maintained by controlling the pumping speed by adjusting the needle valve attached to the pump.

The actual points were obtained by admitting a pressure, P_1 , to the calibrated section with the sample chamber isolated. The amount of gas entering the sample chamber was measured on the oil manometer; the sample chamber was then isolated and a fresh charge of gas was put in. At the end of each point the pressure in the bath at the level of the sample chamber was measured, the calibrated volumes used noted, and the helium level measured in all but the first run.

When the combined oil and mercury manometers were used, the standard-temperature-and-pressure volume of gas in the adsorption chamber, V_{ai} , after the i^{th} point

on the isotherm could be calculated from

$$V_{ai} = \frac{\sum_{j=1}^i (P_{dj}(V_{cj}) + P_{2j}\Delta V_j)}{1033.258} \frac{273.15}{T_r(^{\circ}\text{K})},$$

T_r being the room temperature and 1033.258, standard pressure in grams per square centimeter. The other symbols were defined in Table 2. When the oil manometer alone was used, ΔV_j was added to the calibrated volume V_{cj} to allow for the increased volume caused by the displacement of the oil manometer when it was reading P_{o2j} . The term, $\Delta V_j' P_{o1j}$, allowed for the volume available when the manometer was reading P_{o1j} , but not when it was reading P_{o2j} . Thus when the oil manometer was used, the equation was

$$V_{ai} = \frac{\sum_{j=1}^i (P_{dj}(V_{cj} + \Delta V_j) + P_{o1j} \Delta V_j')}{1033.258} \frac{273.15}{T_r(^{\circ}\text{K})}.$$

During the desorption isotherm, the volume left in the adsorption chamber, V_{di} , after the i^{th} desorption point could be obtained by subtracting the same terms from the total amount adsorbed if all quantities were defined as being positive. Thus if the combined manometers were being used,

$$V_{di} = V_{a_{tot}} - \frac{\sum_{j=1}^i (P_{dj} V_{cj} + P_{2j} \Delta V_j)}{1033.258} \frac{273.15}{T_r(^{\circ}\text{K})} .$$

If the oil manometer alone was used on a desorption point, i , the term,

$$\frac{(P_{di}(V_{ci} + \Delta V_i) + P_{o2i} \Delta V_i)}{1033.258} \frac{273.15}{T_r(^{\circ}\text{K})} ,$$

was subtracted. In this ΔV_i was added to the calibrated volume to allow for the displacement of the oil manometer when it was reading P_{oli} . Similarly $\Delta V_i P_{o2i}$ allowed for the volume available when the manometer was reading P_{o2i} but not when it was reading P_{oli} . Schematic diagrams showing some of the pressure measurements are contained in Appendix VI.

Certain variations existed in applying the correction terms. On the first four-degree isotherm and the two-degree one the temperature, T_r , was the temperature actually measured on the thermometer at the time the point was terminated; however, this was not really justified and on the last four-degree one T_r was chosen as 20.5°C which was the mean room temperature to the nearest half degree. On the first four-degree one the total displacement of the oil

manometer was halved to obtain the corrections ΔV and ΔP ; however, on the second one the null height was measured for each point and the corrections were obtained from the displacement in each arm. On the last isotherm no attempt was made to allow for the small changes in height in the mercury manometer caused by the movement of the oil manometer; this was allowed for on the first isotherm. Since the changes in room temperature caused small changes in the mercury level which were just at the limit of the cathetometers* resolution, experimental attempts to allow for the change in mercury level actually increased the error and made the use of the oil manometer meaningless. For this reason the changes in the mercury level were ignored. All these variations were smaller than the one per cent error allowed.

A discussion of the dead space corrections and accuracy of the system will be deferred to the next chapter as they are not directly associated with the operation of the apparatus.

The first part of the paper is devoted to a general discussion of the problem of the existence of solutions of the system of equations (1) for arbitrary values of the parameters α and β . It is shown that the system (1) has solutions for arbitrary values of the parameters α and β if and only if the conditions (2) are satisfied. The second part of the paper is devoted to a detailed study of the properties of the solutions of the system (1) for arbitrary values of the parameters α and β . It is shown that the solutions of the system (1) are unique and depend continuously on the parameters α and β . The third part of the paper is devoted to a study of the asymptotic properties of the solutions of the system (1) for large values of the parameters α and β . It is shown that the solutions of the system (1) approach a certain limit as the parameters α and β approach infinity.

The author wishes to express his sincere thanks to the members of the Institute of Mathematics of the Academy of Sciences of the USSR for their interest in the work and for the facilities provided for the research.

Chapter 4. RESULTS OF THE ADSORPTION EXPERIMENTS

To check the method and the apparatus, a trial run at liquid-nitrogen temperatures was done using standard anatase (80) (i.e. anatase form of TiO_2) prepared by the late W. D. Harkins^{*}. The apparatus was modified slightly as only a short dewar was required and an all-glass sample chamber could be used. The effective volume of the sample chamber was measured using helium under the assumption that helium was not adsorbed and that virial-coefficient corrections for nitrogen were negligible. The nitrogen isotherm was then done in a similar manner to the helium ones. The results as calculated were in good agreement with the $13.8 \text{ m}^2/\text{g.}$ quoted for this powder (29, p. 220). They were about $13.7 \text{ m}^2/\text{g.}$ if the area of the nitrogen molecule was 16.2 square angstroms. The calculation was done before the error^{**} in the oil density was discovered. Since the results were of no further interest, they have never been recalculated.

Dead Space Corrections

Since the dead space could not be measured with the

* The Chemistry Department of the University of Chicago very kindly sent me a sample.

** (Appendix I) The error was approximately two per cent.

THE HISTORY OF THE UNITED STATES

OF THE UNITED STATES OF AMERICA

FROM THE FIRST SETTLEMENTS TO THE PRESENT TIME

BY JAMES M. SMITH

NEW YORK: PUBLISHED BY J. B. LIPPINCOTT & CO.

1850

THE HISTORY OF THE UNITED STATES

OF THE UNITED STATES OF AMERICA

FROM THE FIRST SETTLEMENTS TO THE PRESENT TIME

BY JAMES M. SMITH

NEW YORK: PUBLISHED BY J. B. LIPPINCOTT & CO.

1850

THE HISTORY OF THE UNITED STATES

OF THE UNITED STATES OF AMERICA

FROM THE FIRST SETTLEMENTS TO THE PRESENT TIME

BY JAMES M. SMITH

NEW YORK: PUBLISHED BY J. B. LIPPINCOTT & CO.

1850

THE HISTORY OF THE UNITED STATES

OF THE UNITED STATES OF AMERICA

FROM THE FIRST SETTLEMENTS TO THE PRESENT TIME

BY JAMES M. SMITH

NEW YORK: PUBLISHED BY J. B. LIPPINCOTT & CO.

1850

THE HISTORY OF THE UNITED STATES

OF THE UNITED STATES OF AMERICA

FROM THE FIRST SETTLEMENTS TO THE PRESENT TIME

BY JAMES M. SMITH

zeolite powder in the chamber and an attempt to measure the effective volume of the empty chamber proved useless because of the large scatter in the volumes obtained, the dead-space corrections were made from the known volume of the sample chamber at room temperature, the volume of the tubing at four degrees, and the volume occupied by the powder. The one-millimeter tube was assumed to be at room temperature except for the length in liquid helium. The volume of the dead space in the sample-chamber section with the empty glass sample chamber was measured at room temperature. Once the volume of the sample chamber, itself, had been subtracted the volume was 10.45 ± 0.1 c.c. An extra 0.14 c.c. was added to partially compensate for the increased volume of gas in the tube below room temperature. When the kovar seal in this section broke, it was replaced without recalibrating the apparatus as the error introduced would be negligible compared to the other errors present.

The volume at four degrees or two degrees was calculated in three different ways. Basically the number of moles, n , present in the unoccupied volume, had to be found and converted to standard-temperature and pressure-cubic centimeters. The perfect gas law, the inverse-volume-virial-coefficient expansion, and the pressure-virial-coefficient expansion were used. Since the experimental

results of Keller (81) showed that only the second virial coefficient was important, the equations were the following:

$$n = PV/RT \quad (A)$$

$$n = (-1 + (1 + 4PB/RT)^{\frac{1}{2}})V/2B \quad (B)$$

$$n = PV/(RT + BP - (BP)^2/RT + 2(BP)^3/(RT)^2) \quad (C)$$

The denominator of the last expansion was an infinite series. Except for pressures close to one atmosphere this expansion was sufficient. For calculations involving pressures near atmospheric higher-order virial coefficients should also be included in this expansion. Since this information was lacking, the expansion was terminated after the fourth term. The virial coefficients, B, actually used in the calculations were the theoretical ones of Kilpatrick et al. (82). The temperature, T, was obtained from the bath pressure with the aid of the NBS tables (83) of the 1958-helium-four-temperature scale. The pressure, P, was known from the adsorption isotherm. When it was necessary, the thermomolecular corrections to pressures, as calculated by Roberts and Sydoriak (84), were applied. The volume, V, was obtained from the room-temperature volume of the sample chamber. The amount of gas contained in the part of the sample chamber section at room temperature was calculated from

1870
The first of the year was a very dry one
and the crops were much injured by the
drought. The wheat was particularly
suffered and the yield was very small.
The corn was also much injured and
the yield was very small.

The second of the year was a very wet one
and the crops were much injured by the
floods. The wheat was particularly
suffered and the yield was very small.
The corn was also much injured and
the yield was very small.

The third of the year was a very dry one
and the crops were much injured by the
drought. The wheat was particularly
suffered and the yield was very small.
The corn was also much injured and
the yield was very small.

The fourth of the year was a very wet one
and the crops were much injured by the
floods. The wheat was particularly
suffered and the yield was very small.
The corn was also much injured and
the yield was very small.

The fifth of the year was a very dry one
and the crops were much injured by the
drought. The wheat was particularly
suffered and the yield was very small.
The corn was also much injured and
the yield was very small.

The sixth of the year was a very wet one
and the crops were much injured by the
floods. The wheat was particularly
suffered and the yield was very small.
The corn was also much injured and
the yield was very small.

The seventh of the year was a very dry one
and the crops were much injured by the
drought. The wheat was particularly
suffered and the yield was very small.
The corn was also much injured and
the yield was very small.

The eighth of the year was a very wet one
and the crops were much injured by the
floods. The wheat was particularly
suffered and the yield was very small.
The corn was also much injured and
the yield was very small.

The ninth of the year was a very dry one
and the crops were much injured by the
drought. The wheat was particularly
suffered and the yield was very small.
The corn was also much injured and
the yield was very small.

The tenth of the year was a very wet one
and the crops were much injured by the
floods. The wheat was particularly
suffered and the yield was very small.
The corn was also much injured and
the yield was very small.

the perfect-gas law and added to the low-temperature contribution.

Errors in the Isotherm

From the formulae in Chapter 3, it was obvious that any errors in the amount of gas in the sample-chamber section were accumulative. This has made it very difficult to estimate the error. In addition the temperature was not really constant as it varied by 0.1° on the four-degree isotherms and 0.01° on the two-degree isotherm. Since the graph of the isotherms showing the volume adsorbed against the relative pressure, P/P_0 , was relatively smooth, the effect of the temperature variation may not have been too serious. The saturated-vapour pressure, P_0 , was equated with the bath pressure. The volume of the dead space was probably not known to more than two or three per cent. Since in the first four-degree isotherm the dead-space volume at high pressures was several times the volume of gas adsorbed in the powder, this error could be very serious and probably caused much of the apparent desorption observed in this isotherm. The last four-degree isotherm probably was valid to within from one to ten percent. The lower limit was set by fluctuations in the room temperature.

The first part of the paper is devoted to a discussion of the general principles of the theory of the structure of the atom.

The second part of the paper is devoted to a discussion of the general principles of the theory of the structure of the atom.

The third part of the paper is devoted to a discussion of the general principles of the theory of the structure of the atom.

The fourth part of the paper is devoted to a discussion of the general principles of the theory of the structure of the atom.

The fifth part of the paper is devoted to a discussion of the general principles of the theory of the structure of the atom.

The sixth part of the paper is devoted to a discussion of the general principles of the theory of the structure of the atom.

The seventh part of the paper is devoted to a discussion of the general principles of the theory of the structure of the atom.

The eighth part of the paper is devoted to a discussion of the general principles of the theory of the structure of the atom.

The ninth part of the paper is devoted to a discussion of the general principles of the theory of the structure of the atom.

The tenth part of the paper is devoted to a discussion of the general principles of the theory of the structure of the atom.

The eleventh part of the paper is devoted to a discussion of the general principles of the theory of the structure of the atom.

Density of Zeolite Crystals

To correct the sample-chamber volume for the volume occupied by the sample, it was necessary to calculate the density of the crystals and to determine the extent that they were dehydrated. To measure the latter, samples of 13X zeolite were placed under an inverted beaker which also contained a beaker of distilled water. The samples were weighed each day for several days and the amount of hydration was recorded. This was done before the isotherm and heat-capacity experiments were started and again after their completion. A sample, sample I, taken directly from the storage can gained approximately twenty-five per cent of its hydrated weight in this check. This sample was partially hydrated in air before being placed under the beaker. Another sample, sample II, having been evacuated for a approximately a week and heated to $350^{\circ}\text{C}.$, gained twenty-six per cent of its hydrated weight; however, it adsorbed water more slowly than the first sample probably because some structural damage had been induced by the heating. After the experiments had been completed, two more samples were hydrated. The one, sample III, from the can gained twenty per cent of its hydrated weight. The sample, sample IV, that had been heated to approximately $250^{\circ}\text{C}.$ gained twenty-four per cent of its hydrated weight. This sample was

Figure 6

The Hydration of 13X-zeolite

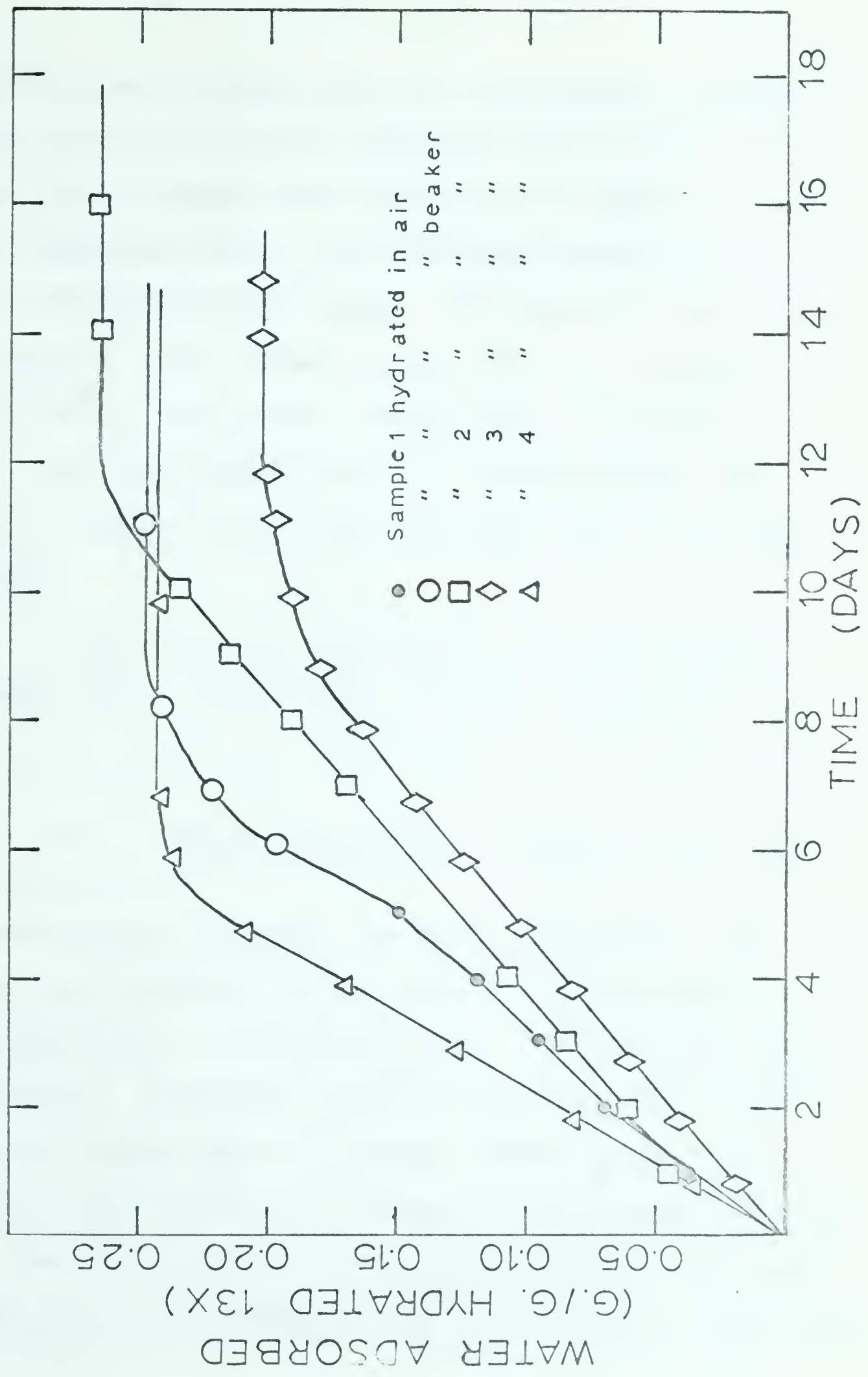
The amount of water adsorbed in grams per gram of hydrated zeolite is plotted against the time taken to hydrate the zeolite. The zero on the time scale is the moment measuring started. Because the amount of water in the 13X-zeolite cavities is not known, only the water adsorbed in these observations is considered, the water adsorbed at zero time being the zero amount.

Sample 1 - sample taken from can before experiments started

Sample 2 - sample dehydrated at 350°C before experiments

Sample 3 - sample taken from can after experiments completed

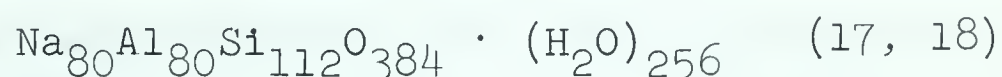
Sample 4 - sample dehydrated at approximately 260°C after experiments.





weighed before heating, sealed to the pumping system in a glass container, heated, and then cut from the system. If the initial weight were assumed to be eighty per cent of the hydrated weight, then the sample gained twenty-five percent of its hydrated weight. The error may have been introduced by glass chips falling into the container when it was cut off the system. These would have been removed with the powder before the empty chamber was weighed. Figure 6 shows the hydration curves for these samples.

The volume of a unit cell was 15,513 cubic angstroms (18). Hence if the chemical formula was given by



the density was 1.93 grams per cubic centimeter. The amount of water was derived from the estimate of the amount contained in a large cavity in reference (13). With this information approximately twenty-six percent of the hydrated crystal's weight was attributable to water. Barrer et al. (13) estimated that twenty-seven percent of the weight was due to this. Two extra molecules per cavity would be sufficient to increase the percentage to the latter level. This would

mean 272 molecules of water per unit cell and a density of 1.95 grams per cubic centimeter. The first density calculated was used to estimate the volume occupied by the powder, which had lost about twenty-five percent of its hydrated weight when weighed.

The Results

The first sample used in the isotherms weighed 0.202 grams and was contained in a chamber with a room-temperature volume of 6.77 cubic centimeters. After allowance had been made for the volume occupied by the powder and the volume of the tube immersed in liquid helium, the volume used in the dead-space calculations was 6.68 cubic centimeters. This sample was used in the first isotherm at four degrees (approximately 4.1°) and the isotherm at two degrees (2.1°).

The second sample used weighed 0.516 grams. The volume of the container was 1.700 cubic centimeters. After the volume of the powder, 0.356 cubic centimeters, the volume of the small piece of copper gauze in the container, 0.020 cubic centimeters, and the volume of the tube immersed in helium, 0.030 cubic centimeters, had been taken into consideration, the calculated volume was 1.368 cubic centimeters. An additional allowance was made if

the helium level was not at the reference mark. This sample was used in the other four-degree isotherm. Figures 7, 8 and 9 show the results graphically. Tables in Appendix III give the results in greater detail.

Constants used in Calculations (85)

Molar Volume 22.42×10^3 c.c.

Avogadros' number 6.025×10^{23} /mole

Gas constant, R, 8.317×10^7 erg/gram-mole- $^{\circ}$ K

THE UNIVERSITY OF CHICAGO
DEPARTMENT OF CHEMISTRY
5408 S. DICKINSON AVE.
CHICAGO, ILL. 60637

RECEIVED
JAN 10 1964
FROM
J. H. HARRIS
100-100000-100000

Figure 7

Helium Adsorption in .202g. 13X-zeolite

The amount of helium, in cubic centimeters (S.T.P.), adsorbed in the .202g. sample is plotted against the relative pressure, P/P_0 . The letters A, B, C refer to different methods of applying the dead-space corrections (Chapter 4, p. 59). When two or more methods agree only one symbol for the point is shown. No attempt has been made to indicate the experimental error in the points.

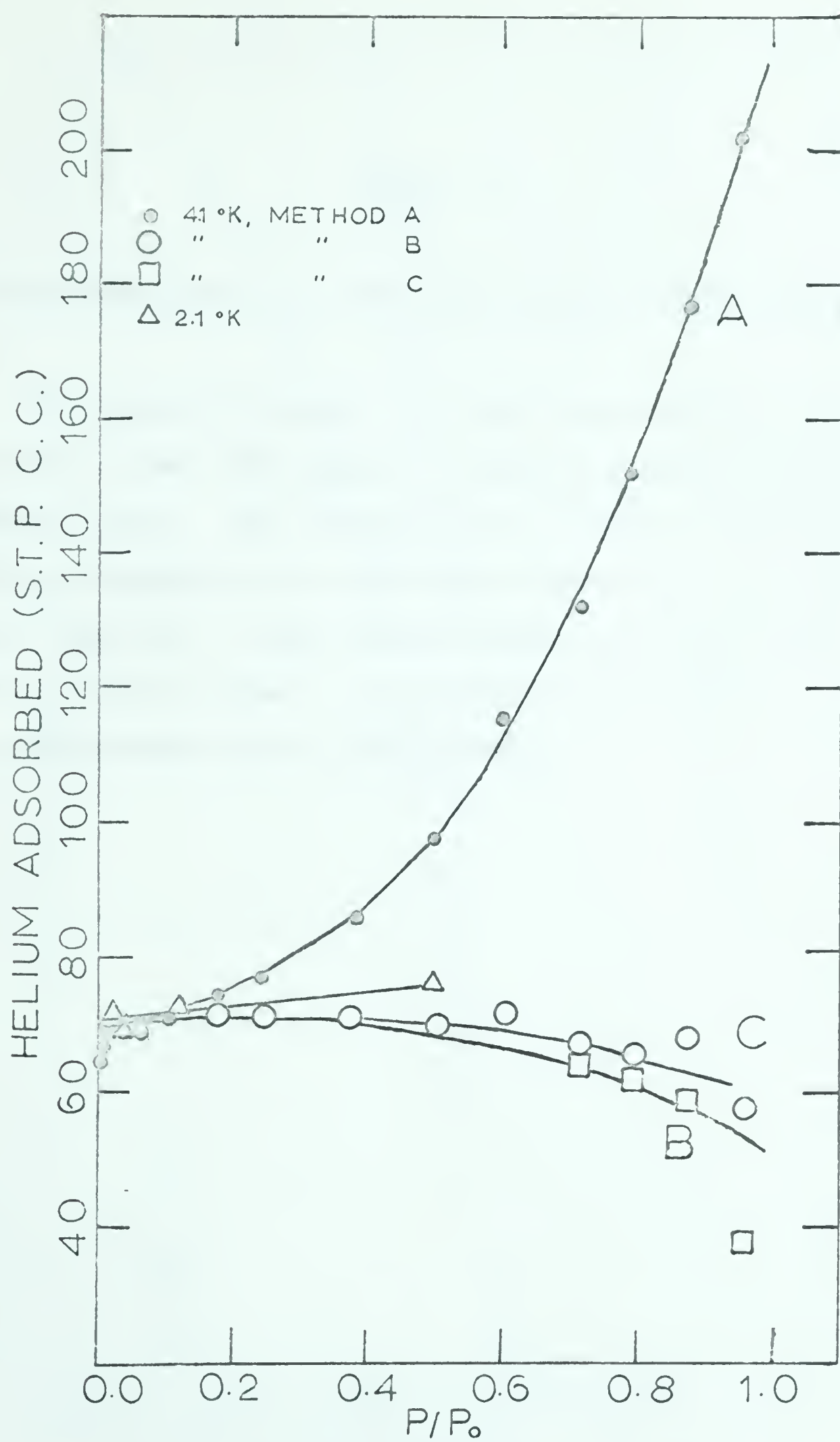




Figure 8

Helium Adsorption in .516g. 13X-zeolite at Approximately 4.1°K

The amount of helium, in cubic centimeters (S.T.P.), adsorbed in the .516g. sample is plotted against the relative pressure (P/P_0). The letters A, B, C refer to different methods of applying the dead-space corrections (Chapter 4, p.59). When two or more methods agree, only one symbol for the point is shown. No attempt has been made to indicate the experimental error in the points.

1870

1871

1872

1873

1874

1875

1876

1877

1878

1879

1880

1881

1882

1883

1884

1885

1886

1887

1888

1889

1890

1891

1892

1893

1894

1895

1896

1897

1898

1899

1900

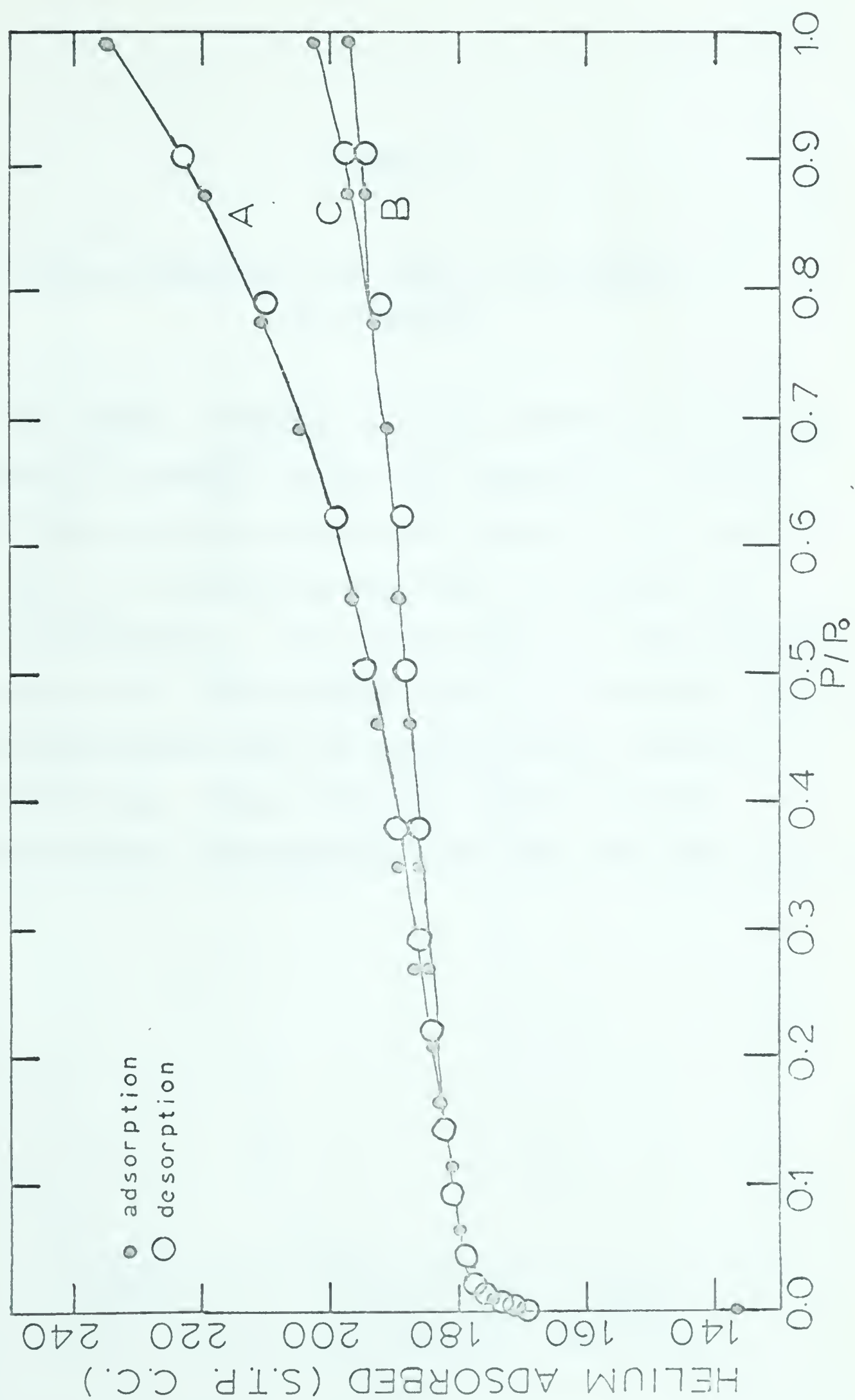
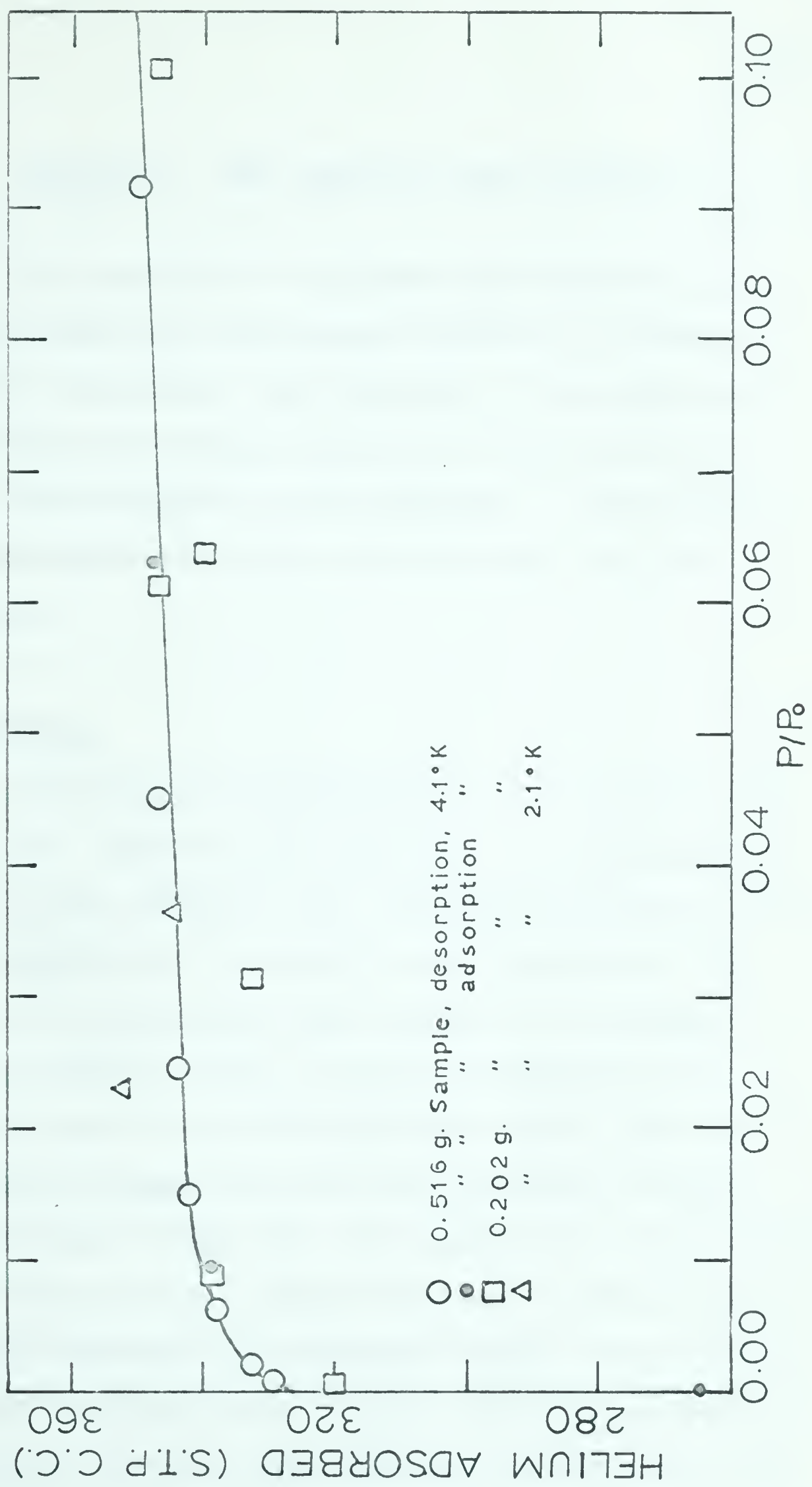


Figure 9

Helium Adsorption per Gram of 13X-zeolite
(as weighed)

The amount of helium in cubic centimeters (S.T.P.), adsorbed in a gram of zeolite (as weighed) is plotted against the relative pressure for values of P/P_0 less than .105. No attempt has been made to indicate the error in the points. Some of the points at four degrees belonging to the .202 g. sample show that the helium was not completely removed from the zeolite lattice between adsorption runs. These were taken after the first isotherm and are substantially lower than the other points.



Chapter 5. THE SPECIFIC-HEAT APPARATUS

The specific-heat apparatus was basically a standard helium-four, exchange-gas cryostat in which a sealed, bomb calorimeter was suspended. A description of the calorimeter and suspension will be followed by an outline of the structure of the cryostat. A discussion of the thermometer and heater circuits will conclude this chapter.

The Calorimeter

Since it was inconvenient to put the calibrated volumes on the specific-heat cryostat, the calorimeter has to be filled with helium in the adsorption apparatus, sealed, and then suspended in the specific-heat apparatus. For this reason the calorimeter was designed to withstand a bursting pressure of about a thousand atmospheres if a tensile strength of 32×10^3 pounds per square inch was assumed for the copper walls and the monograph in Kurti, Hoare, and Jackson (86) used. The dimensions of the calorimeter and the amount of zeolite used were chosen so that, if the heat capacity of the adsorbed helium did not differ greatly from earlier results (22,57), the heat capacity of the calorimeter would be approximately ten per cent of the total.

The body of the calorimeter, made from oxygen-free copper, is shown in Figure 10. A cavity, one centimeter in height and 1.15 centimeters in diameter, provided 1.04 cubic centimeters space for the powder. The neck of the cavity was sealed by a half-inch-long, copper plug that was screwed into position and sealed with soft-solder. Since the powder was a poor heat conductor and the amount of free helium vapour in the dead space small, the thermal contact with the powder inside the calorimeter was improved by a spiral of fine silver mesh silver-soldered to the bottom of the plug. Most of the powder was pressed into the mesh when the plug was screwed into the calorimeter. The gas inlet was through a high-pressure-steel tube, 0.025 inches in outer diameter with a 0.00625-inch wall. This tube was soldered into a hole in the top of the screw.

The volume in the dead space of the sealed calorimeter was estimated fairly easily. Since the calorimeter was sealed with about twenty inches of steel tube attached, the tube contributed about 0.04 c.c. to the dead space. The silver gauze weighed about 1.24 grams and thus occupied about 0.12 cubic centimeters. The sample of powder, weighing 0.556 grams, occupied 0.38 cubic centimeters if the sample had lost twenty-five per cent of its weight by dehydration at the time of its weighing. Thus the designed dead space

was 0.58 cubic centimeters. Actually when the copper plug was sealed into the calorimeter, it did not quite fit into its proper place; about 0.2 cubic centimeters were added to the dead space. As approximately 180 (S.T.P.) cubic centimeters of helium were sealed in the calorimeter, the maximum working pressure was 230 atmospheres. Helium is adsorbed in zeolite to some extent even at room temperature; therefore the actual pressure would be lower than the calculated one.

The heater frame was a piece of copper tubing with two lugs, the lugs being designed to fit into grooves cut into the top of the calorimeter. After an insulating coating of Plasti-Glo^{*} had been applied to the frame, 1100 ohms of manganin wire (double-silk cover, 74.48 ohms per foot) was wound on the frame and varnished into place. At four degrees the resistance was approximately a thousand ohms. Copper wires, used as heater and thermometer terminals, were glued to the top of the heater frame; this time an insulating layer of paper was used in addition to the Plasti-Glo varnish. The frame was soldered with Wood's metal to the calorimeter body before the calorimeter was loaded with helium but after the plug was in position. To provide a place for mounting the resistance thermometer (Chapter 5, p85), a screw socket was tapped in the side

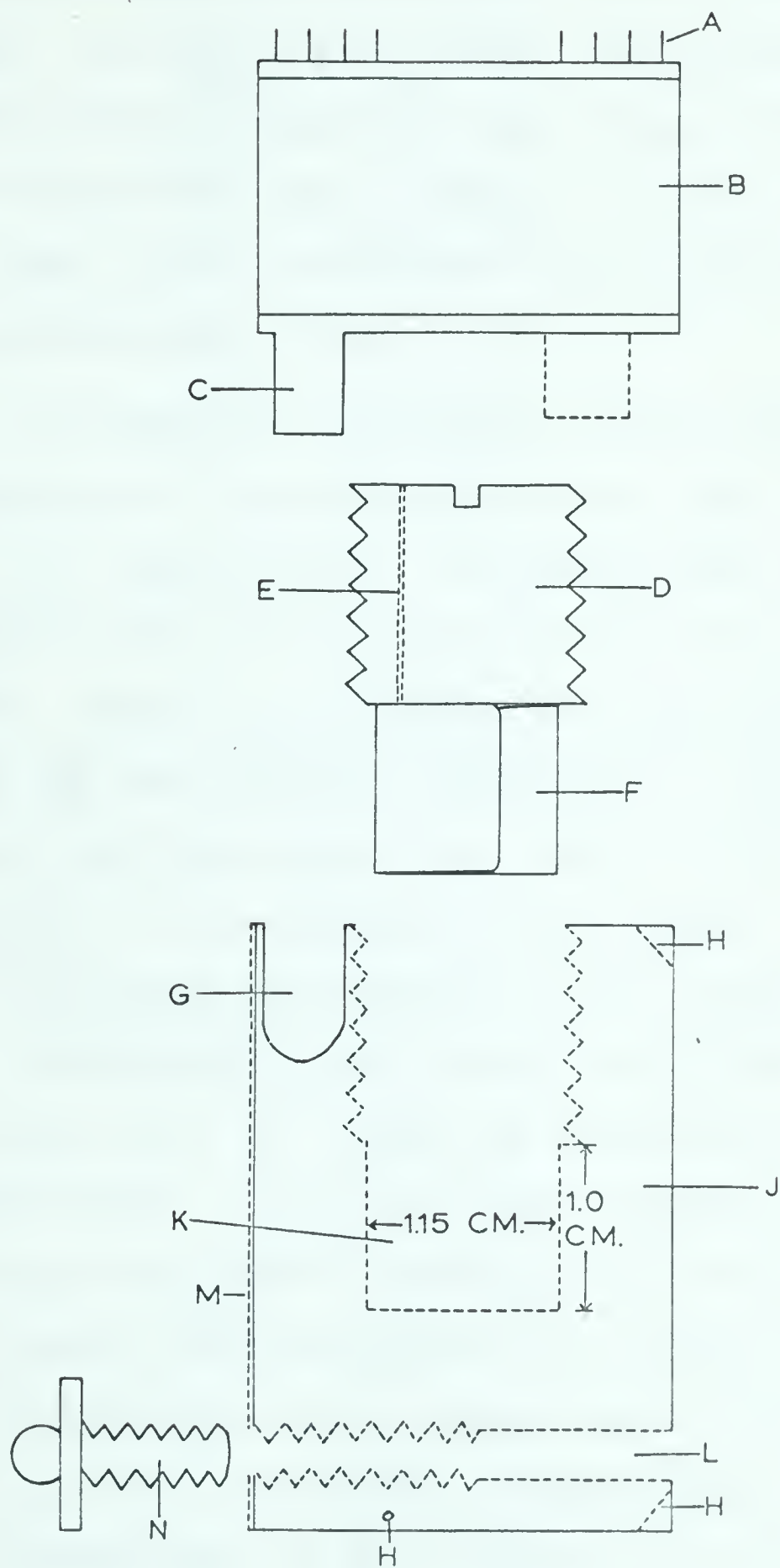
* a poly-urethane cold-setting varnish.

Figure 10.

Schematic Diagram of Calorimeter
(not accurately scaled)

- A - terminals on heater
- B - heater frame
- C - lugs for attaching heater frame to calorimeter
1/4" x 3/16"
- D - copper plug with screw slot
- E - hole for steel tube
- F - silver gauge
- G - slot for heater lug
- H - hole for attaching filament used in suspending
calorimeter
- J - calorimeter body
- K - cavity for containing zeolite
- L - hole for mounting thermometer
- M - strip milled flat to provide good thermal contact
between the thermometer and calorimeter
- N - thermometer

Dotted lines show interior features of the calorimeter body and plug.



of the calorimeter below the powder chamber for the resistance thermometer. To insure good thermal contact between the calorimeter and the thermometer the surface of the calorimeter was milled flat over a strip, 0.35 inches wide, which ran the length of the calorimeter and was centered horizontally around the screw socket.

To suspend the calorimeter, three holes were drilled in the top edge of the calorimeter at an angle of forty-five degrees to the nearest side. Vertically under these holes, three similar holes were drilled in the bottom of the calorimeter. Once the calorimeter had been loaded and sealed, it was leak tested (Chapter 6, p. 91). The thermometer was then screwed into place, and its leads were connected to the terminals on the heater frame. After this the calorimeter was suspended in the cradle (Figure 11) by nylon monofilaments, the thermal conductivity of which was less than 1.25×10^{-4} watts per square-centimeter-degree Kelvin (87). Coiled one-meter lengths of 0.0025 inch, lead-coated, manganin wire, insulated with poly-urethane, served to connect the terminals on the heater with the leads in the platinum-glass seal on the bottom of the helium pot (Chapter 5, p. 84). Since lead is superconducting at the operating temperatures of this cryostat, the lead-coated, manganin wire was chosen because the manganin core minimized

Figure 11.

Photograph of Suspended Calorimeter

- A - helium pot
- B - inner-can joint
- C - cradle
- D - platinum-glass seal containing electrical leads
- E - calorimeter (note flat surface on which thermometer sits)
- F - steel capillary
- G - thermometer
- H - post for mounting thermometer for calibration



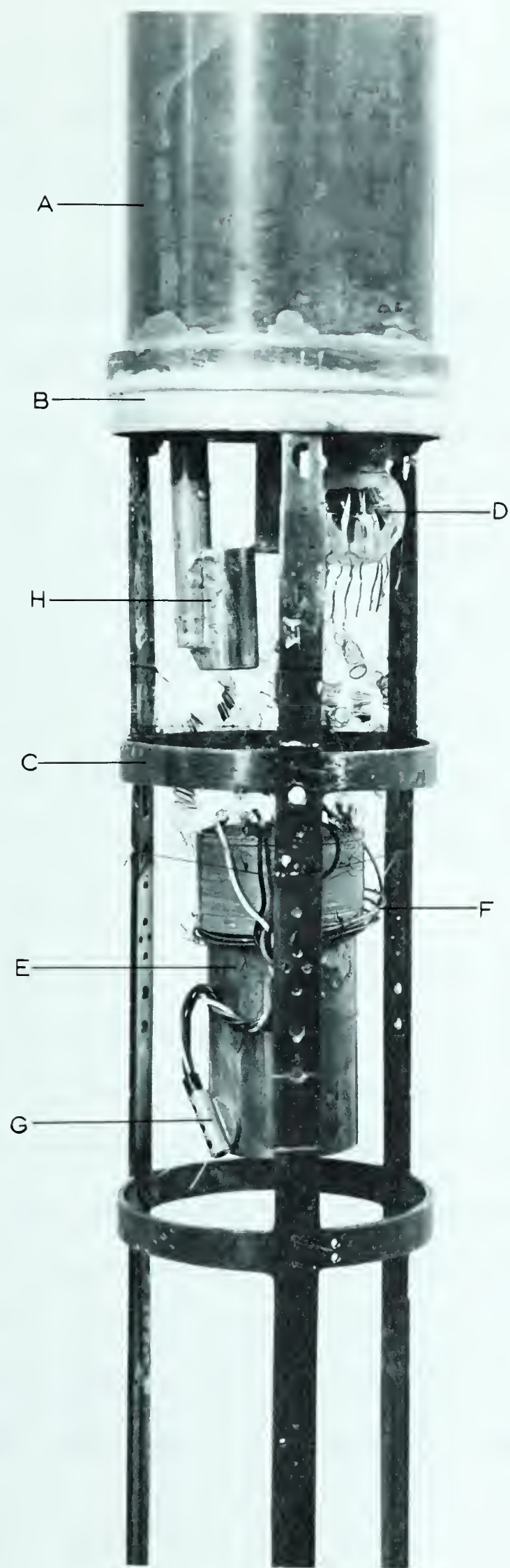
Faint title text, possibly a chapter or section heading.

Faint text block on the right side of the page, possibly a date or a short paragraph.

A line of faint text spanning across the middle of the page.

Faint text block on the right side, below the previous one.

A line of faint text at the bottom of the main content area.





the thermal conduction to the calorimeter at the same time as the lead coating minimized joule heating in the wires.

General Features of the Specific-Heat Cryostat

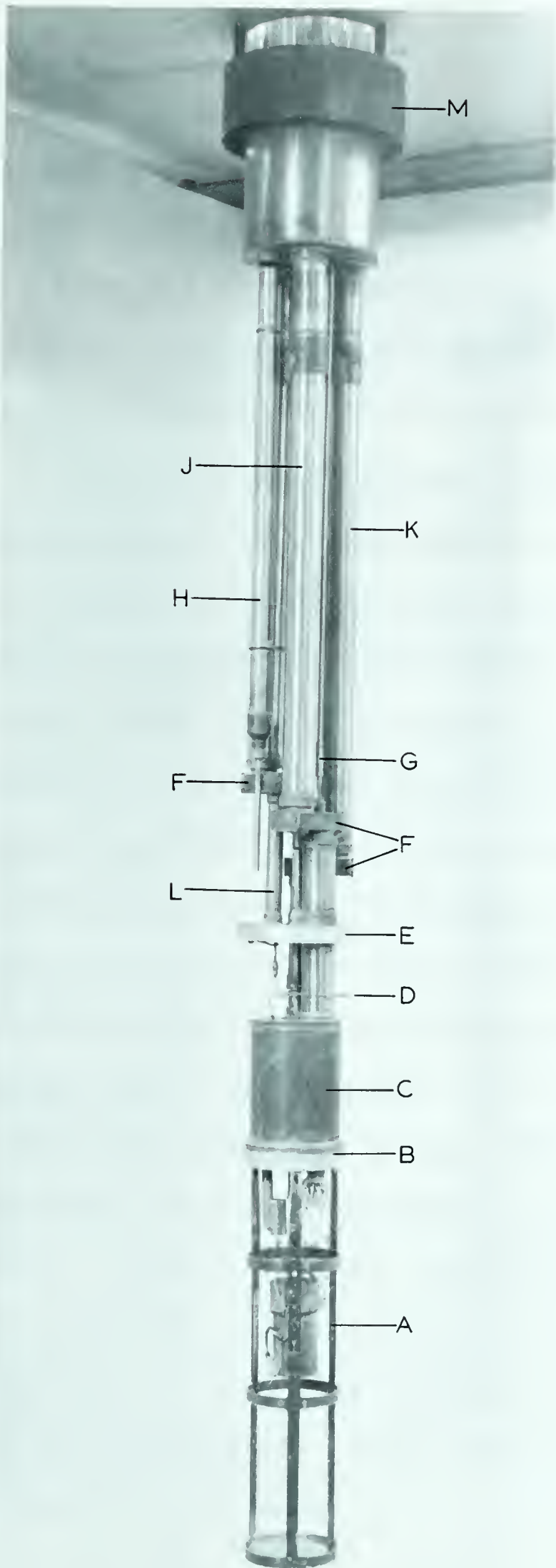
Basically the cryostat was like many other helium-four cryostats which use exchange gas as the cooling mechanism and was very similar to the one described by Buckley (88) except for the absence of demagnetization features in the present case. The cryostat consisted of three separate vacuum systems which can be referred to as the inner-can, the outer-can and the helium-pot systems. To reduce the heat influx by radiation, each pumping line was broken by a rectangular, brass fitting which acted as a radiation trap.

The inner can, covering the cradle and calorimeter, was soldered with Wood's metal to the joint above the cradle but below the helium pot and was used to provide a vacuum to thermally isolate the calorimeter from the helium pot. The outer can, shielding the inner can and helium pot, was attached in the same way to the joint above the helium pot and was used to isolate the helium pot from the liquid helium in the dewar which surrounded the outer can during a run. Both systems were pumped by separate oil-diffusion

Figure 12

Photograph of Specific-Heat Cryostat

- A - cradle containing calorimeter
- B - inner-can joint
- C - helium pot
- D - manometer tube for helium pot
- E - outer-can joint
- F - radiator traps
- G - needle valve for helium pot
- H - syphon guide
- J - helium-pot pumping tube
- K - inner-can pumping tube
- L - outer-can pumping tube
- M - dewar cap



pumps backed by mechanical pumps. In addition the inner-can system had a liquid-air trap between the oil pump and the experimental chamber to prevent hot-oil vapour from flowing into the experimental chamber. Normally the pumps could attain pressures of approximately 10^{-7} millimeters of mercury once the experimental area had been cooled.

The helium-pot vacuum system, used only to lower the bath temperature, consisted of a mechanical pump to which a Cartesian manostat (89), a needle valve, and a Jamesbury valve had been attached so that the pumping speed and, hence, the bath pressure could be controlled. The helium pot was a metal cylinder through which the pumping line to the inner chamber passed. Once it had been evacuated, it could be filled with liquid helium by opening a needle valve in the radiation trap. Affixed to the bottom of the helium pot was a platinum-glass seal containing twelve metal-glass seals to provide electrical connections for the calorimeter. The electrical connections were brought to room temperature by running wires through the helium-pot pumping tube and connecting them to a set of copper terminals. These wires were thermally anchored in the radiation trap at four degrees and also in the helium pot at its temperature. A wax seal provided the room-temperature-vacuum seal.

A one-millimeter-diameter, metal tube, which reached room temperature through the outer-can pumping tube, connected the helium pot with a set of oil and mercury manometers. With the backing pump for the inner can providing the reference pressure, these manometers were used to measure the bath pressure.

The Thermometer

The thermometer was a Honeywell germanium resistance thermometer, model MHSP4301E, suitable for measuring temperatures between 0.4 and 10°K. The Honeywell germanium thermometers are specified as giving temperature reproducibility of better than 0.005°K even after repeated cycling to room temperature. The germanium element was mounted in a gold-plated frame with a flat base, 0.35 inch in diameter; the base included a gold-plate 6-32 screw, 0.34 inch long, to insure good thermal contact with the mounting surface and also easy demounting of the thermometer. The calibration of the thermometer is discussed in Appendix II.

The thermometer resistance was measured by one of the standard thermometer circuits available in the laboratory for this purpose. These circuits were slightly adapted versions of the Dauphinee-Mooser circuit (90), altered so

that the signal could be amplified by a chopper amplifier (91) and recorded on a Leeds and Northrup Speedomax, type B, chart recorder. The chart, moving at two inches per minute, essentially recorded resistance against time. The circuit operated on the principle of an isolating potential comparator (92). So that errors in the reference resistor could be neglected, the same set of resistance boxes was used as the standard in each run.

Heater Circuit

The heater circuit is shown in Figure 13, together with a list of equipment. Heating intervals for the specific-heat measurements were timed using a Standard electric clock capable of measuring time to about one-fiftieth of a second. Because it had an electromagnetic clutch, the clock could be switched on and off with the heater so that the time of the heating period was measured automatically.

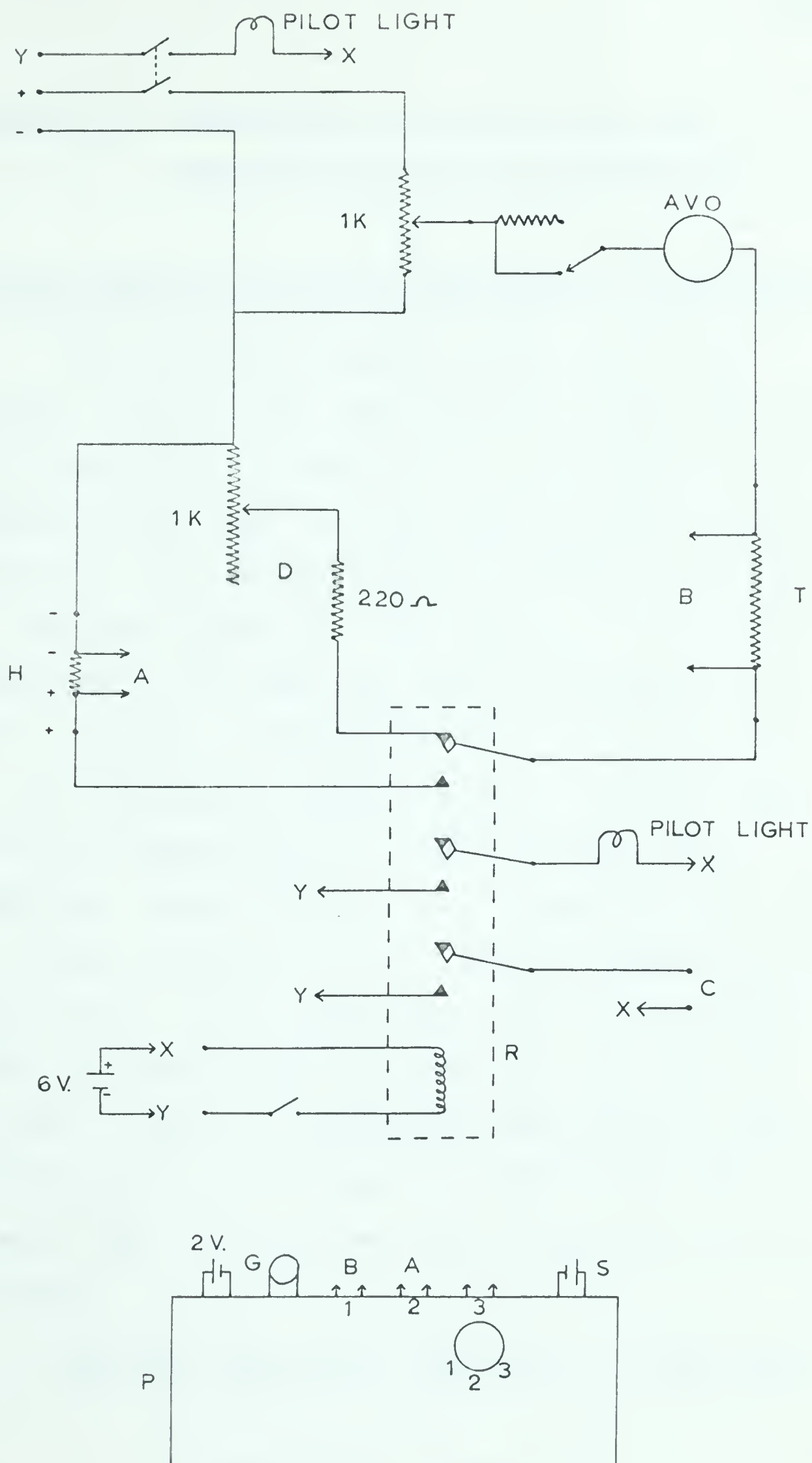
The circuit was designed so that the current through the heater could be measured by using the potential difference across a good quality 1000-ohm resistor (Leeds and Northrup number 776863). An AVO meter in the circuit provided a very rough check on the current measurements of the potentiometer.

To stabilize the batteries so that fluctuations caused by turning a circuit on would not affect the heat-capacity points, a dummy heater took the place of the actual heater except when a heat-capacity point was being taken. Since the dummy resistance was set very close to the resistance of the heater, the rough balance of the current through the heater could be obtained before the heater was turned on. Because speed was important in taking the heat-capacity measurements, the resistance of the heater, described earlier, was chosen so that it would be approximately 1000 ohms at liquid-helium temperatures. Thus both the voltage across it and the current through it could be measured with small changes in the potentiometer settings.

Figure 13

Heater Circuit

- C - connection to clock clutch
- G - Scalamp Galvanometer 24 mm./ μ a.
- P - Cambridge Vernier Potentiometer L375327
- H - heater
- D - dummy heater
- R - Relay Potter and Brumfield KL14D 6V. DC
- S - Weston Normal Cell L353404
- T - 1000 Ω resistor Leeds and Northrup 776863



Chapter 6. EXPERIMENTAL PROCEDURE ASSOCIATED WITH THE HEAT CAPACITY MEASUREMENTS

The Loading, Leak Detection and Evacuation of the Calorimeter

After the screw threads on the neck of the calorimeter and the copper plug had been tinned, the dehydrated sample of zeolite was packed into the calorimeter's cavity. The plug and steel tube were then soft-soldered in position. As soon as the tube had been found unblocked, it was soldered to the adsorption apparatus. The loading of the calorimeter then proceeded in the same way that an isotherm was started. (Chapter 3, p. 53). Equilibrium times were much longer than on the isotherms presumably because the steel tube had a smaller diameter than the one-millimeter tube normally used. When enough gas was in the calorimeter, the steel tube was quickly cut in the desired length, sealed and capped with a brass end ferrule while the calorimeter was still at liquid-helium temperatures. Once the end ferrule was in place the calorimeter was warmed to room temperature and the steel tube was coiled around the calorimeter body. The tube was held in position by small copper wires.

After the calorimeter was sealed, it was placed

in a bell jar which could be evacuated by a mechanical pump. The Veeco helium-leak detector was "teed" into the system. The leak detector is a small mass spectrometer which is set to detect helium. When samples of gas from a vacuum system are passed through the leak detector, it can detect very small traces of helium if they are present in the sample. During this test of the loaded calorimeter, the leak recorded was less than 0.1 corresponding to 1.5×10^{-9} standard cubic centimeters per second; however, after the calorimeter had been suspended and the vacuum systems started, the leak reading was 0.66. This was 0.7×10^{-8} standard cubic centimeters per second or 6×10^{-4} standard cubic centimeters per day. The assumption was made that the steel tube, having been bent into a smaller coil between the leak tests, had opened slightly but that the run could be made. With the calorimeter at liquid-air temperatures for two days after the run, August 3 and 4, the leak reading was between 1.6 and 1.2. On the fifth it was significantly lower. The increased readings may have been caused by remnants of the exchange gas present in the inner chamber.

Before the second run with the calorimeter the helium gas was removed. To do this the calorimeter was evacuated at room temperature through the steel-capillary

tube for more than a week. At the end of this time the leak-detector reading was about 3.6 above the background when the sample chamber was opened to the system after it had been isolated for twenty minutes. The calorimeter was then sealed and re-suspended as before. However, because of some trouble with the vacuum in the specific-heat apparatus, the calorimeter was re-opened and heated on the vacuum system to about 164°C . for a few hours to determine if the calorimeter had been leaking. At the end of this time the vacuum was about 1×10^{-6} millimeters of mercury; the leak detector read 2.0 above the background after the calorimeter had been isolated for ten minutes but did not indicate any leak from the calorimeter at room temperature. The purpose of isolating the calorimeter was to accumulate a larger sample of helium than would be present if the calorimeter were continuously evacuated and thereby to increase the sensitivity of the leak detector. These observations showed that the calorimeter had not developed any major leaks. The calorimeter was then sealed and suspended again.

Heat-Capacity Measurements

After the calorimeter was suspended and wired electrically, the circuits were checked at room temperature.

Since the pressures in both high-vacuum systems were 10^{-5} mm. of mercury or lower before cooling was started, the systems were pumped at least overnight before a run began. The system was then pre-cooled to liquid-air temperatures. With exchange gas in both the inner and outer can, it took almost three hours to pre-cool the calorimeter. After the liquid-helium transfer, the helium pot was filled. At this time the exchange gas was pumped out of the outer can, thermally isolating the helium pot from the liquid helium in the dewar at four degrees. The helium-pot pressure was lowered until the temperature in the inner can was lower than that of the first heat-capacity point desired. The minimum temperature attainable was about 1.6°K . The exchange gas was evacuated from the inner can for about half an hour at which time the heat leak to the surroundings had decreased noticeably and the pressure was on the 10^{-7} mm. of mercury scale on the Martin gauge if the vacuum system was working. In Run B the vacuum system refused to go below 2×10^{-6} mm. of mercury even when the inner can was isolated from the pump.

The system was then ready for the taking of heat-capacity points. The temperature in terms of the resistance of the thermometer was recorded continuously on the chart recorder.

Since the resistance actually being recorded at any time was that which would shift the record to the middle of the chart (Fig. 21), the sensitivity of the chart was checked before and after each point by changing the resistance value of the reference resistance. The change in resistance divided by the shift in position of the record yielded the sensitivity. A value of resistance which moved the record to the low-temperature side of the chart having been chosen, the pen was allowed to write undisturbed for several minutes so that the slope of the fore-period could be obtained. The heating period could then be started.

The dummy heater was turned on nearly an hour before the first point was taken, that is while the calorimeter was being cooled. Once the heater had been turned on the voltage across it and the current through it were measured quickly on the potentiometer. As mentioned earlier the time of the heating period was measured automatically by a clock with an electromagnetic clutch. The time the heater was left on was controlled so that the change in temperature, ΔT , was small enough that the error, caused by assuming the heat capacity measured was the true heat capacity at the mean temperature of the heating period, was less than 0.1 per cent if the T^3 specific-heat law were applicable. Calculation showed that at 1.7° the ΔT should be

$\leq 0.10^{\circ}\text{K}$. The ΔT increased monotonically with temperature to about 0.25° at four degrees; however, even close to four degrees the experimental-temperature changes were always below 0.16°K .

Before the heater was switched off the record on the chart was centered by changing the reference-resistance value. The heater was then turned off, and the after-period was recorded. This could take nearly half an hour. When the calorimeter had reached a steady state, the process was repeated until the helium pot became empty. When the helium pot was empty, exchange gas was put in the inner can, the helium pot was pumped on, and the rest of the process was repeated.

Two heat-capacity runs were done: one on the calorimeter with adsorbed helium, Run A, and the other on the calorimeter with the helium removed, Run B. The heating periods in Run A varied from approximately 100 seconds to over 1000 seconds and the heating rates from 3.14×10^{-5} watts near four degrees to 3.83×10^{-7} watts below two degrees. Faster heating rates below two degrees adversely affected the equilibrium time of the calorimeter; and, since an exchange-gas cryostat was used, there was no possibility of separating the contribution of the heat leak to the surroundings, mainly caused by gas desorption

from the walls of the calorimeter, from that of the non-equilibrium processes inside the calorimeter. During the second run the heating period varied between 100 and 600 seconds and the heating rates from 9.85×10^{-6} around four degrees to 1.55×10^{-6} watts near two degrees. The procedure was essentially the same in both runs.

Chapter 7. THE HEAT CAPACITY RESULTS

Method of Calculation

Before the results can be interpreted, the method of analysis must be considered. To calculate the heat capacity from a given measurement, the changes in temperature caused by the heat leak to the surroundings had to be separated from the changes caused by the known heat input. Since the temperature changes before, during, and after a heat-capacity point were recorded on a chart as resistance versus time, tangents from the fore-period and after-period on the chart were extended to the mid-point of the heating period to estimate the effect of the heat leak. The intersections of the mid-point line with the tangents were used to calculate the effective resistances, the estimates of the resistances that would have been recorded if no heat leak had been present, at the beginning and end of the heating period. Since the value of the resistance being recorded on the chart at any time and the displacement from equilibrium were known and the sensitivity could be calculated, the effective resistance was obtained fairly easily (Appendix IV). A set of graphs, one graph for each filling of the helium pot, with ohms per large chart division plotted against equilibrium resistance, was used

to facilitate the calculations. The resistance value could then be converted to temperature with the aid of the thermometer calibration (Appendix II).

The fore-period was almost a straight line; therefore, this was no problem to extrapolate. The after-period was always curved and sometimes contained a temperature minimum so that the position of the tangent was very difficult to determine. Several papers (93, 94) have been written on the methods of correcting heat-capacity points for the heat leak to the surroundings; finite conduction times in the calorimeter have also been included (95). However, the heat-capacity points did not warrant the detailed analysis required to apply any of these methods; instead the tangent for the after-period was chosen in three ways.

In the first method no non-linear heat leak to the surroundings was assumed. When the after-period contained a temperature minimum, a relaxation time, τ , was calculated crudely by assuming the minimum was the base line for an exponential decay. The tangent was drawn at 4τ from the point at which the heat was turned off. When there was no minimum, the tangent was drawn at a place where the after-period was fairly straight. This method produced too much scatter on the " 4τ " points to be useful.

The B run was analyzed in two other ways, called two and three. In method two, M2, if a point contained a minimum in the after-period, the tangent was drawn at τ ; for the B run this meant sometime within the first three minutes of the after-period run-off. When this method was applied to Run A, τ was occasionally as large as eight or ten minutes. If a period contained no minimum, the tangent was again drawn when the after-period became a fairly straight line; usually this was someplace in the first seven minutes of the after-period.

The third method, M3, was to assume that the heat leak to the surroundings completely dominated any non-equilibrium effects in the calorimeter. In this case the tangent was almost always drawn someplace in the first minute of the run-off. Usually the after-period resistance increased very rapidly for approximately a half minute and then the rate of increase slowed slightly. The tangent was drawn near this point. Both the last two methods gave fairly smooth results; and, when the smoothed values of the heat capacities were subtracted so that A - B was obtained, there was only a small difference in the resulting curves.

The heat capacity of the adsorbed helium was obtained by subtracting the heat capacity of Run B from

that of Run A. The subtracted curve had to be corrected for changes in the heat capacity of the calorimeter caused by slight changes in the weight of the calorimeter between the runs. Reworking the solder joints, between the runs added about 1.17 grams of soft-solder and Wood's metal to the calorimeter and the repeated opening of the steel tube caused the calorimeter to lose 0.05 grams of steel. Unfortunately the specific heats of steel and soft solder were unavailable; however, the corrections were estimated from the specific heat (96) of alpha-iron in the case of steel and from the mean of the specific heats of lead and tin in the case of soft solder (50-50) and Wood's metal. These corrections contributed four per cent or less to the heat capacity of the helium. Since the specific heat of Wood's metal is slightly less than that of lead, unless the soft solder has a very large heat-capacity term caused by the mixing of the two metals, it is very unlikely that the heat-capacity corrections applied in this case are in error by more than fifty per cent. Thus the error introduced by the weight-change in the calorimeter was reduced to a maximum of two per cent.

Errors in Procedure and Analysis

The finite ability of the heater frame to conduct heat to the body of the calorimeter should have resulted

in a small amount of over-heating at the end of the heating period. When over-heating occurs the temperature of the calorimeter increases for a short time after the heater is turned off because the heat-conduction times in the system are finite. From the measurements of the thermal-conductivity of copper-Wood's-metal-copper sandwiches (97) a heat-conduction rate of 3×10^{-2} watts per degree Kelvin at two degrees and 1.5×10^{-1} watts per degree Kelvin at four degrees was obtained if the Wood's-metal seal controlled the heat conductivity. Thus for the heating rates used, the heater was never more than a millidegree hotter than the body of the calorimeter. The weight of the heater was eleven grams, whereas the calorimeter weighed about 168 grams, but the heater had addenda, having specific heats greater than that of copper, attached to it.

Since the heater had a varnish coating the heat capacity was difficult to calculate; however, an estimate could be made from the heat capacity of the dummy calorimeter which weighed 119 grams, 3.1 grams of this being addenda including the thermometer. This calorimeter was the copper block used in the first two thermometer-calibration runs (Appendix II). During the second run a few crude, heat-capacity points were taken to test the equipment. The heat capacity, as analyzed by method three,

was approximately ten per cent above that of the same weight of pure copper. As the weight of the varnish and heater wires, the main contributors to the excess heat capacity of both the block and the heater frame, would be approximately the same, the percentage contribution of the heat capacity of the heater frame to that of the calorimeter could be estimated. It was about fifteen per cent. Thus the higher temperatures of the heater at the end of the heating period should have caused the temperature of the body of the calorimeter to increase by less than 0.2 millidegrees after the heater had been turned off. Indeed only very slight signs of over-heating were recorded on the chart during the runs. The thermometer leads being attached to the heater frame may have partially inhibited the observation of any over-heating present as some of the heat from the frame would be conducted directly to the thermometer. This would be important only if the thermal contact between the thermometer and the calorimeter were poor. Another inhibiting factor was the heat leak.

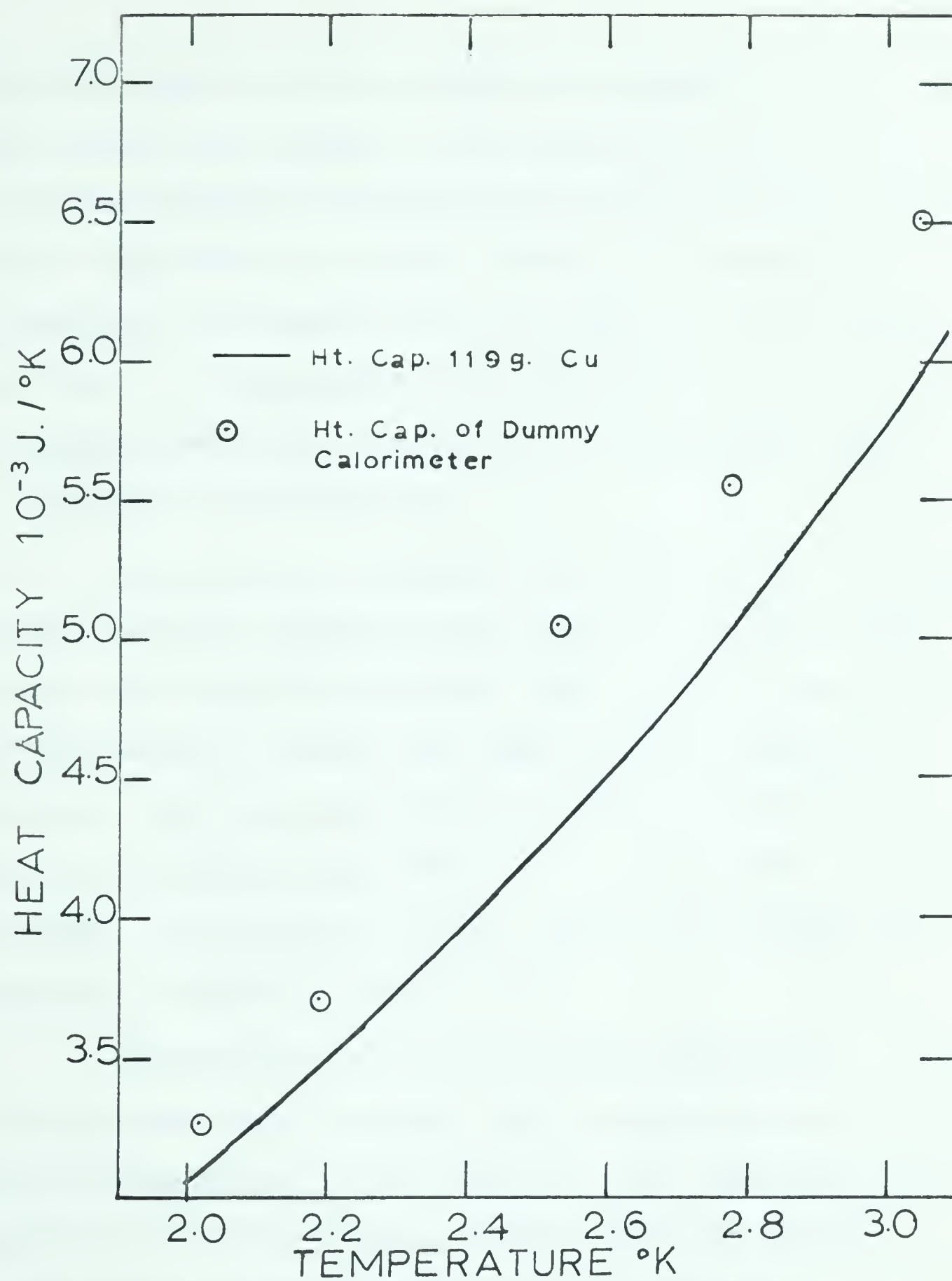
The heat leak from the calorimeter to the surroundings was fairly large and very variable. In Run A, the leak was usually about 5×10^{-7} joules per second before the first point was taken in any filling of the helium pot. The leak in Run B was nearly an order of

Figure 14

Heat Capacity of Dummy Calorimeter

Experimental points analyzed by method three are compared with the heat capacity of pure copper(98).

The confidence limits are not shown but are about $\pm 10\%$ (p. 105-106).



magnitude higher probably because the pressure in the inner can was much higher. The effect of the heat leak on the heat-capacity measurements will not be known until further experiments are done; however, the possibility for error in the results was much higher with the large heat leaks. In the analysis the heat input by the two-microampere, measuring current of the thermometer would be included in the heat leak.

The time was measured to a fiftieth of a second and the frequency variation was monitored on WWV during Run A. The variation was about 0.01 per cent during the time the reported points were taken (on the August 1-3 weekend). Run B was not monitored but the points were taken on a weekend (Sept. 26-27) to minimize the frequency variation. The errors in time, current and voltage were negligible compared to other errors.

Theoretically the temperature difference could be calculated to better than one per cent and the absolute temperature to at least 0.1 per cent after the position of the after-period tangent had been chosen; however the thermometer calibration (Appendix II) appeared to have larger errors than the theoretical ones and the exact effect of the heat leak was unknown. Since the experimental curves were relatively smooth and the

two methods of calculation, M2 and M3, agreed within a few per cent, the results have some significance. Thus the experimental error was probably around ten per cent.

The Results

The specific-heat sample was 180 cubic centimeters of helium adsorbed in 0.556 grams of zeolite which was weighed when it was taken from the storage can. About 0.29 cubic centimeters of helium was contained in the dead space at four degrees. Thus dead-space corrections were small in the adsorption part of the experiment and probably also in the heat-capacity part; however, until more isotherm data is available, no desorption corrections to the heat-capacity data can be made.

The calorimeter leak, mentioned in Chapter 6, probably did not increase much when the calorimeter was cooled. Run A was spread over almost five days. Although only points A43-A99, the points taken in the last two days, are reported here, the other points A1-A42 were analyzed by the first method (Chapter 7, p. 96) and fitted into the scatter of the later points quite well. Time did not permit the re-analysis of these points. Apparent gaps in the numbering of the reported points were caused by the helium pot having emptied near the missing point. There

were similar gaps in the unreported section.

The results of both methods two and three for Runs A and B are shown graphically in Figures 15 and 16 and in tabular form in Appendix V. Certain points only have one calculated value which is assigned to both methods. This was caused by two situations. Something happened to invalidate the slope of the after-period close to the end of the heating period. Usually this was caused by the helium pot going dry. In several cases the run-off became linear almost immediately after the heating period ended. Since the discrepancy between the methods was very small in this case, only one value was calculated.

The heat-capacity curves for the A and B runs were fitted graphically. All the reported points were included in the fit except for two classes of points; the first point after the helium pot had been refilled if the heat capacity of that point were above that of the next point, and the last point before the helium pot emptied if the heat capacity of that point were lower than that of the one before. The heat leak sometimes changed considerably while these points were being taken so that the heat leaks which existed during the heating period could not even be approximated by the methods of calculation used here. Since the temperature region of

Figure 15

Heat Capacity of Runs A and B
(analyzed by method 2)

The results of run A, the run with the calorimeter filled with 180 c.c. of helium, and run B, the run without helium are compared with the heat capacity of approximately the same weight of copper (98). The confidence limits on the experimental points are about $\pm 10\%$ (p. 105-106).

A slash through a point indicates that it has been excluded from the graphical fit.

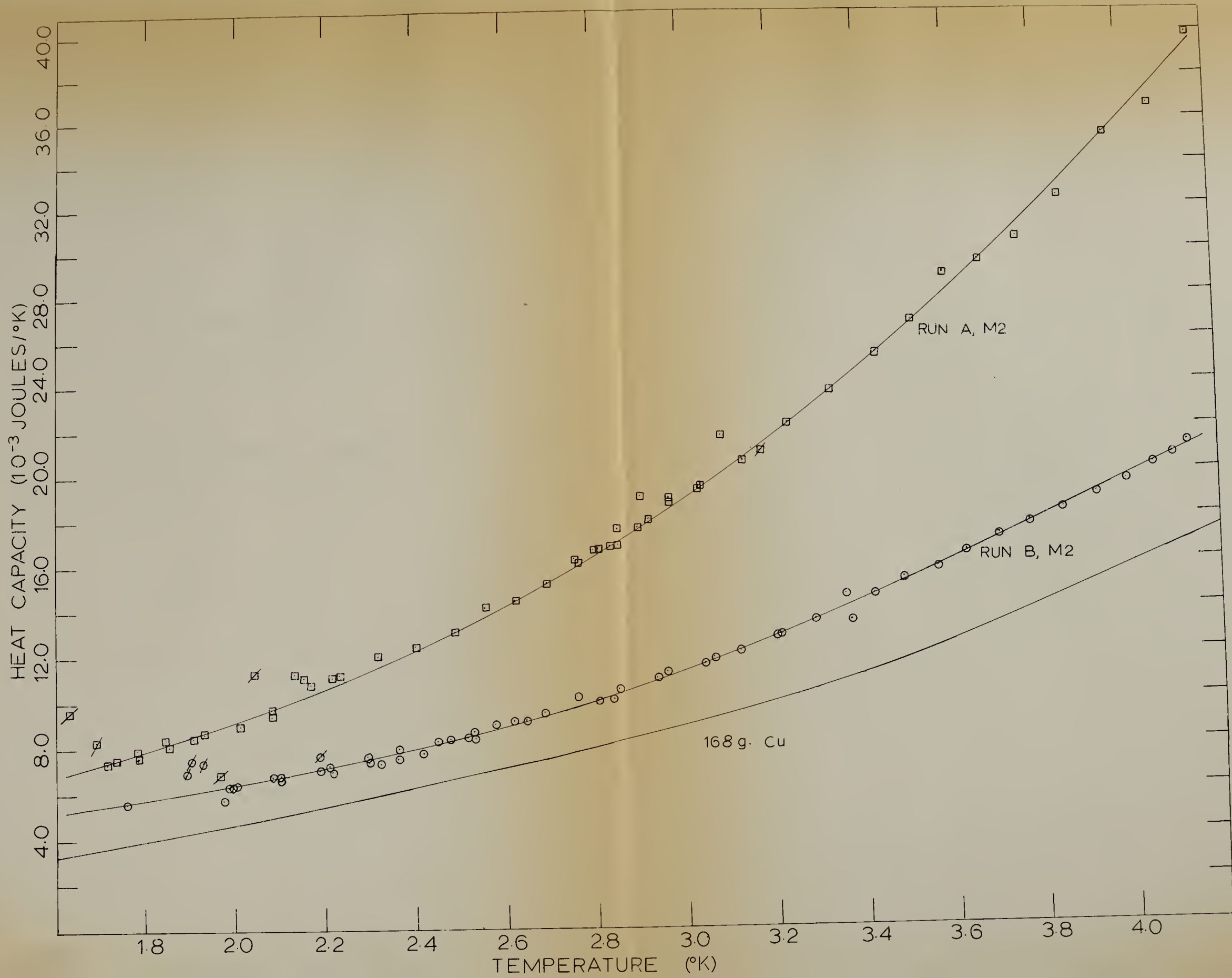
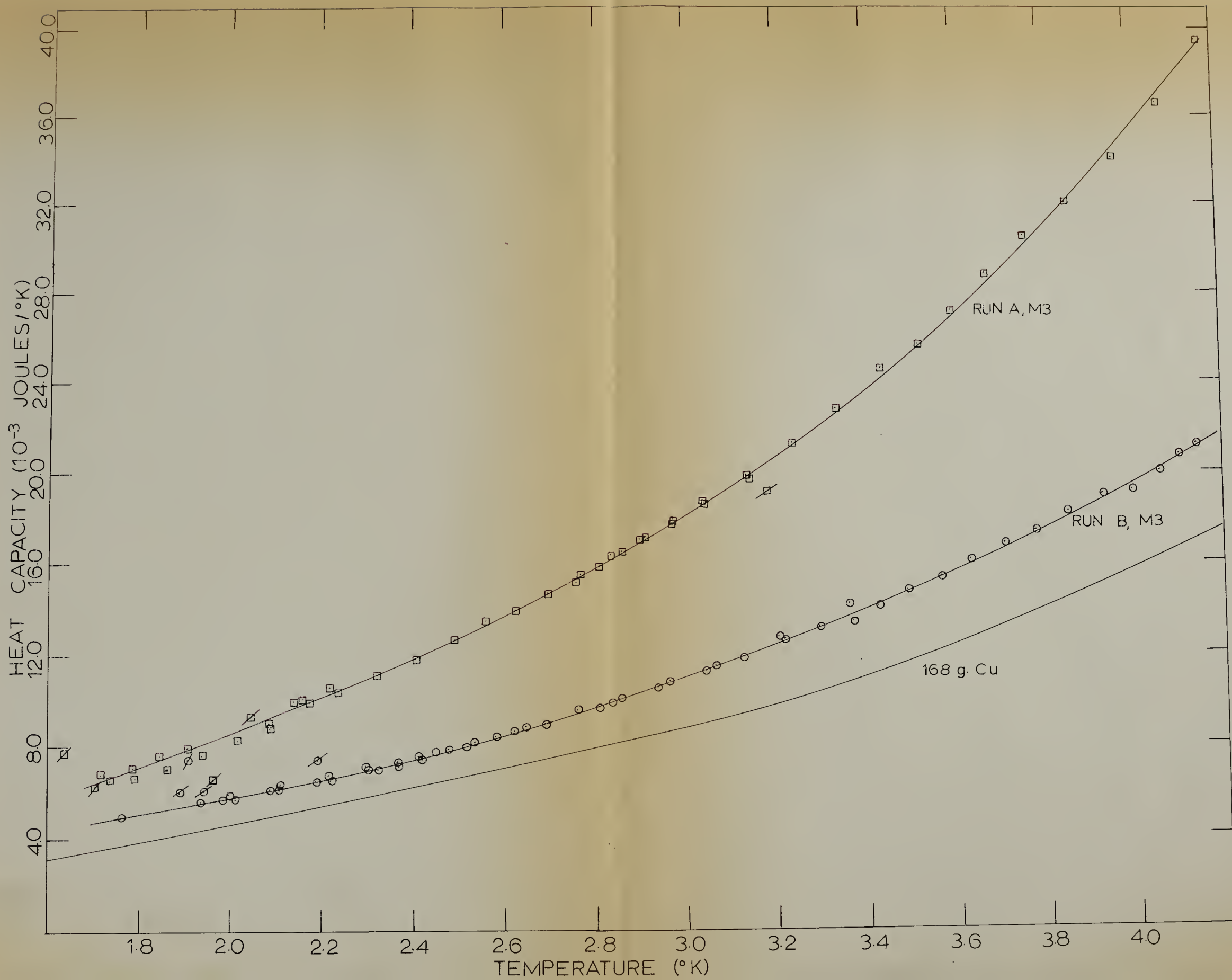


Figure 16

Heat Capacity of Runs A and B
(analyzed by method 3)

The only difference between Figures 15 and 16
is the difference in the method of analysis.



the measurements was only two degrees and each measurement was spread over approximately a tenth of a degree, a numerical analysis was not warranted.

The heat capacity of the adsorbed helium was obtained by subtracting the curve of Run B from that of Run A. Because no other criterion was available, only the difference between curves using the same method of analysis were calculated. The results were then corrected for the small change in the heat capacity of the calorimeter between the runs. These results are shown graphically in Figures 17, 18, and 19. Unless there is some large unknown error in the heat-capacity runs caused by the heat leak, the error in the heat capacity of helium is probably about twenty per cent. In view of the results on adsorbed helium-three published by Lambert (22), the reproducibility of the experiment must be checked before much significance can be attached to the results.

Figure 17

Heat Capacity of Adsorbed Helium Obtained from Figure 15

The heat capacity of the 180 c.c. of (S.T.P.) of helium adsorbed in the cavity is shown. The lower curve was obtained by subtracting the smoothed curves of A and B in Figure 15. The upper curve is corrected for the change in the composition of the calorimeter (p. 100). The error in the results is approximately $\pm 20\%$ (p. 105-106, 112).

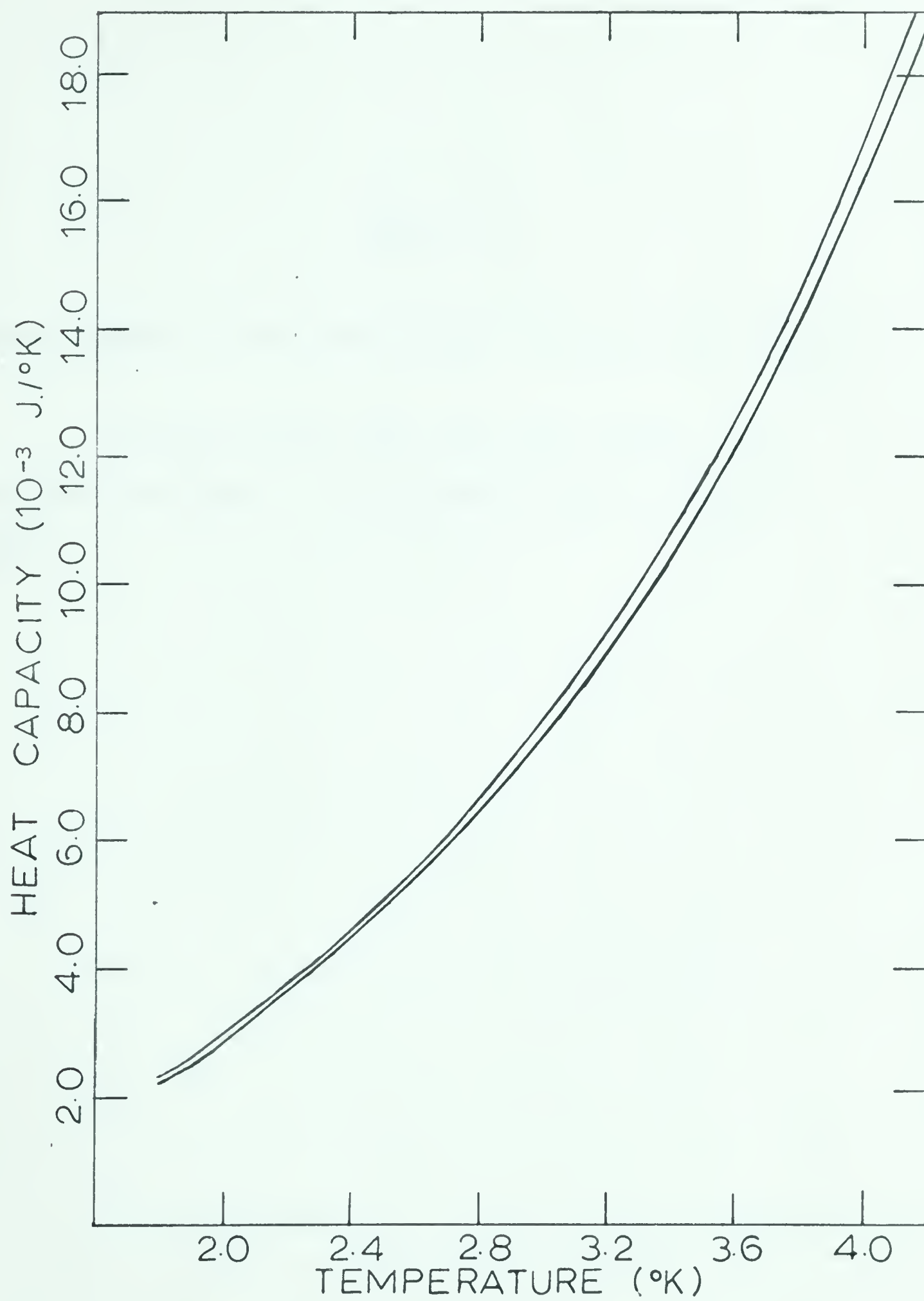


Figure 18

Heat Capacity of Adsorbed Helium Obtained from Figure 16

Except for the fact that the results are obtained from Figure 16 the comments about Figure 17 apply.

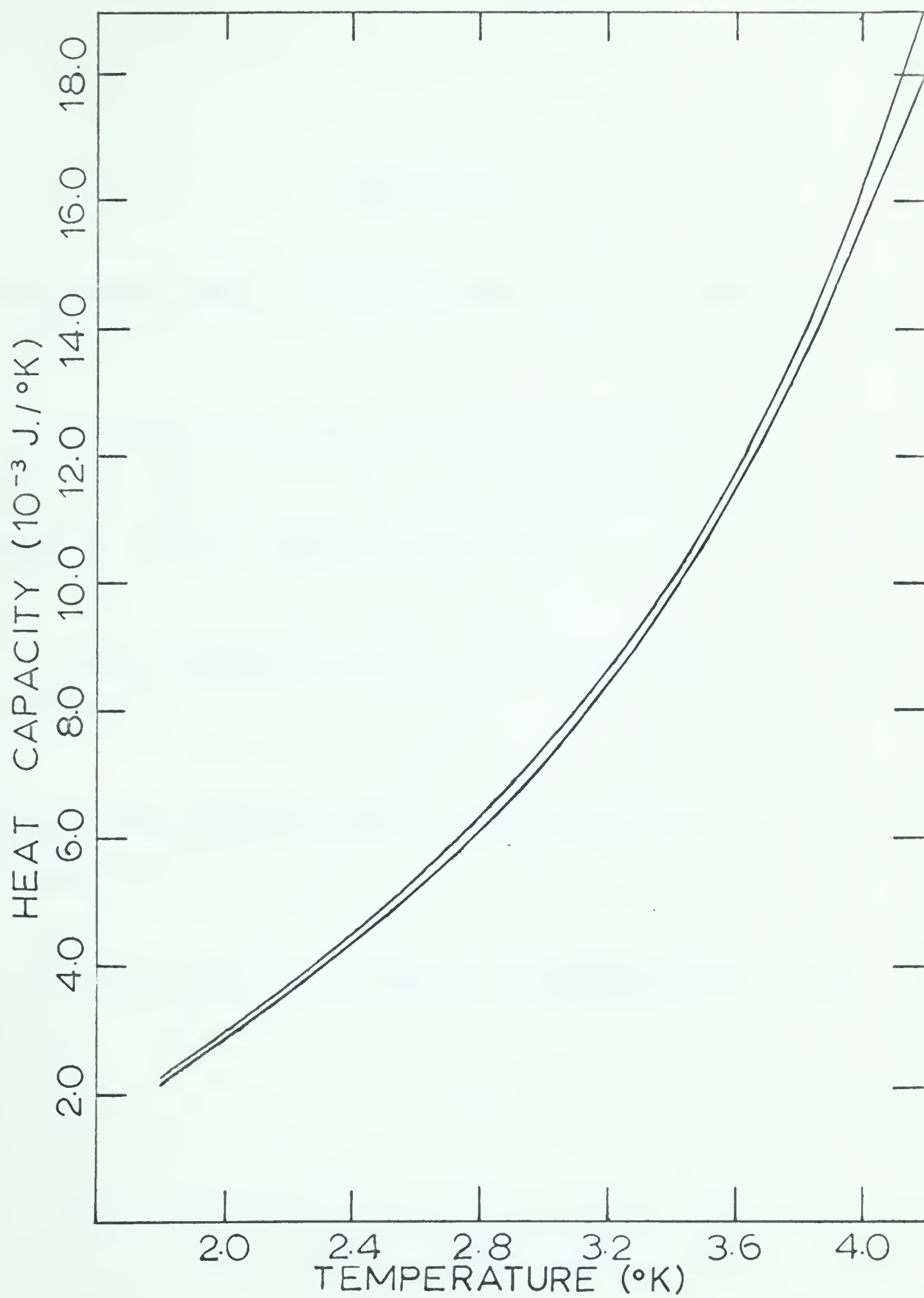


Figure 19

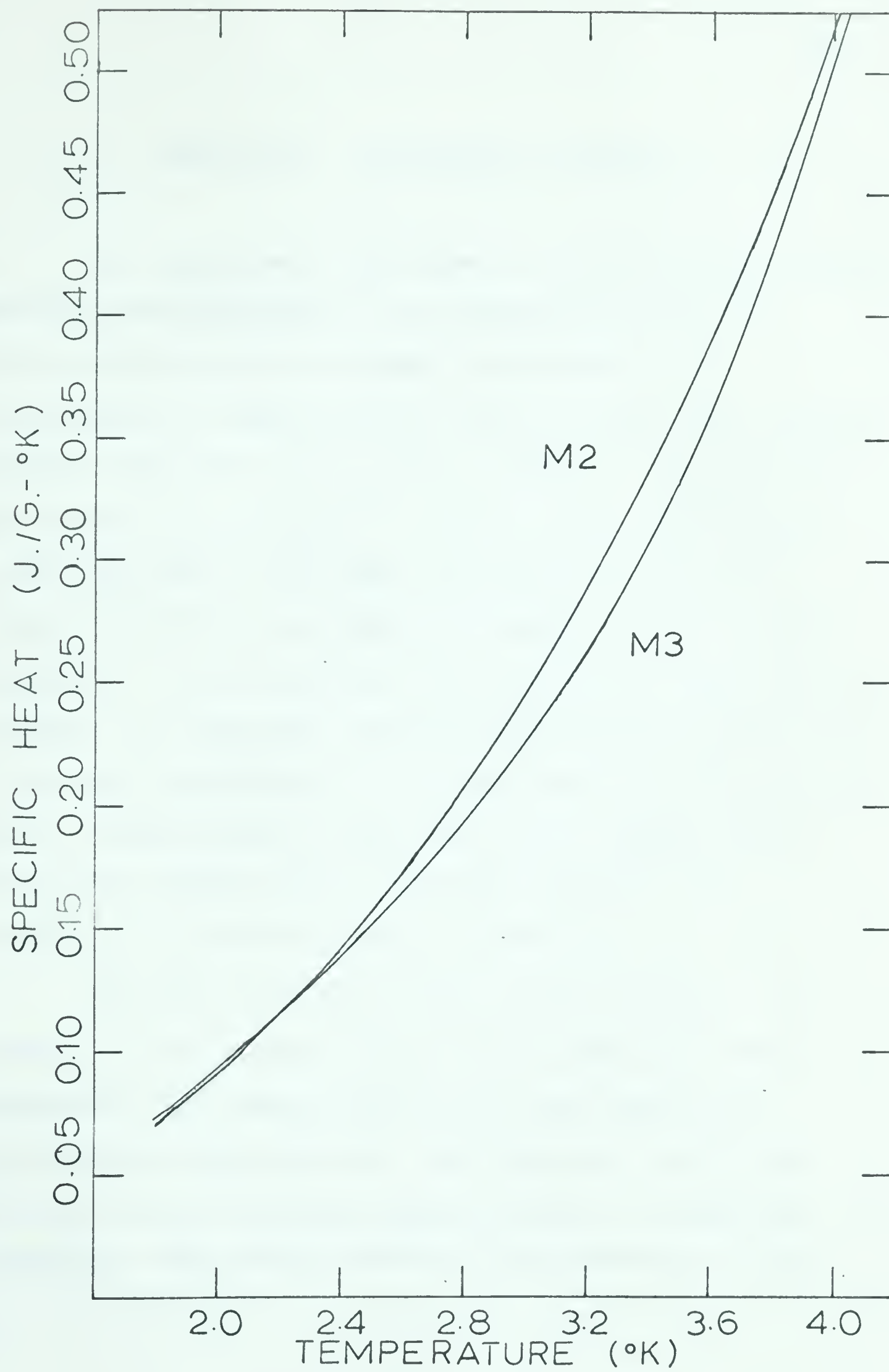
The Specific Heat of Helium Adsorbed in 13X-Zeolite

The specific heat of helium adsorbed in 13X-Zeolite (326 c.c. (S.T.P.) per gram of zeolite as weighed) is plotted against temperature.

M2 - the curve obtained from the corrected curve in Figure 17.

M3 - the curve obtained from the corrected curve in Figure 18.

The error in the results is approximately $\pm 20\%$.



Chapter 8. DISCUSSION OF RESULTS

The experiments described in the preceding chapters consist of the measurement of an adsorption-desorption isotherm of helium four adsorbed in 13X-zeolite at approximately 4.1 degrees Kelvin and two other less accurate adsorption isotherms at 4.1 and 2.1 degrees in the pressure range between P/P_0 equal to 0.002 and 0.98. In addition the specific heat of 326 cubic centimeters (S.T.P.) of helium four adsorbed per gram (as weighed) of 13X-zeolite was measured. The experiments have shown that significant quantities of helium are adsorbed at low relative pressures and that the specific heat of helium adsorbed in the zeolite lattice is significantly below that of the bulk liquid. Before these results can be discussed properly, the structure of the zeolite must be considered.

The shape and size of the zeolite cavity is very important in the interpretation of the results of these experiments. Each large cavity is at the centre of a tetrahedron of large cavities; therefore each cavity has four rather large entrances, approximately 7.5 angstroms (17) in diameter. The cavity cannot be considered as a single,

isolated unit but must be considered more as a member of an interconnected mesh of like cavities. Similarly, the adsorbed helium cannot really be considered as a film on the surface of a solid but is more like a network of filaments connecting periodic bulges.

A very rough estimate of the number of helium atoms that can fit inside the cavities can be obtained by considering them as spheres. From Dubinin's (18) estimate of the cavity size, each large cavity has a volume of approximately 813 cubic angstroms and each small cavity a volume of 150 cubic angstroms. The spherical radius of these cavities is respectively 5.79 angstroms and 3.30 angstroms. If the atoms are assumed to be packed either in a hexagon or in a square so that there is no overlap between layers, the atomic distribution can be calculated. The results are shown in Table 3. A question mark indicates there is some doubt that the molecules listed could enter the cavity at that time. A variety of radii for the helium atoms have been chosen rather arbitrarily from several sources. As can be seen from the table, it is very doubtful that the small cavities contain any adsorbed helium atoms, and the probability becomes less as the effective size of helium atom increases.

Table 3 Helium Atoms in 13X-Zeolite Cavities

Helium Atom				Large Cavity					Small Cavity		
Diameter (Å)	Ref.	SP (Å ²)	A HP (Å ²)	LN	R (Å)	S (Å ²)	SP N	HP	R (Å)	S (Å ²)	N SP
3.70	99	13.7	11.9	1 2	3.94	195	14 1	16or17 2?			4?
3.55	100	12.6	11.0	1 2	4.01 0.5	202	16 1	18 or 2?			4?
3.30		10.9	9.4	1 2	4.14 0.84	216	19 2?	23			4?
3.20		10.2	8.9	1 2	4.19 0.99	221	22 2?	25			4?
3.00		9.0	7.8	1 2	4.29 1.29	232 20.9	26 2	30 3			4?
2.84	38	8.07		1 2	4.37 1.53	240 29.5	30 4		1.88	44.5	6
2.35	35	5.52		1 2 3	4.61 2.26	267 64.2	49 12 1?		2.12	56.5	10 1?

LN - layer no. from cavity wall
A - area occupied by the atom
HP - hexagonal packing
SP - square packing
N - no. of atoms in layer

R - Radius from cavity centre to half-depth of layer
S - Surface area of layer at half-depth
? - there is some doubt that the atoms can enter the cavity

The interaction of the helium atom with the cavity is essentially a Van der Waals interaction; however, since the wavelength of helium is about eight angstroms at liquid-helium temperatures, it is hard to imagine the interaction being described in terms of the nearest-neighbour approximation. The potential to describe the interaction of helium with the zeolite lattice must describe the following effects: the effect that the walls of at least an entire zeolite cavity have on an adsorbed helium atom and the effect that the other helium atoms in the cavity have on a particular helium atom. In addition, the description must be quantum mechanical. The adsorption and specific-heat results can now be considered with the above perspective.

At the lowest observable pressures in the isotherms reported here only one or two layers of helium could be adsorbed on the outer surface of the zeolite. Thus the maximum amount adsorbed in the cavities must be somewhere between the amount adsorbed at the lowest pressure recorded and the maximum amount adsorbed if the isotherm was taken to saturation. Thus for the first sample, 0.202 grams of 13X-zeolite, the volume of gas adsorbed at four degrees was between 69 and 71 cubic centimeters (S.T.P.); at two degrees it was between 70 and 73 cubic centimeters. Similarly for the second sample, weighing 0.516 grams, somewhere

between 174 and 195 cubic centimeters (S.T.P.) of helium were adsorbed in the cavities.

The amount adsorbed in the cavities depended on the amount adsorbed on the outer surface of the zeolite. This could have been checked roughly by using completely hydrated zeolite in an isotherm. Until multilayer adsorption is present, the surface contributions should be less than one per cent. Since the surface has an area of from one to three square meters* per gram, the layer on the surface would contain between 1.1 and 3.3×10^{19} atoms per gram-layer** or 0.4 to 1.1 cubic centimeters (S.T.P.) per gram-layer if the area of the helium atom be nine square-angstroms. At pressures near the saturation pressure multilayers of helium can be thirty or more atoms thick (101). Thus much of the gas adsorbed in the pressure range of these isotherms could have been adsorbing on the surface and not in the cavities. The cavities are certainly filled to a large degree at pressures lower than those observable on the manometers.

In Table 4 the density of the helium adsorbed in the zeolite cavities is calculated from these results.

* manufacturer's specifications

** A gram-layer is the adsorbate atoms or molecules adsorbed to form a film one atom(molecule) deep on the surface of one gram of the adsorbent.

Table 4

Helium Adsorbed in Zeolite Cavities

Sample	c.c. (STP) of He adsorbed	He atoms per unit cell of zeolite	He atoms in one large and one small cavity	Wt. of gas (10^{-2} g.)	vol. available for adsorption (10^{-1} c.c.)		density (grams/cc.)	
					a	b	a	b
1 (0.202 g.)	68	202	25	1.21	.691	.584	.176	.208
	70	208	26	1.25			.181	.212
	73	218	27	1.30			.188	.223
2 (0.516 g.)	174	203	25	3.11	.77	1.49	.176	.209
	195	227	28	3.48			.197	.234

a - all cavities

b - large cavities

To perform the calculations the number of cavities was estimated by assuming both samples weighed twenty-five per cent less than the hydrated weight at the time of weighing; however, no allowance has been made for the volume occupied by the residual water in the cavities. The error introduced by this was not over ten per cent as the zeolite was at least ninety per cent dehydrated. Because the position of these water molecules is not known, the effect they have on the density is unknown. For instance, if the residual, water molecules are contained in the small cavities and the helium is adsorbed only in the large cavities, there is no change in the density of helium for case b, Table 4.

From Tables 3 and 4 it appears that little more than a "monolayer" is adsorbed in the large cavities. Apparently the helium atom has an effective diameter slightly over three angstroms in this system. The effect of increased pressure on the packing is slight for the pressures observed.

Whether helium is adsorbed in the small cavity or not is questionable. Sodium ions close the entrances to the small cavities almost entirely. Water enters one of these cavities by hydrating a sodium ion and floating it from the entrance. It is doubtful that helium can do this when the cell is almost completely dehydrated.

There is a fairly high probability that the density of the adsorbed helium is below that of solid helium. At four degrees, the minimum density of solid helium, the density along the melting line, (102) is 0.231 grams per cubic centimeter and the density of liquid helium at the same pressure is 0.217 grams per cubic centimeter. At two degrees the respective densities are 0.197 and 0.184 grams per cubic centimeter. Unless there is very little adsorption on the surface the helium in the cavities is almost certainly at a liquid density at 4°K even when the relative pressure is high. The situation is less optimistic at the lower temperature. For the density of the adsorbed helium to be in the liquid-density range there must either be significant surface adsorption even at low pressures or the small cavities must be accessible to helium atoms.

The experimental accuracy was not great enough to determine the temperature dependence of the isotherms. It seems fairly safe to conclude that the powder adsorbed at least the amount of gas at two degrees as it did at four for a given relative pressure.

Because of the interest in capillary condensation in small pores an adsorption-desorption cycle was carried out. If the condensation occurs the pore is filled with

adsorbate at one pressure but the adsorbate is not desorbed until a lower pressure; hence, a reproducible hysteresis loop is formed. Since the adsorbate is often viewed as being in a liquid state, an equation linking the pore radius with the condensation pressure has been developed. This equation, the one for the so-called Kelvin radius, is

$$\ln P_0/P = 2 M S \cos\theta / (RT \rho r_k), \quad (103)$$

M being the molar mass, ρ the density of the liquid, S the surface tension, R the gas constant, T the temperature, r_k the pore-radius, and θ the angle of wetting between the adsorbate and the adsorbent. If the angle of contact between the adsorbed helium and the surface of the cavities were zero, then from the above equation the hysteresis loop should be visible somewhere between the relative pressures, P/P_0 , 0.48 and 0.26. The spread in the calculated values is caused by the uncertainty as to what part of the large cavity would control the capillary condensation. Within the experimental error of the isotherm measurements no hysteresis was observed. The non-appearance of the hysteresis loop could be explained in several ways. Firstly the pores could easily have been filled at lower relative pressures. Secondly, the open structure of the large cavities with four entrances would not be conducive to

capillary condensation. Thirdly, the hysteresis loop could occur at very low relative pressures beyond the pressure-measurement range available in the present experiments.

The densities calculated from the isotherm measurements (Table 4) indicate that if the small cavity is unavailable to helium atoms there should be a solid-liquid-phase change between two degrees and four degrees. This is assuming, without any foundation, that the phase-density relation in the bulk is also present in the film. If there is not a solid-liquid-phase transition then, unless the cavities are inhibiting the ordering of the helium atoms in some way, a lambda transition should occur at a reduced temperature. No phase transition was observed in the crude measurements taken in these experiments. That the lambda transition was not observed is not surprising as the filaments of helium are so thin and the relative pressure is so low that the phase transition would be at a lower temperature than could be observed on the present cryostat. The lowest temperature at which measurements were taken was approximately 1.8°K . Any lower temperature measurements attempted had to be discarded because considerable amounts of gas desorbed from the walls of the calorimeter during these measurements. In film-flow experiments the transition temperature is approximately 1.1°K (Figure 3) (9) at a

relative pressure, P/P_0 , equal to 0.2. At four degrees the relative pressure of helium contained in the specific-heat, zeolite sample was about 0.006. Thus even allowing for the fact that the shift in the lambda transition is smaller for a given relative pressure in specific-heat experiments than in flow experiments, the lambda transition, if it be there, would not be in the temperature range observable on the cryostat used.

A comparison of the specific-heat results of the adsorbed helium shows that they are much lower than those of the bulk liquid and that, although they are approximately equivalent to the specific heat of solid helium having a density of 0.219 grams per cubic centimeter at two degrees, they are lower at higher temperatures. This means that near four degrees the zeolite lattice is interacting very strongly with the adsorbed helium. The comparison is shown in Table 5.

Lambert's data (22) for helium three were also much lower than that for the bulk liquid and showed a smaller temperature variation than did the solid (109). In his article he indicated that his results for helium four were very low but did not give enough information to make a good comparison.

Table 5

Comparison of Some Specific Heats of Helium

Temperature	Specific Heat (Joules/gram-°K)			Lambert's (22) Experiment
	Liquid	Solid	Adsorbed	
			This Experiment Method 2	Method 3
1.8	2.81 (104)		0.070	0.069
2.0	5.18	0.084** (105)	0.089	0.091
3.0	2.49	0.41**	0.25	0.23
4.0	3.99		0.52	0.51
0.2*	0.86 (107)			0.11
1.4*				0.98
<0.5	<0.003 (108)	<0.005*** (106)		<0.01

* Helium 3 results
 *** Density 0.214 g./c.c.
 ** Density 0.219 g./c.c.

If the zeolite pellets used by Lambert (22) are assumed to be eighty per cent zeolite which has lost twenty-six per cent of its hydrated weight by dehydration, the density of the helium three in the sample was between 0.089 and 0.105 grams per cubic centimeter. The variation in calculated density results from the uncertainty as to whether the small cavities are available for helium adsorption or not. For the sample used in the specific-heat measurements in the present experiments, the density was between 0.169 and 0.200 grams per cubic centimeter if the zeolite had lost twenty-five per cent of its hydrated weight. The density of the bulk liquids at their boiling points is 0.059 and 0.125 (1) grams per cubic centimeter respectively. The relative compression of the helium three appears to be greater than that of the helium four. Even though the density of helium in the samples used in the adsorption isotherms was greater than that used in the specific-heat sample, the relative density present in Lambert's sample was not attained until fairly high saturations in the present adsorption samples; however, the number of helium-three atoms in each zeolite cavity was smaller than the number of helium-four atoms. Therefore, the zeolite cavities did not completely suppress the differences in statistics and zero-point energy which

exist between the helium isotopes. The fact that the helium in the specific-heat zeolite sample appeared to be at a lower density than that in the adsorption samples was probably caused by the gradual hydration of the zeolite in the storage can (Figure 6). Since the zeolite was only weighed before being dehydrated, this additional hydration would increase the apparent number of unit cells in the sample.

Although the experiments reported here have not shown the properties of helium adsorbed in 13X-zeolite to the desired amount of detail they have given an introduction to the techniques involved and shown that it is worthwhile to construct the equipment necessary to continue the experiments. Many of the difficulties encountered in the present experiments could be overcome by an adsorption apparatus with a good set of temperature controls and a cryostat with a thermal switch (e.g. 110). A complete set of isotherms or a calorimeter in which the pressure is observed during the heat capacity runs is necessary to provide the desorption corrections. A very large helium-four cryostat or preferably, a helium-three cryostat is essential to provide the low temperatures necessary for this study. Relative coverages approximately the same as the one used here should be examined. If a transition

occurred at a higher coverage it would necessarily be attributed to the multilayer of helium on the surface of the powder. Lower coverages at the moment would complicate matters by having less helium in the calorimeter, which would cause poorer thermal contact with the calorimeter and also a lower fraction of the heat capacity would be that of the helium. These experimental results can be regarded as preliminary to the use of the helium-three isotope in 13X with of course the extension of the measurements to lower temperatures.

The specific heat of helium four adsorbed in 13X-zeolite has been measured between 1.8 and 4.2 degrees Kelvin at the coverage of 326 cubic centimeters (S.T.P.) of helium adsorbed per gram of zeolite (as weighed). The adsorption isotherm for helium four in 13X-zeolite has also been determined at approximately 4.1 degrees Kelvin from relative pressures slightly below 0.01 to 0.98. As has been indicated in the foregoing discussion, these results in themselves have not been able to resolve any of the problems connected with the adsorption of helium four in a zeolite, but they are preliminary to a more extensive set of measurements which should yield useful information. The experiments are also a necessary first step before undertaking the adsorption of helium three in

zeolites. Since a more detailed study of this system would do much to resolve the controversy concerning the alleged solid-and-immobile layer in helium films, it is to be hoped that these experiments will be continued in greater detail.

REFERENCES

1. K. R. Atkins, 1959, Liquid Helium, University Press, Cambridge, 1957.
2. W. M. Fairbank, M. J. Buckingham, and C. F. Kellers, 1957, Proc. Fifth Confr. Low Temp. Phys., Madison, Wis., 50. Reviewed by W. M. Farbank, 1963, Rendiconti della Scuola Internazionale di Fisica "Enrico Fermi", 21 Corso, 293.
3. N. Bernades and D. F. Brewer, 1962, Rev. Mod. Phys., 34, 190.
4. V. P. Peshkov, 1964, J.E.T.P., 19, 1023*
1964, Zh. Eksper. Teor. Fiz., 46, 1510.
5. C. T. Lane, 1962, Superfluid Physics, McGraw-Hill, New York, Chapter 5.
6. K. A. Bruekner, 1960, Helium 3, Ohio State, Columbus, 70.
7. L. C. Jackson and L. G. Grimes, 1958, Adv. in Phys. (Suppl. of Phil. Mag.), 7, 435.
8. F. D. Manchester and A. Buckley, 1961, Proc. Seventh Int. Conf. Low Temp. Phys., University of Toronto, Toronto, 519.
9. F. D. Manchester, Proc. Ninth Int. Conf. Low Temp. Phys., Columbus, to be published.
10. A. M. Toxen, 1961, Phys. Rev., 123, 442
11. D. D. Betts, F. D. Manchester, and E. J. Woods, 1964, Physics Letters, 10, 59.
12. A. D. Singh and R. K. Pathria, 1960, Prog. Theor. Phys., 24, 229.
13. R. M. Barrer, F. W. Bultitude, and J. W. Sutherland, 1957, Trans. Faraday Soc., 53, 1111.
14. A. F. Wells, 1962, Structural Inorganic Chemistry, 3rd. Ed., 810, Clarendon Press, Oxford.
15. D. W. Breck and J. V. Smith, 1959. Sci. Amer., Jan., 85.

16. R. M. Barrer, 1938, Proc. Roy. Soc., A167, 392.
17. L. Broussard and D. P. Shoemaker, 1960, J. Am. Chem. Soc., 82, 1041.
18. M. M. Dubinin, 1961, Doklady Akad. Nauk. U. S. S. R.,* 138, 866.
19. R. M. Barrer and G. C. Bratt, 1959, J. Phys. Chem. Solids, 12, 130.
20. M. Santini, 1963, Proc. Eighth Int. Conf. on Low Temp. Phys., Butterworths, London, 59.
21. G. Careri, M. Guira, and M. Santini, 1963, Phys. Letters, 4, 61; 5, 102.
22. M. H. Lambert, 1964, Phys. Rev. Letters, 12, 67; 13, 266.
23. M. Santini and G. Signorelli
G. Careri, Proc. Ninth Int. Conf. on Low Temp. Phys.,
Columbus, to be published.
24. H. Weinstock and C. E. Long, Proc. Ninth Int. Conf. on Low Temp. Phys., Columbus, to be published.
25. D. L. Goodstein, W. D. McCormick, and J. G. Dash, Proc. Ninth Int. Conf. on Low Temp. Phys., Columbus, to be published.
26. D. F. Brewer, A. J. Symonds, and A. L. Thomson, Proc. Ninth Int. Conf. on Low Temp. Phys., Columbus, to be published.
27. T. S. Hill, 1949, J. Chem. Phys., 17, 520.
28. J. A. Morrison, J. M. Los, and L. E. Drain, 1951, Trans. Faraday Soc., 47, 1023.
29. D. M. Young and A. D. Crowell, 1962, Physical Adsorption of Gases, Butterworths, London.
30. W. H. Keesom and J. Schweers, 1941, Physica, 8, 1020; 1032.
31. J. W. Stout and W. F. Giaque, 1938, J. Am. Chem. Soc., 60, 393.
32. A. van Itterbeek, W. van Dingenen, and J. Borghs, 1939, Physica, 6, 951.

33. J. Kistemaker, 1947, Physica, 13, 81.
34. S. Brunauer, P. H. Emmett, and E. Teller, 1938, J. Am. Chem. Soc., 60, 309.
35. H. P. R. Frederikse and C. J. Gorter, 1950, Physica, 16, 402.
36. A. J. Strauss, 1952, Thesis, Chicago. Reviewed by E. Long and L. Meyer, 1953, Adv. in Physics (Suppl. of Phil. Mag.), 2, 1.
37. E. Long and L. Meyer, 1949, Phys. Rev., 76, 440.
38. W. D. Schaeffer, W. R. Smith, and C. R. Wendall, 1949, J. Am. Chem. Soc., 71, 863.
39. S. V. R. Mastrangelo and J. G. Aston. 1951, J. Chem. Phys., 19, 1370.
40. L. Meyer, 1956, Phys. Rev., 103, 1593.
41. R. Bowers, 1953, Phil. Mag., Ser. 7, 44, 485.
42. J. P. Hobson, 1959, Can. J. Phys., 37, 300.
43. W. A. Steele, 1956, J. Chem. Phys. 25, 819.
44. R. P. Singh and W. Band, 1955, J. Phys. Chem., 59, 663.
45. J. G. Aston, S. V. R. Mastrangelo, and R. J. Tykodi, 1955, J. Chem. Phys., 23, 1633.
46. D. White, C. Chou, H. L. Johnston, 1952, J. Chem. Phys., 20, 1819.
47. H. H. Tjerkstra, F. J. Hoofman, and C. J. N. van den Meydenberg, 1953, Physica, 19, 935.
48. D. F. Brewer and K. Mendelssohn, 1953, Phil. Mag. Ser. 7, 44, 340.
49. E. L. Pace and A. R. Siebert, 1960, J. Phys. Chem., 64, 961.
50. J. Greyson and J. G. Aston, 1957, J. Phys. Chem., 61, 610.
51. M. Ross and W. A. Steele, 1960, J. Chem. Phys., 33, 464;
1961, J. Chem. Phys., 35, 850,
862, 871.

52. C. J. Hoffman, F. J. Edeskuty, and E. F. Hammel, 1956, J. Chem. Phys., 24, 124.
53. S. Brunauer, 1943, Adsorption of Gases and Vapors Vol. 1, Princeton University Press, Princeton, p. 394.
54. G. L. Kington and P. S. Smith, 1964, Trans. Faraday Soc. 60, 705; 721.
55. D. F. Brewer and D. C. Champeney, 1962, Proc. Phys. Soc. 79, 855.
56. J. R. Dacy and M. H. Edwards, 1964, Can. J. Phys. 42, 241.
57. H. P. R. Frederikse, 1950, Thesis, Leiden;
1949, Physica, 15, 860.
58. S. V. R. Mastrangelo, 1951, Thesis, Pennsylvania State.
59. D. F. Brewer, D. C. Champeney, and K. Mendelssohn, 1960, Cryogenics, 1, 108.
60. J. A. Morrison and L. E. Drain, 1951, J. Chem. Phys., 19, 1063.
61. J. A. Morrison, L. E. Drain, and J. S. Dugdale, 1952, Can. J. Chem., 30, 890.
62. P. H. Keesom and G. Seidel, 1958, Phys. Rev., 111, 422.
63. J. Aslanian and L. Weil, 1963, Cryogenics, 3, 36.
64. E. Long and L. Meyer, 1952, Phys. Rev., 85, 1030.
1955, Phys. Rev. 98, 1616.
65. D. F. Brewer and K. Mendelssohn, 1961, Proc. Roy. Soc. (London), A260, 1.
66. K. R. Atkins, H. Seki and E. U. Condon, 1956, Phys. Rev., 102, 582.
67. J. Ziman, 1953, Phil. Mag. Ser. 7, 44, 548.
68. C. E. Hecht, 1958, Physica, 24, 584.
69. C. E. Hecht, 1958, Physica, 24, 1023.

70. L. I. Schiff, 1941, Phys. Rev., 59, 839.
71. K. R. Atkins, 1954, Can. J. Phys., 32, 347.
72. S. Franchetti, 1957, Nuovo Cimento Ser. 10, 5, 183.
73. H. Matsuda and C. J. N. van den Meijdenberg, 1960, Physica, 26, 939.
74. S. Franchetti and A. Mazza, 1962, Nuovo Cimento, Ser. 10, 26, 1010.
75. V. L. Ginzburg and L. P. Pitaevski, Zh. Eksper Teor Fiz., 34, 1240. (1958), 1958, J. E. T. P., 7, 853*.
76. E. A. Lynton, 1962, Superconductivity (Chapter 5), Menthuen and Company Ltd., London.
77. D. H. Douglass, Jr., 1962, I.B.M. J. Research Develop-
ment, 6, 44.
78. Handbook of Chemistry and Physics, 1961, Chemical Rubber Publishing Company, Cleveland, ed. 43.
79. W. A. Rogers, R. S. Buritz and D. Alpert, 1954, J. Appl. Phys., 25, 868.
80. W. D. Harkins, Physical Chemistry of Surface Films, 1952, Reinhold Publishing Company, p. 227.
81. W. E. Keller, 1955, Phys. Rev., 97, 1
82. J. E. Kilpatrick, W. E. Keller, and E. F. Hammel, 1955, Phys. Rev., 97, 9.
83. The 1958 He⁴ Scale of Temperatures, 1960, NBS monograph 10.
84. T. R. Roberts and S. G. Sydorik, 1956, Phys. Rev., 102, 304.
85. R. D. Present, Kinetic Theory of Gases, 1958, McGraw-Hill, New York, 266.
86. F.E. Hoare, L. C. Jackson, and N. Kurti, 1961, Experimental Cryophysics, Butterworths, London, Chapter 6.
87. R. Bremer, E. L. Foster, H. M. Rosenberg, 1955, Brit. J. Appl. Phys., 6, 181.

88. J. A. Buckley, 1960, Thesis, University of Alberta.
89. G. K. White, 1959, Experimental Techniques in Low Temperature Physics, Clarendon Press, Oxford, 205.
90. T. M. Dauphinee and E. Mooser, 1955, Rev. Sci. Instr. 26, 660.
91. T. M. Dauphinee and S. B. Woods, 1955, Rev. Sci. Instr., 26, 693.
92. T. M. Dauphinee, 1953, Can. J. Phys., 31, 577.
93. W. H. Keesom and S. Kurrelmeyer, 1939, Physica, 6, 633.
94. W. H. Keesom and J. A. Kok, 1932, Proc. Kon. Akad. Amsterdam, 35, 294.
95. H. D. Vasileff, 1952, J. Appl. Phys., 23, 979.
96. A Compendium of the Properties of Materials at Low Temperatures, Phase I, Part II, 1960, National Bureau of Standards.
97. L. J. Challis and J. D. N. Cheeke, 1964, Proc. Phys. Soc. London, 83, 109.
98. W. S. Corak, M. P. Garfunkel, C. B. Satterthwaite, and A. Wexler, 1955, Phys. Rev., 98, 1699.
99. D. G. Hurst and D. G. Henshaw, 1955, Phys. Rev., 100, 994.
100. W. H. Keesom and K. W. Taconis, 1938, Physica, 5, 161.
101. E. Long and L. Meyer, 1952, Adv. in Phys. (Suppl. Phil. Mag.) 2, 1.
102. C. Domb and J. S. Dugdale, 1957, Prog. Low Temp. Phys., 2, 338.
103. Kelvin, Lord, Phil. Mag. 42, 448, (1881).
104. R. W. Hill and O. V. Lounasmaa, 1957, Phil. Mag. Ser. 8, 2, 143.
105. W. H. Keesom and Miss A. P. Keesom, 1936, Physica, 3, 105.

106. F. J. Webb, K. R. Wilkinson, and J. Wilks, 1952, Proc. Roy. Soc., A 214, 546.
107. M. Strongin, G. O. Zimmerman, and H. A. Fairbank, 1962, Phys. Rev., 128, 1983.
108. J. Wiebes, C. G. Niels-Hakkenberg, and H. C. Kramers, 1957, Physica, 23, 625.
109. E. C. Heltemes and C. A. Swenson, 1962, Phys. Rev., 128, 1512.
110. F. D. Manchester, 1959, Can. J. Phys., 37, 989.
111. J. R. Clement and E. H. Quinell, 1952, Rev. Sci. Instr., 23, 213.

Appendix I

Oil Density

During the work on the calibration of a resistance thermometer (Appendix II), comparison of oil-and mercury-manometer readings showed that the density of the oil was not the same as that given by the manufacturer. The density of a sample of Apiezon B* from the same bottle was measured roughly using a water bath, the temperature of which could be controlled to about 0.1°C , and a specific-gravity bottle with a measured volume of approximately 25.09 c.c. The results corrected for buoyancy are shown in Table 6.

Table 6

Density of Apiezon B

Temperature ($^{\circ}\text{C}$)	Density (g./cm. ³)
16.4	0.8738
17.9	0.8731
20.0	0.8716
22.5	0.8701
26.0	0.8683

* Apiezon B was the oil used in the manometers.

Appendix II

Calibration of the Germanium Thermometer

The thermometer was calibrated, when it was in good thermal contact with the helium pot*, using a measuring current of two microamperes by comparing its resistance value with the vapour pressure of the helium pot as recorded by either a mercury or an oil manometer. The same cathetometer used for the adsorption experiments was used to measure the manometer pressure. While the comparison was being made, the pot was held at nearly constant temperature by adjusting one or more of the valves which controlled the pumping speed of the helium-pot system.

The first two calibration runs, Runs 1 and 2, were done with the thermometer mounted on a copper block having a manganin-wire heater wrapped around it. The block was suspended and wired in the same manner as the calorimeter (Chapter 5). Indeed, on the second run with this configuration the apparatus was tested by making a few heat-capacity determinations. Unfortunately, the thermal contact using this suspension was not good enough to calibrate the thermometer. Another run, Run 3, was done with the thermometer mounted on a post attached to the

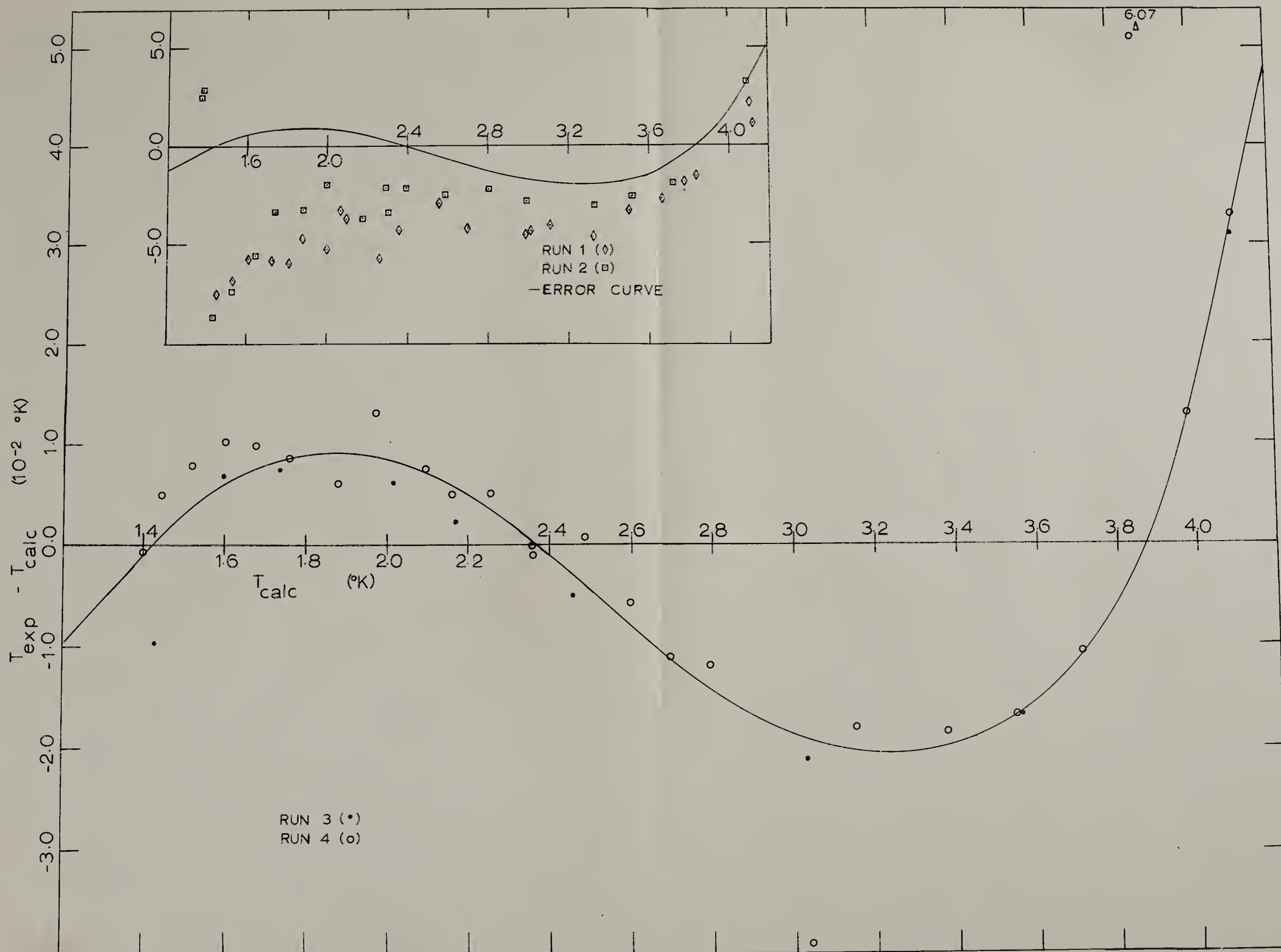
* Chapter 5

Figure 20

The Error Curve for the Thermometer Calibration

The residuals ($T_{\text{exp}} - T_{\text{calc}}$) are plotted against T_{calc} for the third and fourth runs. The solid curve is the error curve used to calculate temperatures. The inset shows the residuals of the first two runs compared with the error curve. The two points above the error curve near 1.4°K were obtained by cooling directly from four degrees to the lowest temperature attainable.

The units in the inset are the same as those for the main graph. The confidence limits are not shown on the graph.



bottom of the helium pot (Fig. 11). The thermal contact, while not ideal, was sufficient to obtain a fairly good calibration of the thermometer. To check the reproducibility of the calibration after the thermometer had been warmed to room temperature, another run, Run 4, was carried out.

The results of the third calibration run were fitted to the semi-empirical curve

$$1/T = a \log_{(10)} R + b + c/\log_{(10)} R \quad (111)$$

by the 1620 version of the standard Computing Centre Multiple Regression Program (G-2010) written by K. Smillie. This gave

$$a = 1.0287272, \quad b = -4.4800306 \text{ and } c = 5.3120814.$$

As the library program did not calculate residuals, a program was written to obtain the difference between the vapour-pressure temperature, T_{exp} , as determined from the 1958 helium-four temperature scale, and the temperature, T_{calc} , calculated from the fitted curve. A plot of $(T_{\text{exp}} - T_{\text{calc}})$ against T_{calc} was made for all the runs (Fig. 20). The residuals of the first two runs showed so much scatter that they were discarded. In spite of some scatter in the points of the last two runs a fairly good

Table 7. Thermometer Calibration

Run 3

Resistance Ω ($\pm .03\%$)	$T_{\text{exp.}}$ ($\pm .0005^{\circ}\text{K}$)	$T_{\text{calc.}}$ ($\pm .001^{\circ}\text{K}$)	$T_{\text{exp.}} - T_{\text{calc.}}$ ($\pm .001^{\circ}\text{K}$)
421.1	4.1315	4.1006	.0309
564.3	3.5403	3.5571	-.0168
771.8	3.0082	3.0294	-.0212
1168	2.4502	2.4552	-.0050
1508	2.1716	2.1693	.0023
1764	2.0223	2.0162	.0061
2461	1.7466	1.7392	.0074
3018	1.6035	1.5968	.0067
3990	1.4196	1.4295	-.0099

curve, the error curve, could be drawn through them; this was used to obtain T_{exp} from $T_{\text{calc.}}$

Since only nine points were taken in the third run, no scatter was observable; however, in the fourth run having more points, there was considerable scatter. There also appeared to be a slight shift in the thermometer calibration between the last two runs. The scatter in the points made the estimation of the magnitude of this shift difficult.

Table 8. Thermometer Calibration

Run 4

Resistance Ω ($\pm .03\%$)	$T_{\text{exp.}}$ ($\pm .0005^{\circ}\text{K}$)	$T_{\text{calc.}}$ ($\pm .001^{\circ}\text{K}$)	$T_{\text{exp.}} - T_{\text{calc.}}$ ($\pm .001^{\circ}\text{K}$)
420.2	4.1376	4.1046	.0330
449.2	3.9919	3.9790	.0129
477.4	3.9254	3.8647	.0607
518.9	3.6991	3.7098	-.0107
568.3	3.5276	3.5444	-.0168
626.6	3.3538	3.3724	-.0186
715.8	3.1312	3.1493	-.0181
905.3	2.7792	2.7912	-.0120
970.3	2.6833	2.6944	-.0111
1044	2.5908	2.5966	-.0058
1139	2.4868	2.4860	.0008
1264	2.3604	2.3617	-.0013
1267	2.3585	2.3589	-.0004
1385	2.2642	2.2592	.0050
1522	2.1647	2.1598	.0049
1624	2.1024	2.0950	.0074
1846	1.9878	1.9747	.0131
2052	1.8889	1.8829	.0060
2384	1.7716	1.7631	.0085
2685	1.6859	1.6761	.0098
2989	1.6135	1.6032	.0103
3407	1.5284	1.5206	.0078
3872	1.4511	1.4461	.0050
4198	1.4012	1.4020	-.0008

Since the resistance was measured to about 0.03 per cent, T_{calc} could be calculated to one millidegree or better. From the vapour-pressure measurement T_{exp} was calculated to 0.5 millidegrees. However the scatter in the results indicated that uncalculated errors existed. For this reason the absolute value of the temperature was probably known only to about 0.02°K . A small temperature change can be calculated much more accurately than an absolute temperature because the error curve must change smoothly. Thus a temperature change of a tenth of a degree could be measured to at least three millidegrees even with the larger uncertainty in the absolute temperature. For the purposes of these experiments, this was adequate.

Because of the design of the calorimeter and cryostat further calibration could not be done during each heat-capacity run. Since the germanium thermometer was supposed to give results reproducible to 0.005°K and because time was short, no further calibrations were done on the thermometer.

Appendix III

Results of Adsorption Experiments

The results of the isotherm experiments are shown in Tables 9 and 10. Letters A, B, and C above columns in the tables refer to the method of calculating the dead-space corrections (Chapter 4, p. 59).

The over-all error in the amount of gas in the sample chamber section is between one and ten per cent in both tables (*).

The error in the room-temperature volume of the sample chamber is about three per cent in Table 9 (**).

The over-all error in the amount of gas adsorbed is between one and ten per cent in Table 10 (***).

The error in temperature is approximately $\pm .0005^{\circ}\text{K}$ and the error in pressure is $\pm .01$ mm. of Hg.

Table 9: Adsorption of Helium in Sample 1 at 4.1 and 2.1°K
(wt. of Zeolite 0.202 g.)

Temperature, T, (°K)	P/P ₀	Vol. of He in sample chamber section*	Vol. of He dead space (S.T.P., cc.)**			Vol. of He adsorbed** (S.T.P. cc.)		
			A	B	C	A	B	C
At 4.1°	4.1260	72.4	3.8	3.8	3.8	68.6	68.6	68.6
	4.1295	95.8	25.2	25.6	25.6	70.5	70.2	70.2
	4.1359	115	44	45	45	71	70	70
	4.1357	150	76	79	79	74	71	71
	4.1348	180	103	109	109	77	72	72
	4.1362	243	157	172	172	86	71	71
	4.1287	307	209	238	237	98	69	69
	4.1407	367	252	296	296	115	71	72
	4.1436	432	300	368	365	132	64	67
	4.1462	486	334	425	420	152	61	66
	4.1361	542	365	483	474	177	59	67
	4.0991	605	403	568	548	203	37	57
	4.1381	68.8	1.3	1.3	1.3	67.5	67.5	67.5
	4.1367	76.4	7.4	7.4	7.4	69.0	68.9	68.9
	4.1209	65.1	.3	.3	.3	64.8	64.8	64.8
at 2.1°	2.1290	72.0	.9	.9	.9	71.1	71.1	71.1
	2.1243	83.8	11.0	11.2	11.2	72.7	72.6	72.6
	2.1291	92.9	19.5	19.9	19.9	73.4	72.9	72.9
	2.1265	71.2	1.4	1.4	1.4	69.8	69.8	69.8

Table 10: Adsorption and Desorption of Helium in Sample 2
(wt. of Zeolite 0.516 g.) at 4.1°

Pressure P (mm. Hg.)	Tempera- ture, T, (°K)	P/P ₀	Vol. of He in sample chamber* section	Vol. of He dead space (S.T.P., cc.)			Vol. of He adsorbed*** (S.T.P., cc.)		
				A	B	C	A	B	C
0?	4.1278		137	0.0	0.0	0.0	137	137	137
6.74	4.1313	.0096	176	0.9	0.9	0.9	175	175	175
44.48	4.1332	.0633	186	6.0	6.1	6.1	180	180	180
78.47	4.1138	.1137	192	11	11	11	181	181	181
118.32	4.1545	.1649	199	16	16	16	183	183	183
149.46	4.1572	.2078	205	20	21	21	185	184	184
192.00	4.1568	.2670	212	26	27	27	186	185	185
249.81	4.1530	.3488	223	34	36	36	189	186	186
322.61	4.1301	.4603	236	43	48	48	193	188	188
395.01	4.1390	.5588	251	54	62	62	197	189	189
481.28	4.1220	.6920	270	65	78	78	205	192	192
545.44	4.1349	.7746	285	74	92	91	211	193	194
618.86	4.1435	.8716	304	84	109	107	220	195	197
705.09	4.1484	.9884	330	95	134	129	235	197	202
642.13	4.1438	.9042	309	86	114	112	223	195	197
551.85	4.1282	.7888	285	74	93	92	210	192	193
438.58	4.1336	.6236	260	61	71	71	199	189	189
349.02	4.1206	.5025	242	47	53	53	195	189	189
268.52	4.1394	.3797	227	37	40	40	190	187	187
204.81	4.1201	.2950	215	28	29	29	187	185	185
150.79	4.1141	.2185	205	21	21	21	185	184	184
104.40	4.1286	.1492	197	14	15	15	183	182	182
64.70	4.1369	.0917	190	8.9	9.1	9.1	181	181	181
32.32	4.1419	.0456	183	4.3	4.4	4.4	179	179	179
17.47	4.1502	.0244	180	2.4	2.4	2.4	177	177	177
10.61	4.1413	.0150	178	1.4	1.5	1.5	176	176	176
4.73	4.1744	.00657	175	.6	.6	.6	174	174	174
1.56	4.1394	.00220	172	.2	.2	.2	172	172	172
.73	4.1634	.00101	170	.1	.1	.1	170	170	170

Appendix IV

Sample Calculation of Heat-Capacity Point

The symbols are defined in Figure 21.

I. Sensitivity

The sensitivity of the chart recorder at a particular equilibrium resistance could be calculated from

$$(1/S(R)) = \frac{\Delta_0}{R_1 - R_2} \quad \text{or} \quad (1/S(R)) = \frac{\Delta_5}{R_3 - R_4}$$

These results were graphed to smooth the scatter and to obtain S for particular values of R .

II. Effective Resistances

The effective resistance at the beginning of the heating period is calculated from

$$R_{e1} = R_2 + \Delta_2 S(R_a),$$

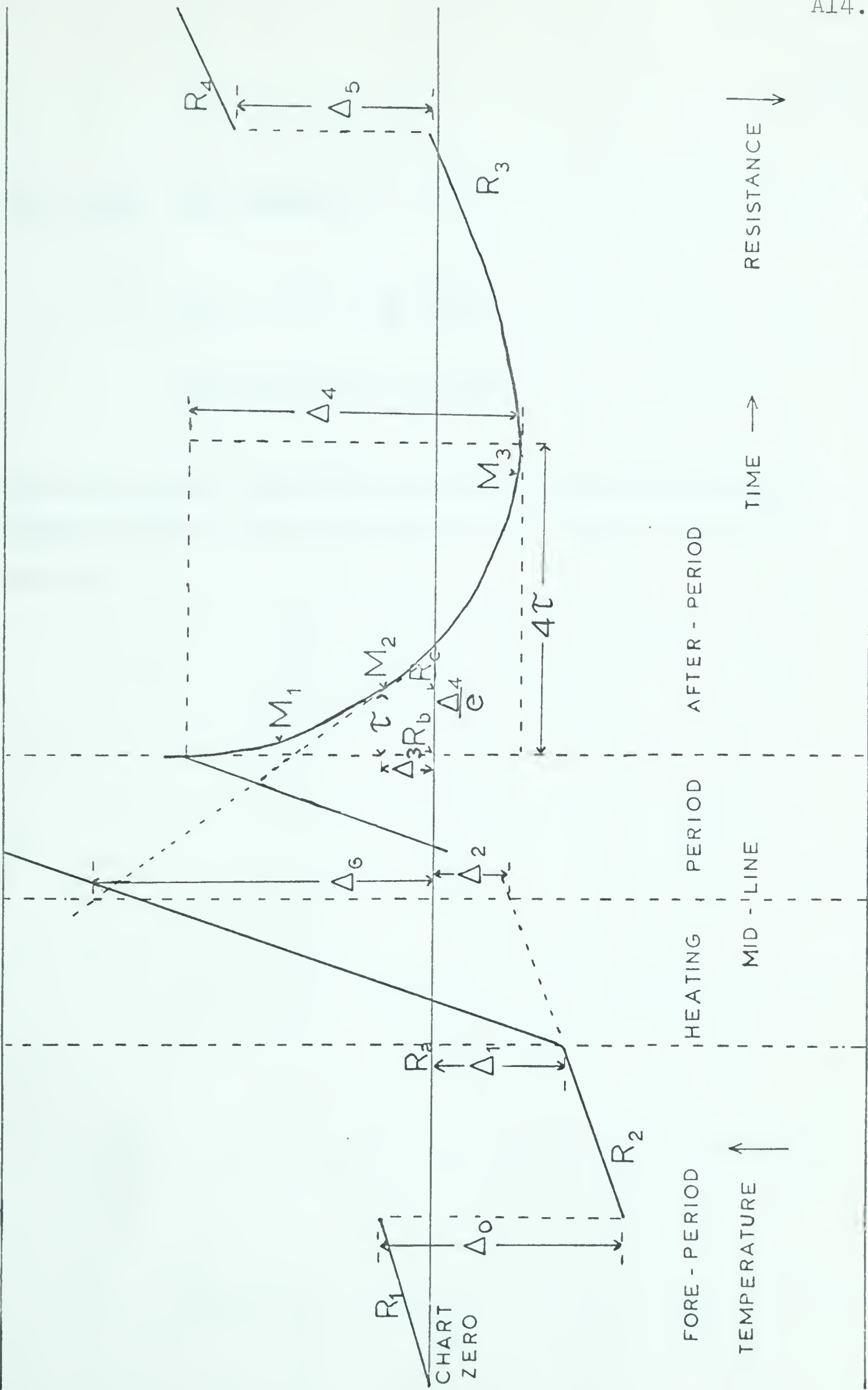
$$R_a \text{ being } R_2 + \Delta_1 S(R_a).$$

The effective resistance at the end of the heating period was calculated by extending the tangent from one of $M1$,

Figure 21

Schematic Diagram of Heat-Capacity Point

The diagram indicates the selection of the points from which the after-period tangent was extended, M1, M2 and M3 referring to Methods 1, 2 and 3 (Chapter 7). The resistances, R_a and R_b , are the equilibrium resistances at the beginning and end of the heating period; R_c the equilibrium resistance at the point M2. The peak at the time the heat was switched off was caused by electronic noise in the switch.



M2, or M3. For example

$$R_{e2} = R_3 - \Delta_5 S(R_c) ,$$

$$R_c \text{ being } R_3 - \Delta_3 S(R_c)$$

The resistances R_{e1} and R_{e2} were used to calculate the temperatures at the beginning and the end of the heating period.

Appendix V

Heat-Capacity Results

An asterisk beside a point indicates that it was disregarded in the graphical fit. M2 and M3 are the methods of analyzing heat-capacity points defined in Chapter 7.

The confidence limits are approximately ten per cent on the heat capacity and one per cent on the temperature. Because the mechanical accuracy is theoretically greater than this (Appendix II and Chapter 7) the points have been quoted to more than the allowed number of figures.

Table 11. Heat Capacity Results of Run A
(Helium-filled calorimeter)

Pt. No.	H e a t e r		I n p u t Time ($\pm .02$ sec.)	Heat Capacity (10^{-3} joules/ $^{\circ}$ K)		Temperature ($^{\circ}$ K)	
	($\pm .00001$ mamps.)	($\pm .00001$ volts)		M3	M2	M3	M2
43	.11078	.10997	103.91	15.09	16.13	2.757	2.755
44	.11078	.10997	104.08	15.85	16.57	2.809	2.808
45	.11078	.10996	100.19	16.36	16.74	2.853	2.852
46	.11077	.10996	130.85	17.08	18.88	2.909	2.904
47	.11077	.10996	107.82	17.70	18.63	2.970	2.969
49	.11076	.10994	99.91	15.78	16.53	2.801	2.799
50	.11075	.10993	118.62	16.45	17.44	2.854	2.852
51	.11075	.10993	99.98	17.10	17.85	2.923	2.921
53	.11055	.10974	147.01	18.62	19.39	3.041	3.039
54	.12768	.12675	139.98	19.80	20.46	3.135	3.133
55	.12767	.12674	151.18	21.27	22.10	3.237	3.235
56	.14739	.14633	116.47	22.75	23.59	3.334	3.332
57	.14738	.14632	141.40	24.51	25.22	3.436	3.434
58	.14737	.14630	99.08	25.58	26.67	3.518	3.516
59	.14735	.14628	129.41	27.06	28.82	3.593	3.589
60	.14733	.14628	141.30	28.76	29.39	3.672	3.670
61	.14731	.14627	152.90	30.45	30.45	3.760	3.760
62	.17822	.17696	127.18	31.96	32.29	3.856	3.855
63	.17820	.17695	158.17	34.04	35.20	3.966	3.964
64	.17818	.17695	128.82	36.49	36.49	4.071	4.071
65	.17817	.17693	155.84	39.43	39.78	4.165	4.165
66*	.07073	.07016	100.67	6.20	8.26	1.705	1.695
67	.07071	.07017	131.50	6.51	7.41	1.740	1.737
68	.07071	.07017	122.26	6.59	7.55	1.795	1.789

Table 11 (cont'd)

Pt. No.	He a t e r		I n p u t Time ($\pm .02$ sec.)	Heat Capacity (10^{-3} joules/ $^{\circ}\text{K}$)		Temperature ($^{\circ}\text{K}$)	
	($\pm .00001$ mamps.)	($\pm .00001$ volts)		M3	M2	M3	M2
69	.07071	.07017	152.55	7.00	8.00	1.864	1.857
70	.07070	.07016	174.69	7.63	8.57	1.940	1.934
71	.07070	.07016	202.40	8.30	8.91	2.019	2.014
72*	.07070	.07016	180.85	8.79	9.35	2.088	2.085
73*	.02408	.02389	1000.10	9.37	11.24	2.047	2.042
74	.03561	.03534	946.78	9.91	11.09	2.142	2.135
75	.03560	.03534	779.22	10.67	11.05	2.219	2.217
77*	.01965	.01950	1867.53	7.80	9.66	1.643	1.634
78	.02271	.02253	999.72	6.84	7.39	1.720	1.717
79	.02270	.02253	1001.09	7.10	7.63	1.789	1.786
80	.02270	.02253	990.31	7.69	8.04	1.850	1.849
81	.02270	.02252	1000.08	8.00	8.44	1.910	1.909
82*	.02407	.02390	783.03	6.66	6.88	1.967	1.966
83	.04267	.04235	376.64	8.99	9.61	2.085	2.083
84	.05076	.05037	412.58	9.91	10.68	2.175	2.171
85	.05076	.05037	354.09	10.06	11.01	2.160	2.156
86	.05076	.05038	417.61	10.36	11.10	2.239	2.236
87	.07167	.07113	226.39	11.10	11.90	2.324	2.321
88	.07165	.07111	252.72	11.74	12.33	2.409	2.406
89	.07165	.07112	264.20	12.62	13.01	2.492	2.491
90	.07165	.07112	281.70	13.45	14.05	2.561	2.558
91	.08627	.08563	171.53	13.89	14.33	2.625	2.623
92	.08626	.08562	216.70	14.64	15.07	2.696	2.694
93	.08626	.08562	230.51	15.49	15.93	2.767	2.766
94	.08626	.08562	238.74	16.33	16.70	2.835	2.834
95	.10156	.10080	193.31	17.00	17.45	2.899	2.898
96	.10156	.10080	231.91	17.88	18.80	2.970	2.967

Table 11 (cont'd)

Pt. No.	H e a t e r		I n p u t Time ($\pm .02$ sec.)	Heat (10^{-3} joules/ $^{\circ}$ K)		Temperature ($^{\circ}$ K)	
	I ($\pm .00001$ mamps.)	V ($\pm .00001$ volts)		M3	M2	M3	M2
97	.10155	.10081	214.08	18.67	19.28	3.036	3.035
98	.10155	.10081	223.69	19.69	21.50	3.091	3.086
99*	.10155	.10081	237.13	19.07	20.86	3.178	3.172

Table 12. Heat Capacity Results of Run B
(Empty calorimeter)

Pt. No.	H e a t e r I ($\pm .00001$ mamps.)	I n p u t V ($\pm .00001$ volts)	Time ($\pm .02$ sec.)	Heat Capacity (10^{-3} joules/ $^{\circ}$ K)		Temperature ($^{\circ}$ K)	
				M3	M2	M3	M2
1	.03920	.03881	124.26	4.87	5.48	1.764	1.762
2	.03923	.03883	259.48	5.65	5.65	1.978	1.978
3*	.03923	.03883	405.39	7.37	7.49	2.191	2.190
4	.03923	.03884	440.81	7.14	7.23	2.299	2.298
5	.05136	.05084	306.19	7.51	7.70	2.415	2.413
6	.05134	.05083	330.01	8.18	8.27	2.532	2.532
7	.05136	.05085	385.81	8.88	9.05	2.648	2.647
8	.05133	.05081	424.92	9.51	10.05	2.761	2.758
9	.06944	.06876	245.96	9.99	10.38	2.853	2.850
10	.06946	.06878	346.25	10.80	11.15	2.963	2.960
11	.06945	.06877	308.85	11.50	11.73	3.065	3.064
12	.06946	.06878	298.80	12.70	12.70	3.205	3.205
13	.06946	.06878	335.31	13.34	13.34	3.368	3.368
14	.06955	.06885	155.78	7.10	7.57	2.365	2.362
15	.06957	.06887	179.20	7.84	8.23	2.479	2.476
16	.06955	.06886	199.29	8.38	8.89	2.582	2.578
17	.06952	.06883	234.36	8.98	9.38	2.689	2.686
18	.06951	.06882	238.51	9.67	9.90	2.806	2.805
19	.06951	.06883	296.63	10.46	10.87	2.937	2.934
20	.06949	.06881	276.71	11.20	11.51	3.044	3.042
21	.06949	.06880	317.90	11.82	12.07	3.125	3.123
22	.07282	.07210	363.36	12.58	12.74	3.216	3.215
23	.07283	.07211	285.92	13.11	13.38	3.291	3.290
24	.09084	.08995	196.32	14.15	14.49	3.358	3.357
25	.09085	.08996	222.5	14.05	14.51	3.423	3.421
26	.09086	.08998	231.29	14.73	15.20	3.489	3.487
27	.09086	.08998	263.87	15.31	15.63	3.564	3.562

Table 12 (cont'd)

Pt. No.	He a t e r		I n p u t Time ($\pm .02$ sec.)	Heat Capacity (10 ⁻³ joules/ $^{\circ}$ K)		Temperature ($^{\circ}$ K)	
	($\pm .00001$ mamps.)	($\pm .00001$ volts)		M3	M2	M3	M2
28	.09086	.08998	255.59	16.06	16.36	3.631	3.630
29	.09085	.08998	304.43	16.76	17.07	3.705	3.703
30	.09978	.09882	218.61	17.30	17.67	3.775	3.774
31	.09978	.09882	285.98	18.19	18.19	3.848	3.848
32	.09980	.09884	259.76	18.87	18.87	3.925	3.925
33	.09979	.09883	300.09	19.11	19.41	3.993	3.992
34	.09979	.09884	270.99	19.96	20.13	4.055	4.055
35	.09978	.09884	227.67	20.60	20.60	4.099	4.099
36	.09979	.09884	170.06	21.13	21.13	4.137	4.137
37*	.03961	.03921	400.10	7.38	7.38	1.907	1.907
38	.03962	.03921	371.89	5.88	6.19	2.002	2.000
39	.05003	.04953	289.82	6.36	7.37	2.112	2.109
40	.05003	.04953	343.81	6.72	7.11	2.217	2.214
41	.05003	.04953	280.30	6.99	7.51	2.299	2.296
42	.05004	.04953	318.22	7.34	7.85	2.368	2.364
43	.05004	.04953	367.35	7.75	8.15	2.453	2.450
44	.05002	.04952	404.73	8.21	8.58	2.534	2.532
45*	.04465	.04420	324.57	6.01	6.79	1.894	1.888
46	.04464	.04419	310.85	5.77	6.20	1.987	1.983
47	.04463	.04418	372.65	6.13	6.66	2.089	2.084
48	.06010	.05949	228.38	6.43	6.96	2.189	2.184
49*	.06009	.05949	235.78	6.06	7.34	1.944	1.932
50	.06010	.05949	188.90	5.66	6.37	2.012	2.005
51	.06010	.05949	210.16	6.09	6.53	2.109	2.104
52	.06010	.05949	240.29	6.53	6.86	2.221	2.218
53	.06009	.05949	181.33	6.98	7.23	2.326	2.324
54	.06008	.05948	183.95	7.49	7.64	2.420	2.419
55	.06008	.05948	227.22	7.99	8.34	2.517	2.515
56	.06008	.05949	273.92	8.63	9.05	2.622	2.620
57	.06009	.05949	244.22	9.86	9.86	2.838	2.838

Appendix VI

Figure 22.

Schematic Diagrams of Manometer Usage in
Adsorption Isotherms

This appendix shows pictorally the four basic ways the manometers were used in the adsorption experiments. The small pair of lines beside each manometer shows its null height.

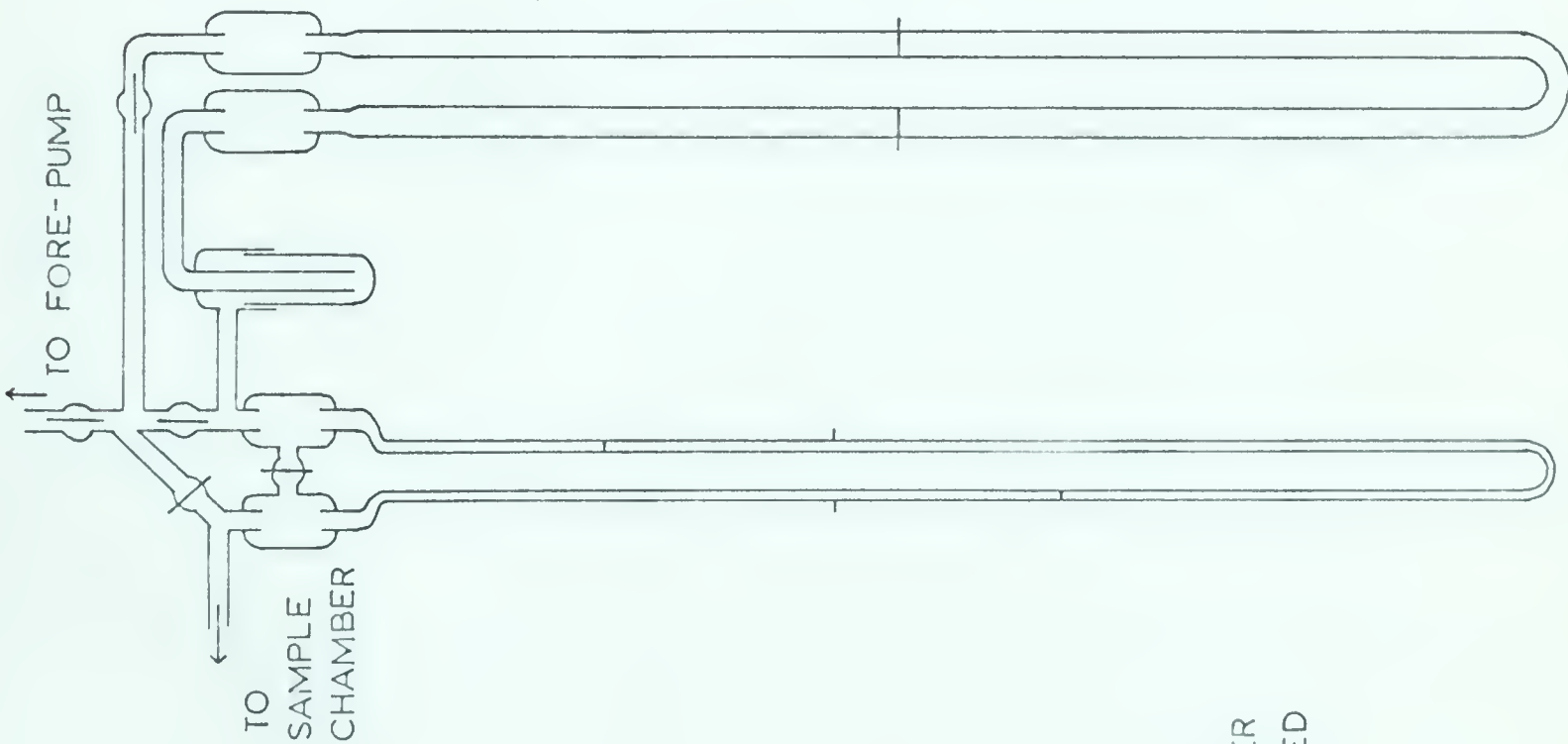
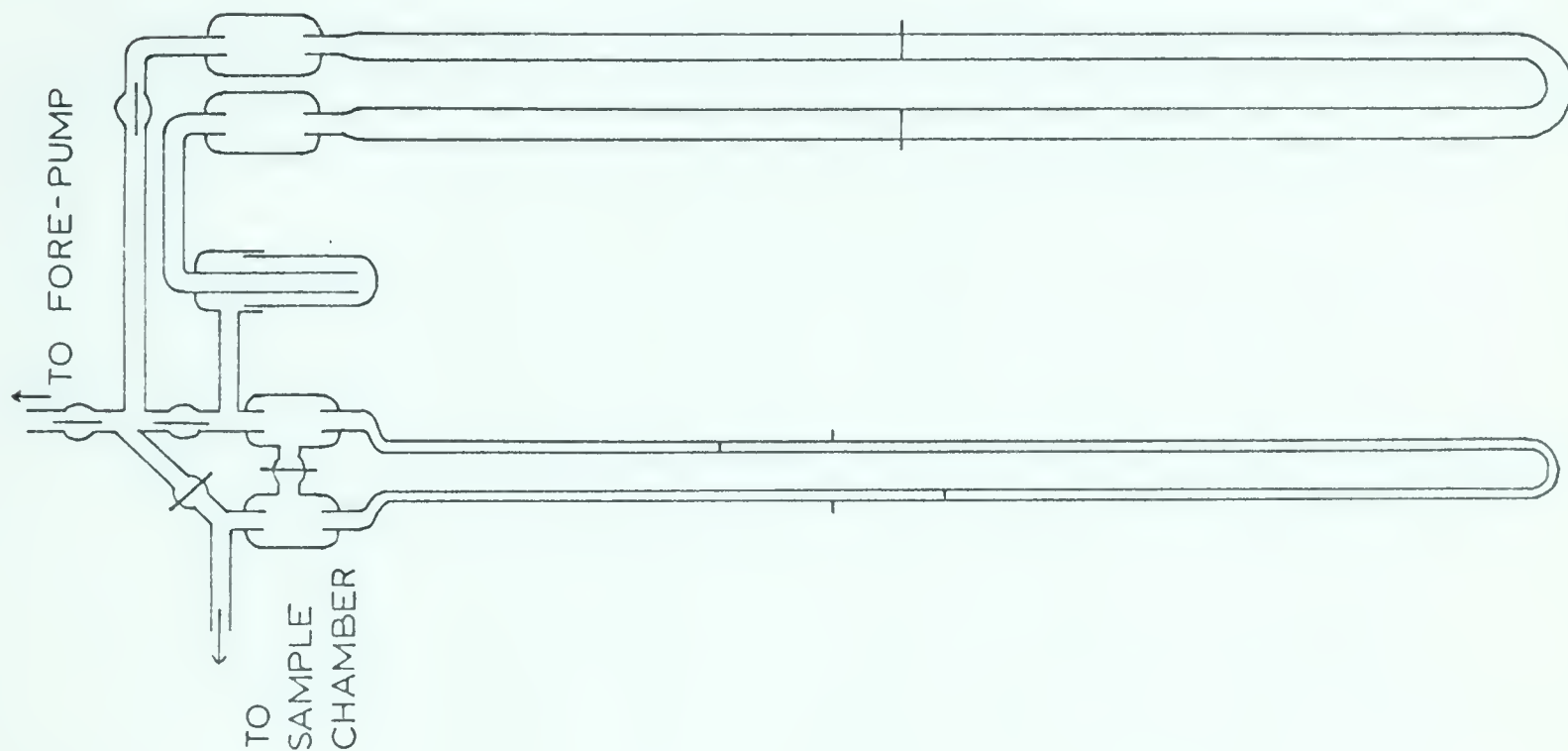
- 22 - 1 Adsorption point using oil manometer only.
- 22 - 2 Desorption point using oil manometer only.
- 22 - 3 Adsorption point using both manometers.
- 22 - 4 Desorption point using both manometers.

The left manometer in each pair is the oil manometer, the right the mercury.

SAMPLE
CHAMBER
OPEN

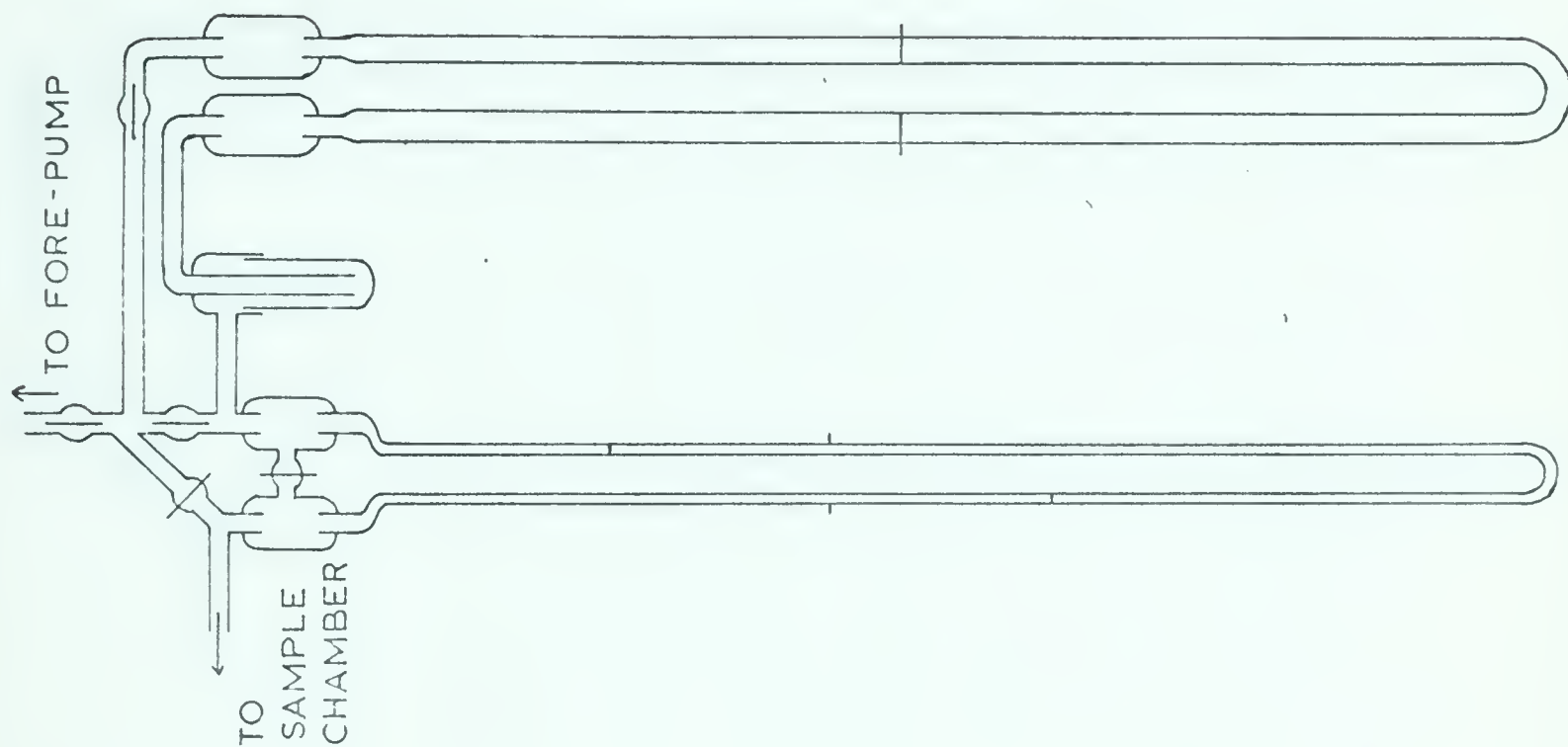
SAMPLE
CHAMBER
ISOLATED

1

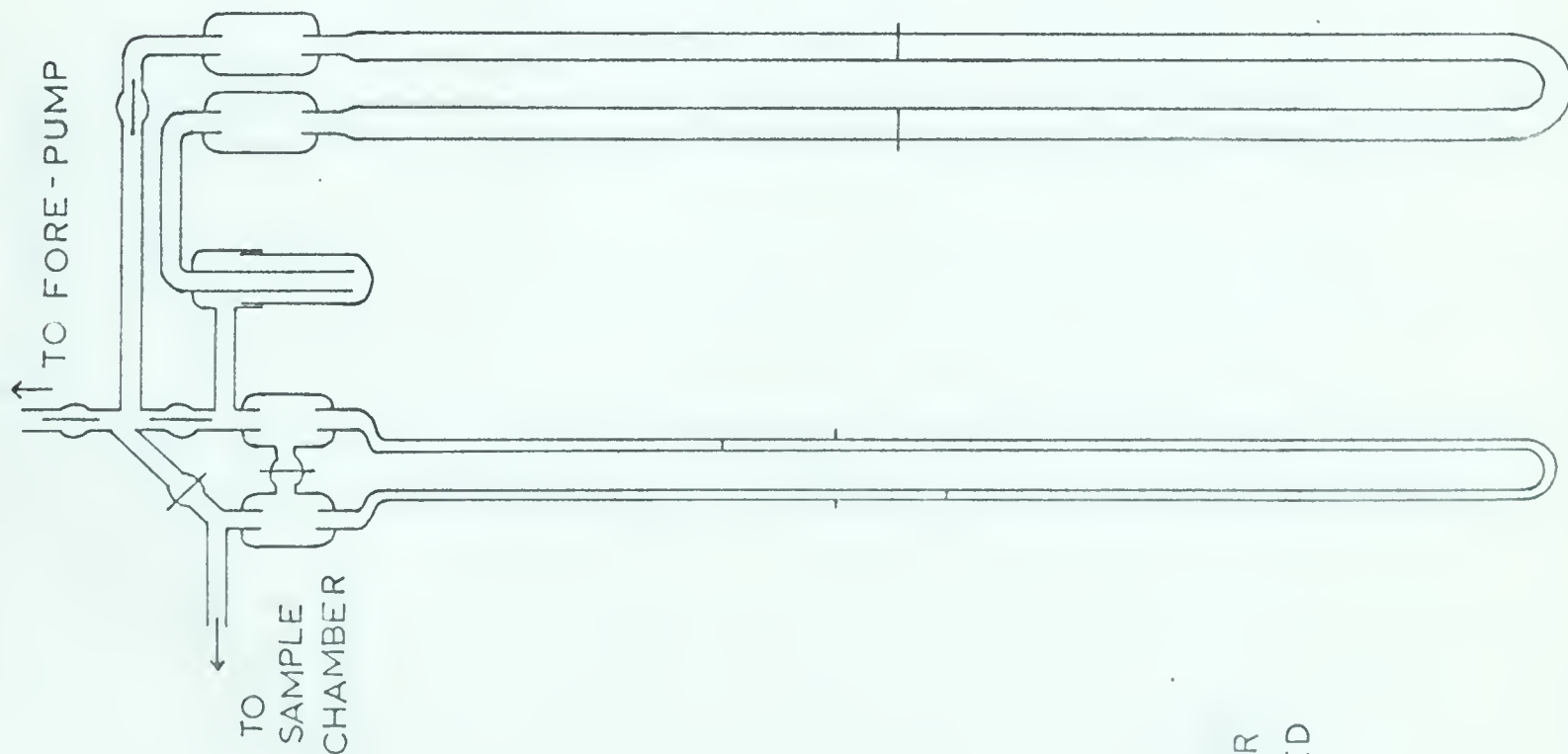


2

SAMPLE
CHAMBER
OPEN



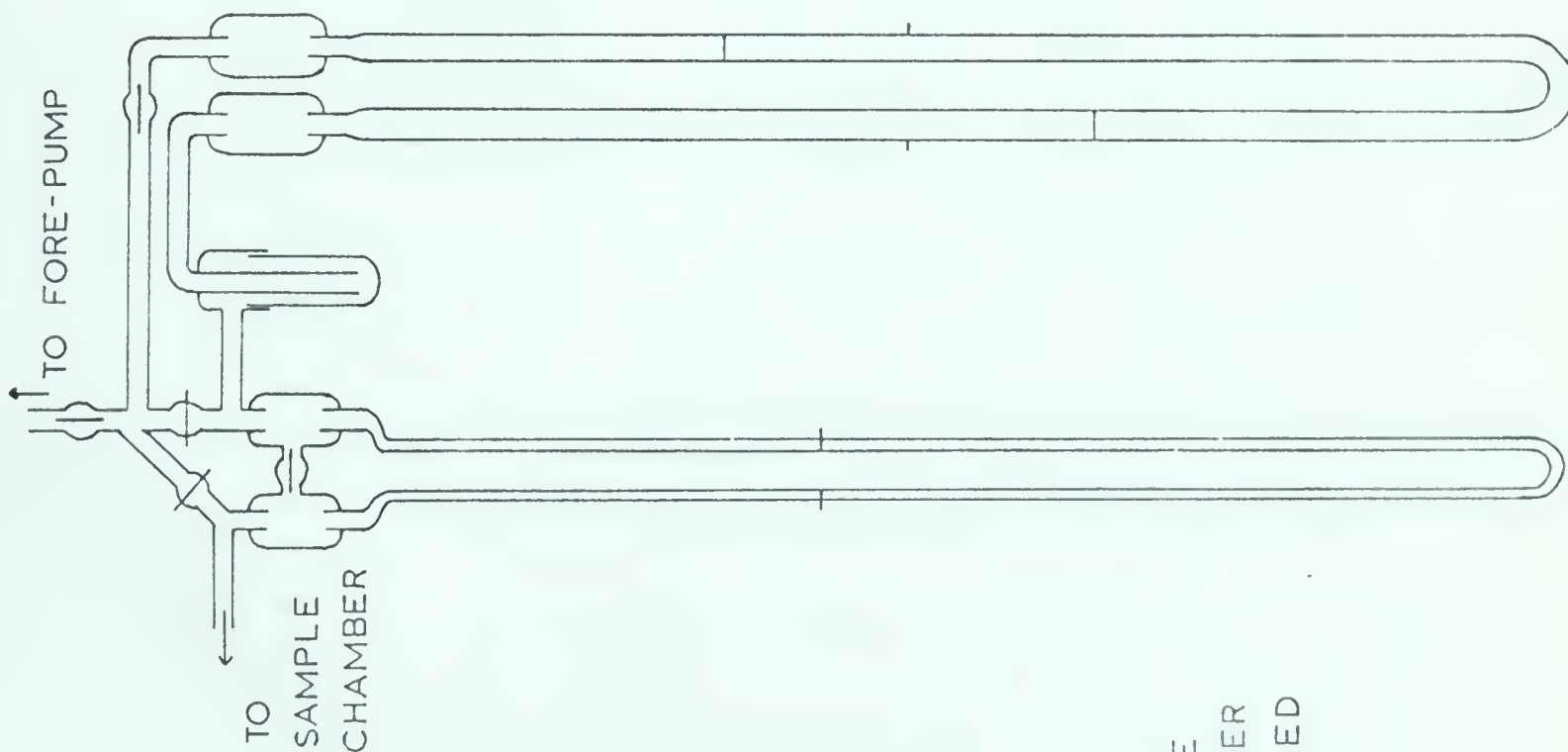
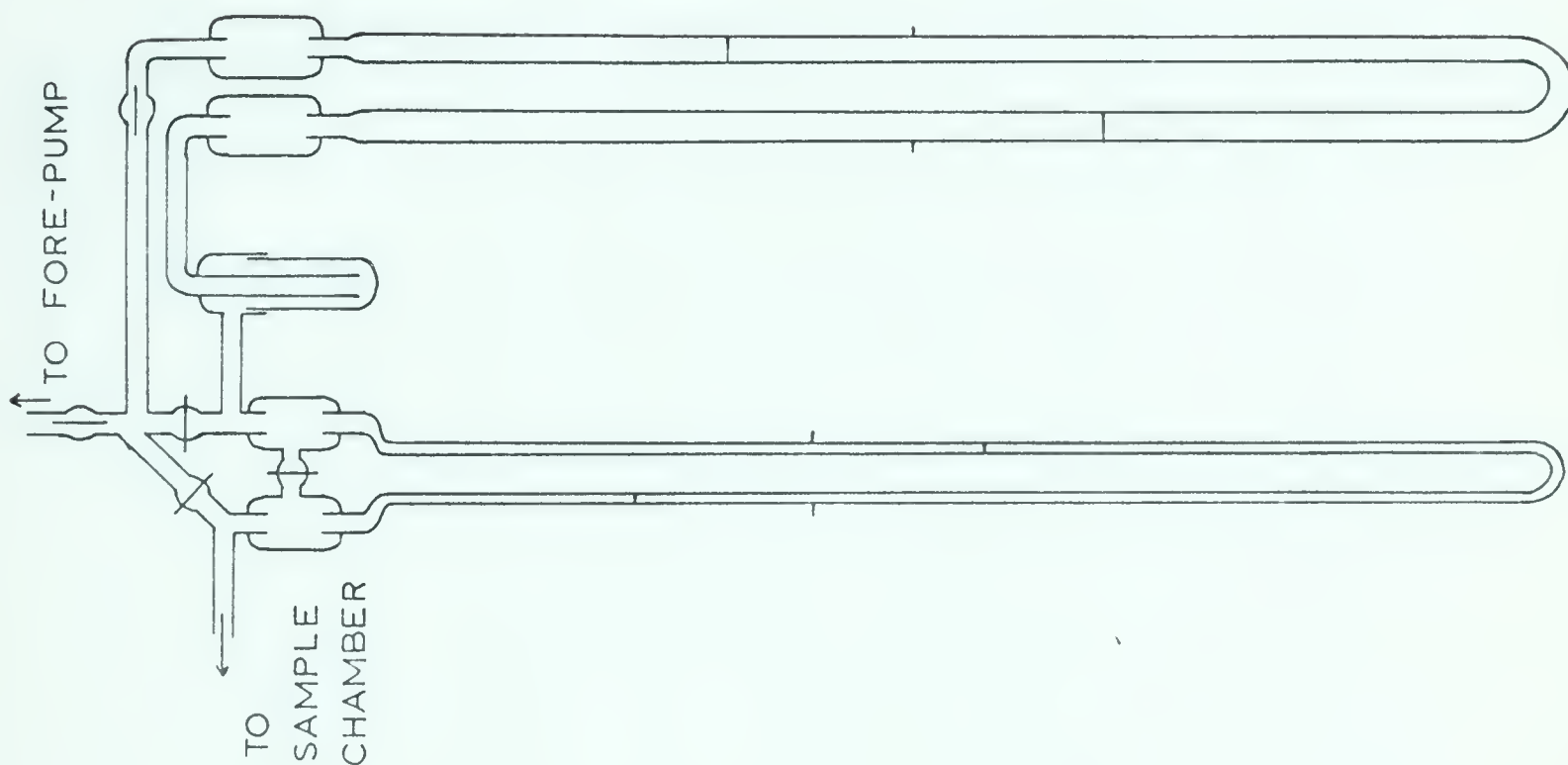
SAMPLE
CHAMBER
ISOLATED



SAMPLE
CHAMBER
OPEN

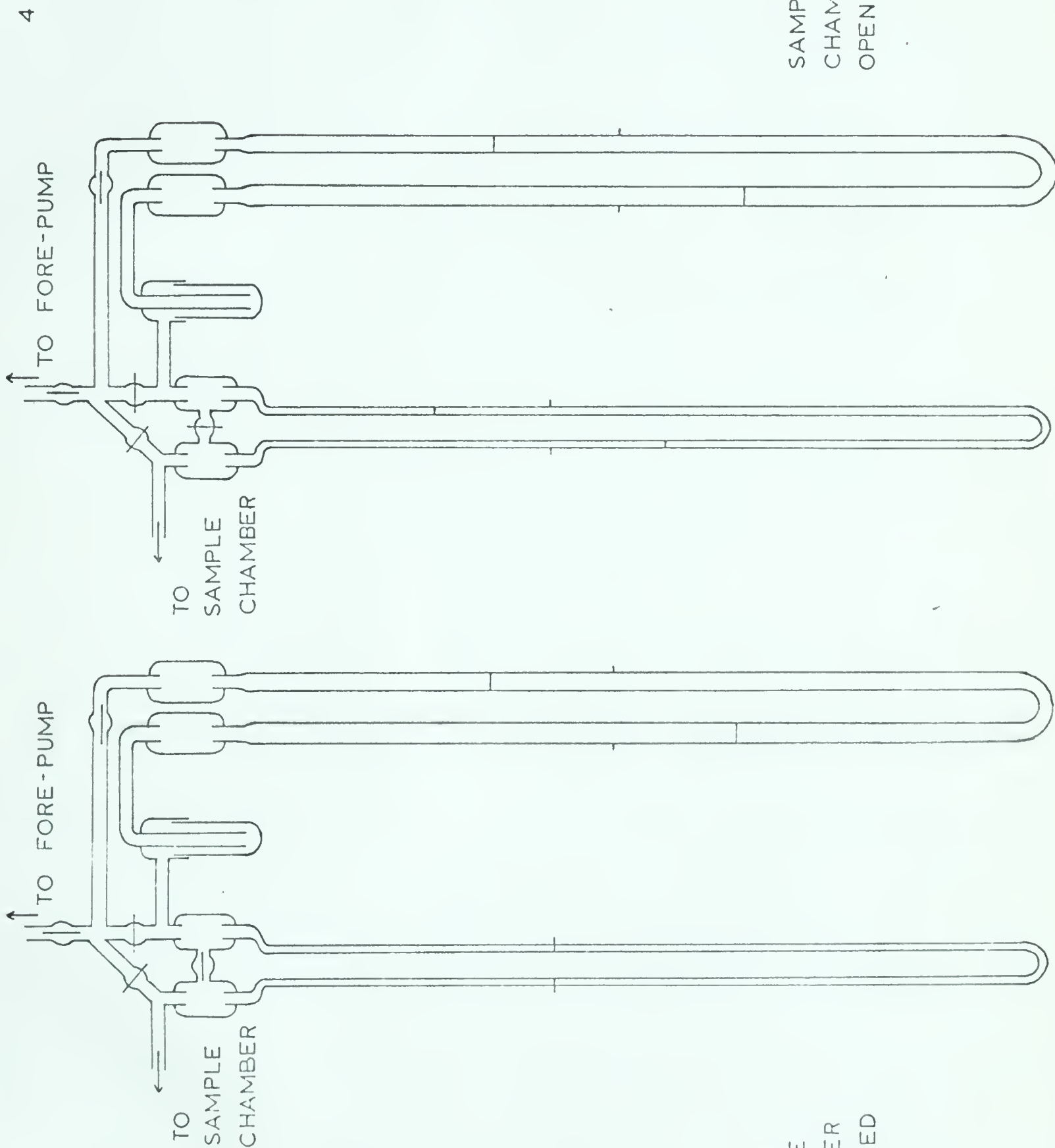
SAMPLE
CHAMBER
ISOLATED

3



SAMPLE
CHAMBER
OPEN

SAMPLE
CHAMBER
ISOLATED





B29828